A Design Tool for Matching UAV Propeller and Power Plant Performance

A THESIS
SUBMITTED TO THE FACULTY OF THE GRADUATE SCHOOL
OF THE UNIVERSITY OF MINNESOTA
BY

Arion L. Mangio

IN PARTIAL FULFILLMENT OF THE REQUIREMENTS
FOR THE DEGREE OF
MASTER OF SCIENCE

Demoz Gebre-Egziabher, co-advisor
William L. Garrard, co-advisor

May 2013

© Arion L. Mangio 2013

Acknowledgments

First, I want to thank those who helped me with my research. My two advisors, William Garrard and Demoz Gebre-Egziabher, helped me formulate the problem to base my research on and have greatly contributed to my writing abilities. I also must thank Gary Balas for hiring me to work in the UAV Lab. Working in the lab allowed me to interact with other MS and PhD students, and this helped develop my desire to further my education. It also led me to pursue a master's degree in Controls Systems, which I previously did not have an interest in. Furthermore, I must thank Peter Seiler for stirring my interest in Controls Systems. After taking his classical controls class, I knew I wanted to pursue Control Systems further. Lastly, I must thank Perry Leo for admitting me into the program.

Second, I thank my family for all they have done. My father, mother, grandparents, aunts, and uncles took me to RC flying fields countless times and spent hours upon hours building airplanes with me throughout my childhood. They saw the gift in me for building things and for flying, and they nurtured that gift the best they possibly could. The talents I have today are a direct result of their investment.

Third, I also must thank Jenny, my beautiful and awesome wife. She has proof read many of the papers I have written, and they are much better because of it. She has lived with me as I struggled at times to complete my degree. She has helped in so many ways, and I would not have finished my degree without her help. She has stood beside me, and I have faith in and trust her with all of my life.

Lastly, I must give credit to God. All those who have helped me along the way deserve great credit, but I must give credit to God for what I personally have done. I know that I would not have made it this far without His blessings and help. There were times that I did not know how I was going to finish my master's degree. The main realization that makes the EPM code work was that the engine RPM could be divided by the gear ratio, and then the propeller and engine power data could be plotted together. I firmly believe that this idea was not my own. Additionally, I was on the wrong path and terribly confused after high school. I thank God that He was able to use my mistakes to humble me and make me a better person. I give all the credit for everything I have done and ever will do to God because He is the only reason I have made it this far.

Dedication

To Jenny, My Family, and Jesus Christ

Abstract

A large body of knowledge is available for matching propellers to engines for large propeller driven aircraft. Small UAV's and model airplanes operate at much lower Reynolds numbers and use fixed pitch propellers so the information for large aircraft is not directly applicable. A design tool is needed that takes into account Reynolds number effects, allows for gear reduction, and the selection of a propeller optimized for the airframe. The tool developed in this thesis does this using propeller performance data generated from vortex theory or wind tunnel experiments and combines that data with an engine power curve. The thrust, steady state power, RPM, and tip Mach number vs. velocity curves are generated. The Reynolds number vs. non dimensional radial station at an operating point is also found. The tool is then used to design a geared power plant for the SAE Aero Design competition. To measure the power plant performance, a purpose built engine test stand was built. The characteristics of the engine test stand are also presented. The engine test stand was then used to characterize the geared power plant. The power plant uses a 26x16 propeller, 100/13 gear ratio, and an LRP 0.30 cubic inch engine turning at 28,000 RPM and producing 2.2 HP. Lastly, the measured power plant performance is presented. An important result is that 17 lbf of static thrust is produced.

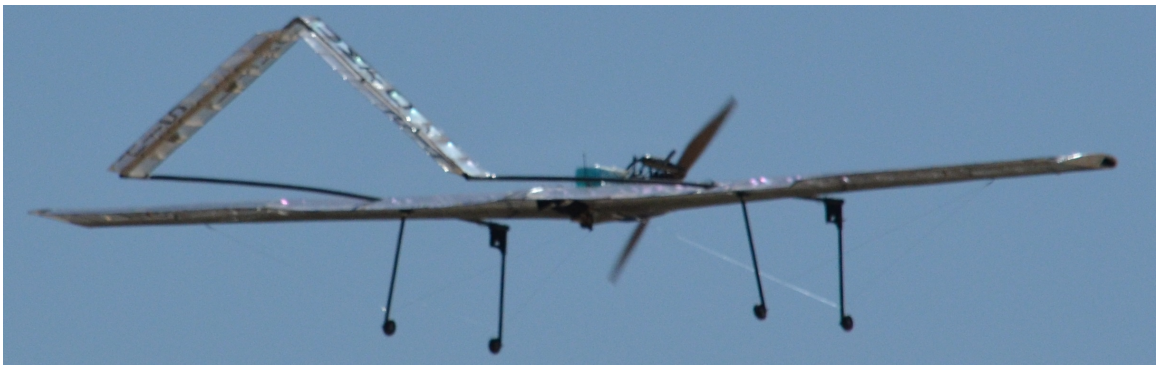

Figure 1: The University of Minnesota SAE Aero Design Advanced Class Airplane.

Contents

List of Tables

List of Figures

Nomenclature

Abbreviations and Acronyms

UAV	Unmanned Aerial Vehicle
RC	Radio Control
$WWII$	World War II
RPM	Revolutions Per Minute
SFC	Specific Fuel Consumption
$COTS$	Commercial Off The Shelf
ICE	Internal Combustion Engine
TDC	Top Dead Center
BDC	Bottom Dead Center
$nitro$	Nitromethane
ABC	Alloy Piston, Brass Cylinder Liner, Chrome Plated
ABL	Advanced Bi-metallic Liner
$LiPo$	Lithium Polymer Battery
$NiCd$	Nickel Cadmium
$NiMH$	Nickel Metal Hydride
ESC	Electronic Speed Control
PWM	Pulse Width Modulation
DC	Direct Current
BEC	Battery Eliminator Circuit
$OpAmp$	Operational Amplifier
POT	Variable Potentiometer
FFT	Fast Fourier Transform
OD	Outside Diameter
ID	Inside Diameter
CNC	Computer Numerically Controlled

List of Symbols

A	Amperage
V_{batt}	Battery Voltage
C	C rating of battery
W	Watts

c	Chord
h	Thickness
r	Radial station
x	Non-dimensional radial position
R	Propeller radius and gas constant for air
c_D	Non-dimensional chord to diameter ratio
D	Propeller diameter or drag
h_c	Non-dimensional thickness to chord ratio
dL	Differential lift
dD	Differential drag
α	Angle of attack
V_E	Relative incoming flow velocity
Re	Reynolds number
V	Velocity
μ	Absolute viscosity coefficient
x_{RE}	Characteristic length
$C\ell$	Lift coefficient
Cd	Drag coefficient
L	Lift
ρ	Density
S	Area
a	Lift slope or speed of sound
ωr	Velocity due to rotation
V_R	Velocity due to rotational velocity and forward velocity
ϕ	Angle between V_R and ωr, degrees
α_i	Induced angle of attack, degrees
ω	Induced velocity
ω_a	Axial component of induced velocity
ω_t	Tangential component of induced velocity
P	Power
β	Sectional blade twist, degrees
T	Thrust or temperature
γ	Heat capacity ratio
V_{Etip}	Relative tip velocity
M_{tip}	Tip mach number

J	Advance Ratio
n	Angular velocity, revolutions per second
η	Efficiency
P_{req}	Power required by propeller
C_T	Thrust coefficient
C_P	Power coefficient
HP	Horsepower
τ	Torque
V_{OPT}	Optimization velocity
P_{avail}	Power available from the power source
RPM_{eng}	Revolutions per minute of the engine
RPM_{prop}	Revolutions per minute of the propeller
G	Gear ratio

Chapter 1

Introduction

This thesis deals with the techniques used for sizing propeller-based power plants for small Unmanned Aerial Vehicles (UAV's). There has been considerable work done for large scale propeller driven aircraft, but these design methods may not be applicable to small UAV's.

UAV's are increasingly important in a variety of applications. In all applications where UAV's are used, it is desirable to have the aircraft be designed in an optimum way. Many UAV's are small, slow flying, and propeller driven. Propeller research reached its prime during World War II (WWII), but with the advent of the jet engine, propeller driven aircraft received little attention. Private and turboprop aircraft continued to use propellers with little change to the design philosophy because the power of the engines and size of the aircraft did not change markedly. It is not until recently that serious attention as been given to small UAV's. Therefore, the design tools for small aircraft have not been substantially improved.

Many small UAV's are the same size as the average radio controlled aircraft. The radio control (RC) community has been steadily advancing and many new types of aircraft are available. There are gliders, pylon racers, gas and electric powered aircraft, all ranging in size from very small to several meters in wingspan and capable of a wide range of speeds. Such aircraft are designed for hobbyists and serve no purpose other than entertainment. Even so, these aircraft have become very advanced. They have centrifugal fan jet engines, single and multi-cylinder internal combustion engines, turboprop/turboshaft engines, and a wide variety of electric motors. The RC

community has helped advance the technology for electric power, and many would say that a brushless motor with a Lithium Polymer (LiPo) battery is more powerful and lighter than a similarly sized internal combustion engine setup. It suffices to say that there are many power options available for UAV's from the RC market. Because there are so many combinations of motors and engines with various propellers and gearboxes, it is hard to predict the performance of a complete power plant. The design philosophy in the RC market has been to basically overpower the airplane to ensure adequate performance is met. Such a philosophy does not lend itself well to minimizing the weight of a power plant or determining the optimal configuration with regards to efficiency. The average RC modeler is not looking for an overly complicated system, and the power plants available are very simple for this reason. This is why most power plants are direct drive and why there are few gear drive systems, except for electric motors. In matching a motor or engine to a propeller, the average modeler will simply follow manufacturers recommendations and perform several trial and error experiments until they get reasonable performance. In general, it is understood by most modelers that larger diameter propellers with less pitch will give good low-speed performance, and small diameter propellers with high pitch and high revolutions per minute (RPM) will have good high-speed performance. Since RC parts are readily available, low cost, and designed for small aircraft, they are often used in small UAV's. The designer must use the same trial and error techniques used for RC aircraft. If the UAV designer has access to a wind tunnel, better testing can be performed but still with the same limitations of trial and error. To do these tests properly, several motors and engines need to be purchased and tested along with several propellers and gearboxes to optimize any particular design. This can result in weeks of testing and may not give the best combination of motor/engine, propeller, and gear ratio, because there are so many gear ratios available. A tool is needed which will analyze these combinations and output the gear ratio, propeller size, and engine. In this way, only one propeller, gear set, and engine or motor needs to be purchased and more time can be spent on the airframe design and optimization. Currently, there are computer programs for RC that only estimate the static thrust, but none accurately predict the thrust vs. velocity curve [1]. There are, however, several methods developed for large propellers to predict the thrust vs. velocity performance along with other parameters. To understand how to match an engine or motor to a propeller, it is advantageous to build upon the techniques already developed and understand the principles behind earlier design choices.

This thesis develops analytical tools that can be used during the design phase of small UAVs. The purpose of these tools are to help the designer, during the conceptual design phase, to select the appropriate power plant and propeller combination for a particular airframe. As previously described, there is considerable prior work related to this problem, but most of the prior work dealt with larger, manned aircraft. The purpose of the work reported here is to examine whether the existing tools are still valid for the smaller UAV which operate in conditions which are not always similar to larger aircraft.

1.1 Aircraft Conceptual Design

Aircraft conceptual design is the first stage of the design process of a new aircraft. At this point, the design requirements are posed in such a way that the general weight and layout of the aircraft can be considered.

To begin, the mission profile of the aircraft is considered. Many aircraft have a simple mission profile, where the aircraft climbs to a cruising altitude, cruises for some distance, descends, loiters, and then lands. Many UAV's do not fly to a new location since they land where they initially took off. The cruise portion of the flight can then be considered loitering over the same area. There are several other mission profiles that can characterize the task a particular aircraft is to perform, but the simple mission profile adequately describes most surveillance tasks for UAV's [2]. The mission profile will determine how long an aircraft is to loiter over a certain area, or how far the aircraft needs to fly. If the goal is to stay aloft for a long time, the design requirements will be different than flying to a certain location quickly.

Each UAV will have to carry a certain amount of sensors to perform its mission. These can sometimes be made lighter, but a basic estimation of the weight of those sensors is required in the conceptual design stage. The combined information of the mission profile and the weight of the electronics allows for the estimation of the empty weight and fuel weight. This is done by considering available power plants and their specific fuel consumption (SFC). The SFC describes how much fuel is consumed for the thrust produced. The power plant must be chosen so that it can propel the aircraft at the desired speed efficiently. Based on how fast the aircraft flies, how far it will fly, and the SFC of the engine, the amount of fuel required can be estimated. The aircraft configuration can then be sketched out to estimate the wingspan, length,

and required wing area. The weight of the structure can then be estimated.

The conceptual design phase requires several iterations on each aspect of the design. The required fuel will change depending on how efficient the airframe is. The airframe design will depend on the SFC of the engine as well, because the fuel required will depend on the SFC of the engine. There is an abundant amount of information for large aircraft that has been compiled into graphs and tables. The data from the large aircraft has been posed in the form of ratios. This creates trends for certain types of aircraft. The trends aid in the prediction of the SFC depending on how fast the aircraft will fly, how much fuel is required compared to the empty weight of the aircraft, and the lift to drag ratio of the wing [2]. This type of information is not available for small UAV's because not many have been built when compared to large aircraft. It is therefore hard to use such tables and graphs for small UAV's. It will generally be required to iterate on the design requirements and build several prototypes to arrive at the final configuration. The hardest to predict is the power plant performance. Traditional methods for power plant sizing will be mentioned next.

1.2 Power Plant Sizing in the Conceptual Design Phase

The power required is calculated from the conceptual design phase, and this is used to find an engine that provides the necessary power. Data has been compiled for many large engines to estimate the size and weight from the required power [2]. Available engines and propellers can then be compared, and a combination can be chosen to meet the required power.

In general, it is best to choose the largest diameter propeller possible because this will give the best efficiency. This is evident from Newtons second law, $F = Ma$, where a larger propeller will accelerate a larger mass of air less in order to get the same force, and this improves efficiency. The diameter can not be too large, however, because the tips of the blades will approach the speed of sound. The rotational speed of the propeller and forward speed of the aircraft must be considered to ensure the tip speed is not too high, otherwise the efficiency will decrease. The pitch of the propeller determines how well it will perform at fast or slow speeds. Fixed pitch propellers are only optimal for certain speeds, so compromises must be made. However, there are variable pitch propellers that can perform well over a wider range of speeds. Propellers

are usually characterized by non-dimensional coefficients. The performance can then be scaled and different propellers can be more easily compared.

There are some additional effects that must be considered. At higher altitudes there is lower pressure. The lower pressure will dramatically reduce the power output of engines. There are superchargers and turbochargers that pressurize the engines intake air, and these allow for high power to be produced at higher altitudes. The altitude of flight from the mission profile must therefore be considered in the selection of an engine.

1.3 Problem Statement

It is not clear if the above noted methods for initial sizing of power plants are valid for small UAVs. The empirical methods in reference [2] were developed as fits to data collected from large aircraft. For example, it is not clear what kind of impact size (captured through Reynolds number, for example) has on the accuracy of the methods. The purpose of this thesis is to examine whether these traditional approaches to initial sizing of manned aircraft are applicable to small UAVs.

1.4 Thesis Contribution

This thesis outlines a procedure that optimally finds the best engine and propeller combination from engine power curves and propeller performance data. The tool developed can be used with any type of power source that can spin a shaft and put power into the shaft. Many aircraft engines are built so that they produce power at an RPM where propellers will be efficient at producing thrust. The problem is that engines can produce much higher power if allowed to run at high RPM. Propellers do not produce efficient thrust at high RPM, however. It seems that optimizations as described in this thesis have not been done for small UAV's and are not generally done for large scale aircraft. Large scale propeller driven aircraft are limited to only a handful of engine choices, because it is very expensive to certify new engines. The tool developed could be used with large propeller driven aircraft in order to more optimally match engines to propellers. This would allow for smaller high RPM engines to be used with much larger propellers. This could improve the propulsive efficiency substantially. Modern hybrid aircraft concepts could also benefit from the use of the tool developed in this thesis. Hybrid aircraft will have different power

sources driving the propeller, and the procedures developed could find the best gear ratio, propeller, electric motor, and engine to optimize the completed power plant. Additionally, the limitations of high pitch propeller performance at low speeds may be improved by the choice of the proper gear ratio. Overall, this thesis, and the tools developed, could drastically improve propeller driven power plant performance.

1.5 Thesis Organization

Chapter 2 summarizes many historically significant engines and gives an interpretation as to what the designers were trying to do to optimize the power plants. The progression from internal combustion engines to the jet age will also be discussed, and the lessons learned will be loosely applied to internal combustion engines.

Chapter 3 describes how model 2 and 4-stroke engines operate and how they should be used. Break-in procedures and tuning characteristics are also discussed. Lastly, electric power plants and the associated batteries, speed controls, and motors are explained.

Chapter 4 describes how propellers can be modeled and how they can be optimally combined with an engine by use of a power vs. RPM curve. The tool explained in this section can be used with vortex propeller theory or experimental data. The thrust, power, RPM, and tip Mach number, vs. velocity are presented along with station Reynolds numbers on the propeller. A design study is also shown comparing a large propeller to a small propeller, and the benefits of gearing a high RPM engine are presented.

Chapter 5 explains the testing of five 26 inch propellers in a wind tunnel where their performance data was gathered experimentally. Chapter 5 also explains the construction and setup of an engine test stand that was built to test the validity of the tools developed. In this chapter, an engines power curve is found, and a geared power plants performance is tested. The measured results are then compared to predictions made with the tools developed.

Chapter 6 summarizes the various results and gives suggestions for future work.

Chapter 2

Overview of Large Scale Power Plants

Many similar principles can be seen in different power plants and applications. The specifics in designing a gear box, cylinder, specific horse power or thrust, or any particular part of one engine or motor is not of huge importance to the UAV designer. A designer of a UAV would rather use commercial off the shelf (COTS) parts. Therefore, it is of benefit to understand how an engine or motor can be set up to efficiently produce thrust to give the highest thrust to weight ratio or greatest efficiency depending on the application. To make a propeller driven aircraft power plant requires a power source that will turn a shaft and a way to connect that power plant to a propeller. WWII and the years after produced some of the most optimized propeller driven power plants in history. The lessons learned from their design features can be applied to new systems. An overview of the internal combustion engine and some famous examples will be presented, along with some ideas about turbine power plants.

Before considering the engines, there are some limiting factors to the propellers that need to be mentioned. The propellers had to operate below certain RPM, based on how fast the airplane was flying and the size of the propeller. Therefore, the output shaft from the power plant had to be geared based on the RPM range of the power plant and the constraints of the propeller.

2.0.1 Large Reciprocating Engine Power Plants

The internal combustion engine concept is fairly simple. It operates by compressing air mixed with fuel, igniting the mixture, and capturing the force delivered by the exploding charge of air and fuel. Most engines use pistons that travel up and down in a cylinder. The piston is connected to a connecting rod, which is connected to the crankshaft. In this way, the vertical motion of the piston is converted into rotary motion of the crankshaft. To control the delivery of air into the cylinder, there are valves that open and close at the proper time, depending on the position of the piston and crankshaft. To inject fuel there is some kind of device, such as a carburetor or fuel injector, positioned somewhere in the air intake. The products of combustion are ejected from the cylinder. When the fuel is burned, it produces heat which is controlled by air or water cooling [3].

To improve performance, several things can be done. The components can be lightened so that the engine produces more power for its weight. More air and fuel can be forced into the cylinder so that the explosion of fuel and air produces more force on the piston. The combustion of fuel and air can be done faster or more completely so that more energy is extracted from the mixture before it exits the engine. The incoming air can be cooled so that it is more dense; this is almost the same as forcing more air into the cylinder. More cylinders can be added to the engine, or the cylinders and pistons can be made larger, so that there is more force going into the crankshaft. The cooling system can be made more efficient to extract more heat. Lastly, the RPM of the engine can be increased so that more combustion events occur per unit time. There are of course many more improvements that can be made, and many of these improvements will affect the others, but the main areas of concern are often the aforementioned items.

One of the most famous examples of an internal combustion engine is the Rolls-Royce Merlin engine of WWII shown in Figure 2.1. The Merlin engine eventually produced about 1,500 horsepower (HP). The heavily modified merlin engine in the unlimited Reno Racer Dago Red produces an estimated 3,500 to 3,800 HP with a reduction gear ratio of 0.42:1 [4]. This engine uses a supercharger driven by the crankshaft to compress the air going into the engine, so that the air will be denser, allowing for more fuel to be burned and more HP to be delivered. The engine uses four valves per cylinder so that the incoming intake air will flow more easily into the combustion

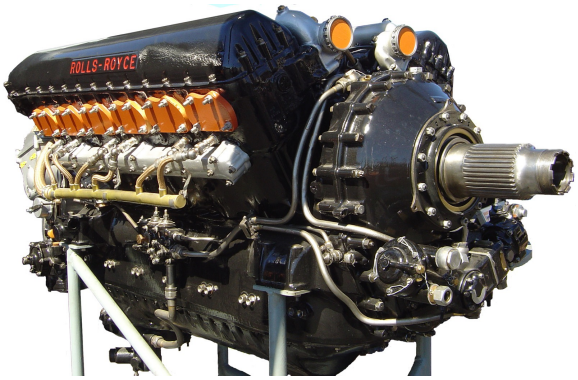

Figure 2.1: Merlin engine.

chamber. An intercooler is used to cool the air making it more dense. The engine uses two spark plugs per cylinder to burn more of the fuel-air mixture and for redundancy. It is liquid cooled to control the engine temperature. This allows for tighter tolerances because the engine can have a more uniform temperature. This overview of features shows that much was done to get maximum power out of the pistons and cylinders.

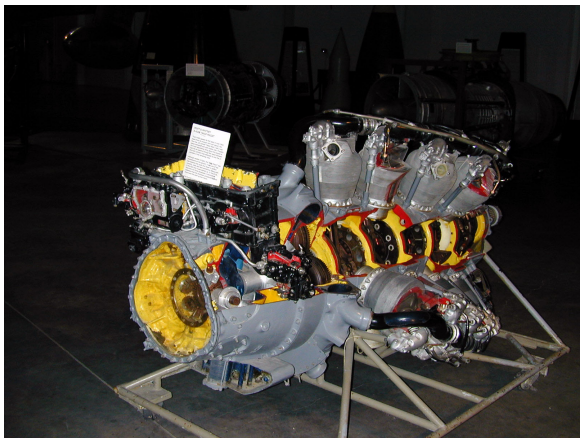

Figure 2.2: Pratt & Whitney R-4360 Wasp Major.

The largest reciprocating engine ever produced for aircraft is the Pratt & Whitney R-4360 Wasp Major, shown in Figure 2.2. The engine was used in the B-36 bomber and several transport aircraft. It produced 3,500 HP and was geared 0.381:1 or 0.425:1 [5]. The engine has 28 cylinders arranged radially around the crankshaft in four rows. It was air-cooled using intricately designed cooling fins on the cylinders. It uses two large valves for each cylinder. Two spark plugs were used in each cylinder, as in the Merlin engine. This engine used a turbo charger in addition to a supercharger, like the Merlin engine, that captured energy from the exhaust gases to be used for

compressing the intake air. The Pratt & Whitney R-3350 engine, similar to the R-4360, used turbo compounding. This basically works like a turbocharger, but adds power to the crankshaft instead of compressing the intake air.

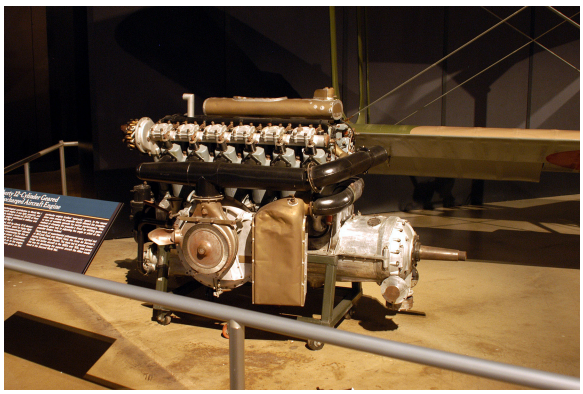

Figure 2.3: Variable gear ratio transmission on a Liberty engine.

The Liberty engine shown in Figure 2.3 was a huge success in WWI [6]. The engine shown is outfitted with a variable gear ratio transmission, although it was usually direct drive. This was done in order to allow the engine to operate at its optimal RPM to get the most thrust out of the propeller. The engine is water cooled, similar to the Merlin engine shown in Figure 2.1. Each cylinder uses two valves, one for the intake air, and one for the burned air and fuel mixture. The engine uses a turbo charger, shown by the circular device on the side of the engine, similar to the R-4360. The engine also uses an intercooler similar to the Merlin engine. The Liberty engine is almost the same size as the Merlin engine, but it only produced about 400 HP. This shows how the technology advanced in the many aspects of engine design.

Additionally, some of the large internal combustion engines used water-methanol or alcohol injection on takeoff to increase the power, but this could not be used for extended periods of time. In summary, all of the internal components of an internal combustion engine could be optimized and lightened, but the basic design would be the same. Therefore, an engine with a supercharger, turbocharger, and turbo compounding would be the practical limit as far as getting the maximum performance out of the internal combustion engine.

2.0.2 Private and Small Aircraft Power Plants

The large internal combustion engines shown are some of the most optimized and refined in their class. When the U.S. Air Force retired their last piston engine transport and bomber aircraft, the only aircraft using piston engines used engines of much lower HP. These aircraft made by Cessna, Piper, Mooney, Beechcraft, and Cirrus, to name a few, generally use direct drive Lycoming or Continental engines, though some are geared. There are several small experimental aircraft that use converted automotive engines or Rotax engines with gear reduction drives. The automotive engine is well optimized for its task. For this reason many auto engine conversions perform very well. This class of engine makes roughly 100-500 HP. These engines sometimes use turbo chargers, but none use turbo compounding, and most do not use a supercharger. The engines are designed for simplicity, minimal cost, and ease of operation more than extracting the absolute maximum power or getting the best performance out of the system. Some of the smaller engines are quite efficient and considered powerful for their class, but they do not compare to the large engines shown in terms of how many components are involved or how complicated they are.

2.0.3 Turbine Power Plants

The reason for the demise of the piston engine in large aircraft is the jet engine. The first jet engines were used toward the end of WWII, and they have been extensively refined. Some reasons that the jet engine is better than a piston engine are (1) it has much more power for its weight (2) it is more reliable, and (3) it can propel an aircraft to faster speeds. Modern jet engines also have incredibly long service intervals. The first jet engines were turbojet engines, but later engines were turbofans. The reason for the change is that a turbofan moves a much greater volume of air than a turbojet, making it more efficient [7]. For slower speeds, the turboprop engine is more efficient than a turbofan. The propfan, currently under development, is expected to further increase efficiency at high subsonic Mach numbers where the turbofan operates.

The turbine engine works in a similar way to an internal combustion engine in that it compresses air, combines it with fuel, burns it, and extracts power from the increase in pressure. This is done using blades arranged around varying size disks. Some of these disks compress air, others extract energy from expanding air. In the front of the engine, the air is slowly compressed through many disks of blades, and the

whole section is known as the compressor [7]. The compressed air is then mixed with fuel, burned in a combustor, and expanded through a few disks of blades, known as the turbine section. The compressor section is connected to the turbine section so that part of the extracted energy is used to compress the air. In this way, there is continuous combustion. This basic layout is known as a turbojet [7]. The turbojet operates by moving a relatively small amount of air very fast. The turbofan engine uses some of the captured energy from the turbine to turn a large fan at the front of the engine. This causes more air to be moved. The turboprop engine also uses some of the energy from the turbine section, but instead of turning a fan, it turns a propeller through a gearbox [7]. Lastly, the propfan engine captures power from the turbine, but instead of driving a shaft to run a fan or gearbox, it drives blades directly attached to the turbine section on the back of the engine [7].

This discussion is meant to highlight the general features of the four turbine engines so that some conclusions can be drawn from the basic operating principles. The engines are better power plants because more power is produced from a given mass of metal, fuel, and air, compared to a piston engine. The other characteristics such as reliability, long service intervals, and higher possible speeds are more dependent on how the basic turbine engine concept is implemented. Basically, any power plant that can turn a shaft can be adapted for many different purposes. This idea is not entirely correct as one would probably not say that a piston engine can be adapted to propel an aircraft faster than the speed of sound. There are always other constraints that limit what a particular power plant can be used for. For relatively slow speed propeller driven flight, anything that turns a shaft, puts power into that shaft, uses the minimal amount of energy to produce that power, or produces a lot of power for a given amount of energy, is desirable. The RPM of the spinning shaft is not of great concern, because a gear reduction unit can be used to convert the power plant RPM into whatever RPM is best for the propeller and design purpose of the aircraft. This is what was done with the turboprop engine, the output shaft spins incredibly fast but is reduced by gears to the proper speed for the propeller.

2.0.4 Summary of Power Plants

There are many power plants available, so the UAV designer should not feel limited in the selection of a power plant. It is better to consider all types of power plants available and select from the most optimized systems in a particular operating prin-

ciple category. Before a power plant is considered, knowledge of what the operating conditions of the aircraft will be must be decided upon. Once these conditions are known, different complete aircraft designs can be considered. Typical power plants for model aircraft will be presented next. These power plants are often used in small UAV's because the aircraft are of the same size.

Chapter 3

Power Plants for Small UAV's

In this chapter, we will describe power plants used on small aerial vehicles. The purpose of this discussion is to familiarize the reader with terminology used to describe power plants. It also provides a quick overview of existing electric and internal combustion engines (ICE's) for small aerial vehicles.

Traditionally, model airplanes have used glow powered ICE's. It is not until recently that electric power has begun to equal or outperform glow powered engines. This is because electric power plants have become much more efficient because of Lithium Polymer batteries and brushless motors. ICE's for model airplanes are usually 2-stroke or 4-stroke. There are Wankel style engines and rotary cylinder 4-strokes, but they are not as common [8] [9].

3.1 Internal Combustion Power Plants

The most common model engine is the 2-stroke engine, an example of which is shown in Figure 3.1. This is because it has a low parts count, high power to weight ratio, and is therefore less expensive in general. There are several references that can be consulted regarding the detailed operation of 2-stroke engines [10]. The basic operation will be summarized next.

The 2-stroke engine has three main moving parts, the crankshaft, piston, and connecting rod. The crankcase holds all the components. Other important parts are the carburetor, muffler, bearings, and glow plug. These will be discussed in further detail

Figure 3.1: Front view of typical model 2-stroke engine.

below. The piston is used to pump the fuel-air charge through the engine. When the piston moves up, it draws a fresh charge of air through the carburetor. As the air is being drawn in, the carburetor adds the proper amount of fuel to the air. As the fuel-air mixture is drawn through the engine, it mixes and becomes more uniform. When the piston reaches the top of its range of travel, top dead center (TDC), the air is no longer allowed to flow into the engine. Now the piston begins to move downward. This compresses the air in the crankcase. As the cylinder continues to move down, the air is compressed more, but eventually ports in the combustion chamber open. These ports are connected to the crankcase and allow the pressurized fuel-air mixture to be forced into the combustion chamber. The piston then moves to bottom dead center (BDC) and begins to move up again. Eventually, the intake ports that were opened are closed because of the piston moving past them. Then, the piston compresses the fuel-air charge until near TDC, where the charge is ignited. The ignited charge then forces the piston down. The piston is connected to the crankshaft by the connecting rod, so the downward force of the piston is transferred to rotary motion in the crankshaft. As the piston is moving down, exhaust ports are opened and these allow the burnt fuel-air mixture to leave the engine. As the burnt gases leave the combustion chamber, they enter a muffler or tuned pipe. The 2-stroke engine is called a 2-stroke because it requires 2 strokes of the piston to complete one cycle of intake, compression, power, and exhaust. The burnt gases tend to leave the combustion chamber with such speed and force that they create a pulse of air that quickly moves to the end of the muffler or tuned pipe. The pulse then reflects off the back of the muffler or tuned pipe and travels back to the exhaust port. The length

of the tuned pipe is tuned so that the reflected pulse arrives back at the exhaust port before the piston has covered it. This increases the pressure in the combustion chamber. As the exhaust ports were uncovered, the intake ports were also uncovered so they are open at the same time. So, the intake charge is coming in at the same time the exhaust is leaving. This creates the potential for some of the intake charge to leave with the exhaust. This can cause a loss in efficiency. The timing of when the ports open and close can be changed to optimize the engine operation, but they are usually still less efficient than 4-strokes with regards to using the fuel energy. Because the crankcase is used to compress the fuel-air charge, it is not usually possible to have a separate oil system in 2-strokes. The oil is therefore mixed with the fuel so that the moving parts are lubricated. This also makes 2-strokes less efficient because they are burning oil and not just fuel.

In model ICE's, the charge is ignited by the use of a glow plug. The glow plug is similar to a spark plug, but the glow plug does not need any external devices to ignite the fuel-air mixture once the engine is running. The glow plug has a platinum coil in it that is initially energized by a 1.5 Volt battery or other voltage source, shown in Figure 3.2(a). The engine is then spun fast enough to start it. Once the engine is running, the voltage source can be removed, and the heat of combustion keeps the coil warm enough to ignite the next fuel-air charge. The operation is similar to a diesel engine, where the compression of the fuel-air mixture ignites the fuel. Some engines have shims between the cylinder head and the crankcase that can alter the timing of the ignition event by changing the compression ratio of the engine. Glow plugs are not as long lasting as spark plugs, however. Figure 3.2(b) shows a used glow plug where some black deposits can be seen. These are byproducts of combustion. Figure 3.2(c) shows a worn out glow plug where the coil is deformed. The engine may still run with a deformed coil, as long as the coil remains attached to the rest of the glow plug. This particular glow plug will not glow when energized, so the engine could not be started. The choice of glow plug is therefore very important to the operation of model ICE's. Glow plugs can be made more robust by making the platinum wire in the coil thicker and shielding the coil from combustion more. This prevents the coil from getting as hot as it would if it were more exposed. This may not allow the engine to idle very well, however. When the engine is idling, there are not as many combustion events per unit time. Therefore, coil may not glow hot enough to ignite the mixture, and the idle RPM may have to be higher to keep the engine running.

(a) Energized Glow Plug (b) Used Glow Plug (c) Worn Out Glow Plug

Figure 3.2: Figures showing energized, used, and worn out glow plugs.

This could make it difficult to land an airplane because the thrust can not be reduced as much as desired. There are glow plugs with a bar across the opening where the coil is. The bar helps the idling performance, but may reduce power output slightly. The choice of glow plug can also affect the timing of the ignition event in the engine which can affect the power output. Glow plug choice is therefore a balance between longevity, idling performance, and power output. The fuel choice will also affect the engine performance, as will be discussed.

Model engine fuel is primarily composed of methyl alcohol, also known as methanol. This is a cool running fuel compared to gasoline, for example. Cool running means that the combustion temperatures are not as high, so the engines can be lighter because less needs to be done to cool them. The fuel also has about 16-20% oil in it. The oil is usually a castor, synthetic, or a blend of castor and synthetic. Most model engine fuel also has nitromethane (nitro) in it. The nitro increases the power output of engines because the nitro has oxygen in it. More fuel can be burned in the combustion chamber for a given volume of fresh air intake because not as much oxygen is needed to burn it. Nitro percentages are anywhere from 10-50 %, but 10-15% is common for model airplane fuel. Because the nitro affects how much fuel-air mixture is burned in the combustion chamber and the intensity of combustion, the glow plug choice may need to be adjusted for different nitro percentages. This is usually only important when using very high nitro percentages, as was used in this project.

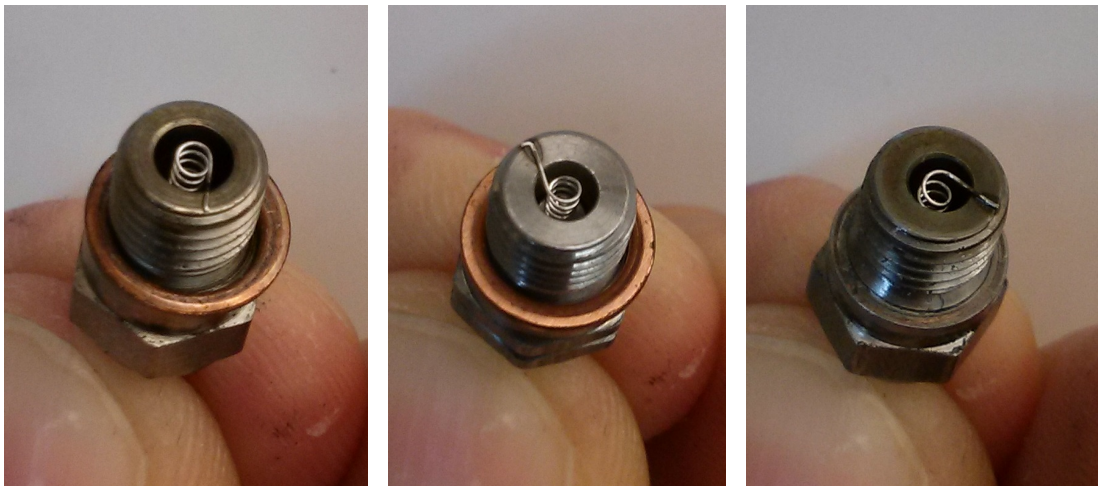

(a) MC-59, Hot (b) MC-8, Medium Cold (c) MC-9, Cold

Figure 3.3: Figures showing McCoy MC-59, MC-8, and MC-9 glow plugs.

Figure 3.3 shows three McCoy RC car type glow plugs. Figure 3.3(a) shows a hot MC-59 glow plug. Hot in this case means that the plug glows hotter or absorbs more of the combustion heat. This is because the hole around the glow plug is larger in comparison to the holes in Figures 3.3(b) and 3.3(c). The coil element is also slightly thinner, but this is not evident from the pictures. The MC-8 glow plug, shown in Figure 3.3(b), is a medium glow plug. This plug is colder than the MC-59. The MC-9 is colder still and is to be used with high nitro percentages and extended high RPM and full throttle settings. The hotter the plug, the better the idle performance will be, as was mentioned. Manufacturers usually list recommended glow plugs and these can be used as a starting point. Hotter or colder plugs can then be experimented with to find the optimum performance in light of idling and power output.

Model engines usually have ball bearing supported crankshafts. Ball bearings reduce the friction in the engine and increase the power output. There are engines that use hydrodynamic bearings, such as the O.S. LA engine series, but these are not as powerful as the equivalent engine with ball bearings [10]. The bearings are lubricated by the oil in the fuel.

Model engines have carburetors on them that change the power output of the engine and control the fuel-air ratio. Figure 3.4(a) shows the side of a typical model 2-stroke engine. Here the throttle lever is seen. The throttle lever can be attached to an RC servo and this will control the power output and RPM of the engine. The throttle lever

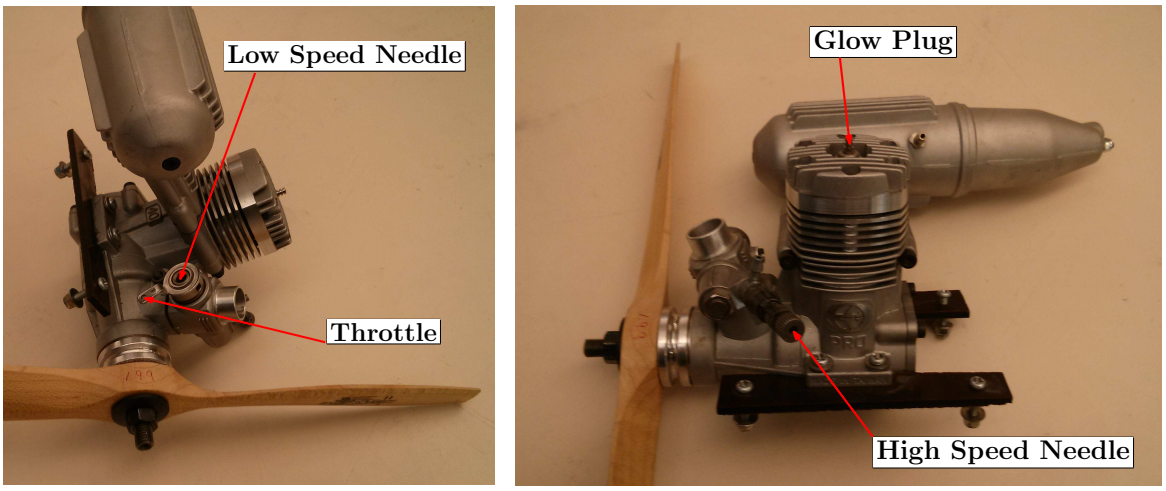

Figure 3.4: Side views of a typical model 2-stroke engine.

will also stop the engine if closed all the way. The ratio of the mixture of fuel and air that the engine is burning will affect how well it runs and the maximum power. There is a low speed needle that controls the low speed mixture. The low speed needle will affect the idle and midrange performance. The high speed needle, shown in Figure 3.4(b), will affect the full throttle performance and the low speed performance. The tuning procedure is usually to set the high speed needle for maximum power and then richen the mixture slightly. Richening the mixture means to turn the mixture screw in a counterclockwise direction unless the needle valve is reverse threaded. Richening the mixture has the effect of injecting more fuel. Leaning the mixture is the opposite of richening. To set the maximum power, the engine is set rich so that it is smoking a fair amount. The extra smoke shows how much extra unburned fuel is leaving the exhaust. Following running the engine rich, the high speed needle is leaned until peak power and RPM is achieved. Then, the mixture is richened about a quarter of a turn, or until the engine is smoking a little extra. The reason for richening the mixture is that the engine will unload slightly when the airplane is flying. This will increase the RPM, and the engine could run lean in the air. If an engine runs lean, it can damage the engine because of lack of lubrication, but usually it results in the engine stopping in flight. It is best to test the engine pointing straight up before flight for this reason, because the engine will have to pull fuel from the fuel tank against gravity, and that will lean out the mixture. There is a port on the muffler that is used to pressurize the fuel tank to help the engine suck in fuel, but pointing the engine or aircraft straight up is still the worst case scenario for the fuel mixture. It never hurts an engine to run

rich, so it is best to run slightly rich at all throttle settings so that the engine does not quit, but not so rich that the engine runs poorly.

After the high speed needle is set, the low speed needle is set. This is done by letting the engine idle for several seconds and then advancing the throttle. If the engine bogs down when the throttle is advanced and there is excessive smoke, the low speed needle is too rich. If the low speed needle is too lean, the engine may quit as the throttle is advanced, and there will be little smoke. If the RPM of the engine slowly increases when the engine is idling, it can mean the mixture is too lean. The engine can also "load up" when it is idling if set too rich. "Loading up" means that excess fuel is pooling in the crankcase. When the throttle is advanced, the engine may bog down and quit because it is abruptly sucking in the unburnt fuel and oil. If the low speed needle is too rich it can sometimes give the symptoms of running too lean, because the engine quits when the throttle is advanced, and it quits before excess smoke is seen. Sometimes if the engine is not running right, it can be best to screw both the high and low speed needles in all the way, and then unscrew them again to the manufacturers recommended starting points. Another issue with the fuel-air mixture is that the needles will need to be readjusted if the propeller size is changed or the weather changes. Usually only the high speed needle needs to be changed once the engine has been tuned well once.

2-stroke engines are usually ringed, ABC, or of the ABL type. ABC cylinder liner construction is an acronym, where A stands for alloy piston, B stands for brass cylinder liner, and C stands for chrome plated cylinder liner. ABL stands for advanced bi-metallic liner and is a more advanced form of the ABC type of construction [8]. Ringed means that the piston has at least one piston ring. The piston ring pushes against the cylinder walls and forms a tight fit to trap the gases being compressed by the piston. ABC type engines do not use piston rings of any kind. They rely on a very tight fit between the piston and the cylinder liner or sleeve. The sleeves are usually tapered so that they are tighter at TDC. When the engine heats up, it expands so that the fit is not as tight. Ringed engines do not develop good compression until they are spun fast, because the compression pressure helps the ring seal against the piston. ABC type engines have good compression immediately but can be prematurely worn out if tuned or broken-in improperly.

Breaking in an engine consists of running it in a prescribed manner where fuel-air

mixtures are rich and the temperature and RPM are relatively low. This is done for several tanks of fuel. In between runs, the engine is allowed to cool completely with the piston at approximately BDC. This is important for ABC type engines because the cylinder sleeve is tapered at the top to account for expansion at higher temperatures. If the engine is cooled with the piston at TDC, it may affect the tightness of the fit. The multiple runs heat cycle the parts and allow them to wear against each other without damaging the engine. This is critical at the top of the sleeve where the fit between the piston and sleeve affects the compression of the engine. If the break-in procedure is not done correctly, the engine can be permanently damaged because the fit between the piston and cylinder liner will be worn out prematurely. The main factors in doing the break-in correctly are getting the engine temperature reasonably high and also having a rich mixture. This causes the tapered fit to expand so it doesn't get worn out, and the extra oil cleans out and protects from any fragments of metal. This can only be done by repeatedly cycling the engine from low to high RPM. As the engine is broken in more and more, the mixture can be leaned out. Many new model airplane engines do not require breaking in on the ground and can be flown in a prescribed manner in the air. Each manufacturer has different procedures, so the instruction manuals have to be consulted for each specific engine.

There are 4-stroke model engines as well. These engines use the familiar Otto cycle, which will be briefly summarized here [10]. Figure 3.5(a) shows a typical model 4-stroke engine. As in the 2-stroke cycle, the piston pulls in a fresh charge of fuel and air. The difference between 2 and 4-stroke engines is that there is a dedicated valve on the top of the cylinder that opens at the proper time to let the fuel-air charge in. The valve is adjusted so that it opens just before the piston begins to move down from TDC. Then when the piston moves down, it sucks in air through the carburetor which adds the proper amount of fuel. The carburetor, shown in Figure 3.5(b), operates the same way as the 2-stroke carburetor. It has a low speed and high speed needle, and a throttle lever. As the piston reaches BDC, the intake valve is closed. The piston then moves up and compresses the fuel-air mixture. At this point, the 4-stroke is operating the same way as the 2-stroke. As the piston reaches TDC, the mixture is ignited by the glow plug. The piston then moves down from the pressure of combustion. This force is transmitted to the crankshaft by the connecting rod the same way as in a 2-stroke. As the piston reaches BDC, the exhaust valve is opened. This starts the blowdown process, where the high pressure in the combustion chamber escapes from

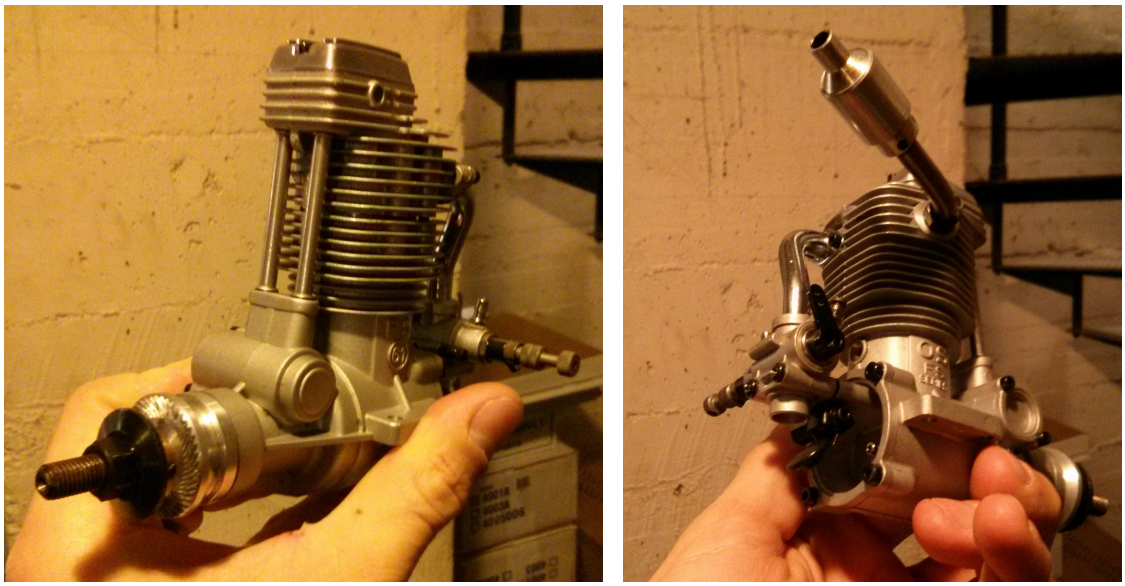

Figure 3.5: Front view (left) and rear view (right) of typical model 4-stroke engine.

the exhaust port. The piston then moves up to TDC with the exhaust valve open, and this forces the remaining products of combustion out the exhaust valve. The exhaust valve is then closed as the intake valve is opened at TDC after the exhaust stroke. The piston then begins moving down again with the intake valve open, and the cycle starts over again. There is a camshaft that spins at half the rotational speed of the crankshaft. This is used to open and close the intake and exhaust valves at the proper time in the pistons travel. The camshaft is contained in the tubular casting, perpendicular to the crankshaft, on the crank case shown in Figure 3.5(a). The valves are actuated by pushrods which the camshaft moves. The pushrod motion is transferred to the valves in the cylinder by small lever arms or tappets. These tappets can usually be adjusted and there should be some clearance between the pushrods and tappets to account for expansion when the engine is running. The tappets and valves are contained in the rectangular structure on the top of the cylinder. 4-strokes do not need a tuned pipe, so a simple muffler can be used instead, shown in Figure 3.5(b). 4-stroke engines usually use a dedicated oil system, but model engines do not. Instead, they use the blow by gases from combustion to lubricate everything below the piston. There is a crank case vent that allows excess oil to leave the crankcase. Model 4-stroke engines can use the same fuel as model 2-stroke engines, but there is fuel available that is just for 4-stroke engines. The difference is usually slightly less oil content. Many prefer high nitro helicopter 2-stroke fuel because higher power is

possible. Basically, almost any model fuel can be used with model 4-stroke engines, but the manufacturer recommendations should be followed. The reason for not having a dedicated oil system is to allow the engine to run well in any orientation. If there was a dedicated oiling system, it may not work properly with the engine upside down because the oil could interfere with the piston motion, and an oil pump would not be able to suck the oil in any orientation. RC pilots need to be able to mount the engine in any orientation because of the aircraft design, and the engine must perform well if the airplane is flown upside down or other aerobatics are performed.

The break-in of 4-stroke model engines is similar to 2-stroke engines. The engines are run rich for several tanks of fuel. Each manufacturer will have a different break-in procedure. The mixtures on the carburetor are set the same way as they are for 2-stroke engines. The only difference in the carburetors is that many 4-stroke engines have a choke to draw in extra fuel for starting. Also, most model 4-stroke engines use piston rings to seal the combustion chamber and use special glow plugs that hold the combustion heat longer to aid the idling performance. 4-stroke engines are usually not as sensitive to glow plug selection as 2-stroke engines are.

There are several differences between model 2 and 4-stroke engines. For the same displacement, a 4 stroke engine can usually use a bigger propeller, but will produce less power. 4-stroke engines will run cleaner and not emit as much smoke and will have a more realistic sound. 4-stroke engines do not need a tuned pipe, but they are taller because of the valves on the cylinder. 4-stroke engines are also more expensive, have more parts to adjust and maintain, and are heavier for the same power. There are very large and impressive multi cylinder 4-stroke engines, however. Some available configurations are flat four, radial, star, or two cylinder horizontally opposed cylinder configurations. 2-stroke engines are generally not available in these multi-cylinder arrangements, except for in two cylinder horizontally opposed configurations. Both 2-stroke and 4-stroke model engines are popular; it will be the cost, application, or personal preference that will determine which kind to use. Recently, many previously glow fueled 2 and 4-stroke engines have become available in gasoline fueled versions. This has the benefit of reducing fuel cost, because a gallon of gasoline is cheaper than a gallon of glow fuel. The gasoline versions use spark plugs, and this requires an ignition unit that usually includes a battery, which adds to the weight of the engine.

Model car engines are only available as 2-strokes. These engines run at incredibly

high RPM compared to model airplane engines and produce much more power for their weight and displacement. The engines are geared to the drive wheels of RC cars and trucks. They also have large cooling heads because of reduced airflow. There are also model boat engines, and these are essentially model car engines with water cooled cylinder heads. There are high RPM ducted fan engines for use in RC model jet airplanes, but these have been mostly replaced by electric motors and model turbojet engines. The ducted fan engines were all 2-stroke high RPM engines and produced high power like the RC car engines. Model car engines operate the same way as airplane engines and use tuned pipes in the same manner. The cooling heads on model car engines can be removed or modified for use on aircraft, as was done in this project. The benefit of model car engines is that they are designed to be geared. The only problem with high RPM engines is that they can't use very large propellers. Small high RPM propellers do not produce much thrust at lower speeds, and this is where most RC airplanes fly. Therefore, RC car engines have not been used in airplanes very much. RC engine distributors seem to highly discourage the use of RC car engines in airplanes as do some manufacturers. The reasoning was that the RC car engines can not hold their tune at a fixed RPM, and they will only last for several gallons of fuel. These claims seem to be false with the exception of longevity, which remains to be tested.

Model engines are usually started by an electric starter that is pushed against the spinner or propeller nut on the front of the crankshaft, shown in Figure 3.6 as the yellow device. RC car engines are usually pull started but can also be started by pushing a rubber disk against the flywheel, shown by the starter to the left of the yellow starter. Figure 3.6 also shows a blue flight box that is commonly used to bring all the equipment to the flying field. The flight box holds the fuel and tools. It also has a battery and power panel to start engines and energize the glow plug. There are two glow drivers shown in Figure 3.6 to the right of the yellow starter. One is battery powered, while the other is connected to the flight box. The battery powered versions are convenient, but many times they run out of battery too early. The glow driver connected to the flight box has the advantage of being able to adjust the current flowing to the glow plug. This can make the coil glow hotter or colder and can help with starting engines.

Another important tool for model engines is a propeller balancer, shown in Figure 3.7. This particular balancer is magnetic, but there are several others available. To

Figure 3.6: Flight box and starting equipment for 2 and 4-stroke model engines.

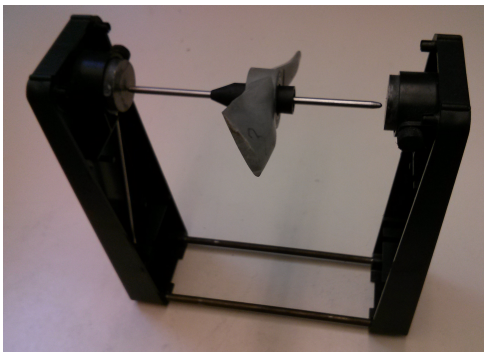

Figure 3.7: Magnetic propeller balancer.

use a propeller balancer, the propeller is installed on the shaft so that it is centered the same way as it would be when mounted to the engine. The propeller should balance so that the propeller blades are horizontal. If not, an x-acto blade can be used to trim away the trailing edge of the propeller blade that is too heavy. Some modelers apply paint or tape to the tips of the propellers to balance them. Tape does not work well on glow or gas powered models because the fuel dissolves the adhesive. It is important to balance the propeller on RC aircraft. If they are not balanced there may be excessive vibration which can damage electronics and the airframe.

3.2 Electric Power Plants

Electric motors are used in many applications and have become very popular in model aircraft. They operate by creating magnetic fields that attract magnets positioned around a shaft, and they switch those magnetic fields to induce rotation in the shaft. The magnetic fields are made by passing a current through coils of wire. There are different designs and configurations depending on the application. A motor with the magnets on the outside of the engine with the coils of wire on the inside, is known as an outrunner in the RC community. These motors are known to produce a lot of torque and therefore do not need a gearbox. A motor with the magnets on the inside and coils of wire on the outside is known as an inrunner. These motors generally run efficiently at high speeds, so a gearbox is needed if spinning a large slow turning propeller is the goal. The outrunner is popular in part because it drives a propeller directly, and it is simpler to install for this reason. Inrunners have the potential to be more efficient but can be more complex because of the gearbox. RC servos use the geared inrunner concept to move a control arm. Servos have many many sets of gears to reduce the high speed of the inrunner motor so that the servo arm can be turned with much greater torque. Electric power plants are becoming more popular in the RC community and also in UAV's because of the simplicity of the systems compared to internal combustion or turbine engine designs. All that needs to be done to fly an electric aircraft is plug in the batteries, turn on all the systems, and fly. There is no fueling, tuning and adjusting, or waiting for the system to warm up. The motors don't stop unless there is catastrophic failure. The only limitation is battery life, but this problem is being solved with solar panels and/or improved battery technology.

There are several considerations that need to be made when making an electric power plant. There are three main parts: the motor, electronic speed control (ESC), and battery. All the components are interrelated in the initial sizing of a power plant. Each component will be discussed, and then conclusions will be made for a complete power plant.

The battery choice is very important to the power and flight time of an electric power plant. The most widely used battery type is lithium polymer (LiPo). There are nickel cadmium (NiCd) and nickel metal hydride (NiMH) batteries as well, but these are not usually used for power plants, only to power servos and RC electronics.

A LiPo battery will usually consist of various cells. Each cell operates in the 3-4.2

voltage range, where 4.2 Volts is fully charged, and 3 Volts is fully discharged. It is extremely important to never charge a LiPo cell over 4.2 Volts, as they can spontaneously ignite if overcharged. Once a LiPo cell is on fire, it cannot be extinguished because the chemicals react mostly with themselves to burn instead of with oxygen. LiPo cells should also never be discharged below 3 Volts when under load. This means that if a motor is using power from the cell, the voltage of the cell should not drop below 3 Volts per cell when in use. Then when the load is removed, the voltage will rise above 3 Volts. The steady un-loaded voltage of a LiPo cell should never drop below 3.2 Volts per cell. If a LiPo cell is discharged below the recommended voltage it will reduce the life of the cell and could cause it too swell. There are different capacity LiPo cells. The capacity of the cell will affect the cells size, but not its voltage. Therefore, a small cell will have the same voltage characteristics as a large cell. The difference will be how long the cell can supply the voltage. Cells are also rated for how many Ampere's (Amps) can be drawn from them, and this is related to the "C" rating. The Amps that can be drawn from a cell is found by multiplying the cell capacity in Amp hours (Ah) by the C rating, shown in Equation 3.1.

$$A(Amps) = Capacity(Ah) \times C = \frac{Capacity(mAh)}{1000} \times C \tag{3.1}$$

Therefore, if a cell has a capacity of 1000 mAh, or 1 Ah, and the C rating is 20, 20 Amps can be drawn from the cell. Most cells have a burst C rating and a continuous C rating. The burst C rating means that the battery can be discharged at a high rate for several seconds, and the continuous C rating denotes the Amps that can be drawn continuously from the battery until the minimum voltage is reached.

To get higher voltages, LiPo cells are wired in series. When a battery or cell of the same capacity are wired in series, the voltage doubles but the capacity remains the same. If a battery or cell of the same capacity is wired in parallel, the capacity will double, but the voltage will remain the same. Battery manufacturers use these two simple facts to make batteries of different size and voltages. It is important to note that the C rating does not change when batteries or cells are wired in series, and it doubles when they are wired in parallel.

To determine how long a cell can supply a certain Amperage, divide the capacity in

Ah by the Amps being drawn from it, shown by Equation 3.2.

$$t(hours) = \frac{Capacity(Ah)}{A(Amps)} = \frac{Capacity(mAh)}{1000 \times A(Amps)} \tag{3.2}$$

For example, if 10 Amps is drawn from a 1000 mAh, or 1 Ah, cell the run time will be $(1Ah)/(10A) = 0.1$ hour or $0.1 \times 60 = 6$ minutes. It is important to realize that the number of cells does not influence how long a particular battery will last. The cell count only affects the voltage supplied. This changes the Watts delivered, given by,

$$W = V_{batt} \times A \tag{3.3}$$

where the V_{batt} denotes the voltage of the battery, A denotes the Amps being drawn from the battery, and W denotes the Watts being produced by the battery.

3.2.1 LiPo Battery Charging

LiPo batteries are charged by taking note of the C rating for charging and the cell count. Most LiPo's can be safely charged at 1 C, but new batteries can be charged significantly faster. The charging Amps can be determined by Equation 3.1. Some chargers will ask for just the battery capacity. These chargers assume a 1 C charge rate. Newer chargers will ask for the C rating and the battery capacity or the charging amps. Chargers have options to choose the number of cells or the voltage of the battery. LiPos are considered to have a nominal voltage of 3.7 Volts per cell. Therefore, if a charger asks for the battery voltage, it will often be based on the nominal voltage. A 3-cell battery will have a nominal voltage of 11.1 volts, for example. It is important to balance the cells when charging as well. As was discussed, the individual cell voltage can not exceed 4.2 Volts. If a battery is charged only by its main leads, it would be possible for one cell to be above 4.2 Volts and another to be below. The overcharged cell will then ignite if over charged too much. Newer chargers have built in balancers that monitor each cells voltage. If a cell is charged more than the others, the charger will discharge the over charged cell as it continues to charge all the cells. The charger will also stop charging the battery if there is too large of a voltage imbalance. There are external balancers, but these can be dangerous if one cell is significantly out of balance from the others because the charger will not stop charging the battery if a cell becomes over charged.

LiPo chargers will charge a battery at the maximum allowable charge C rating until

the individual cell voltages reach 4.2 Volts per cell. At this point, the charger will adjust the current to maintain the battery voltage at 4.2 Volts per cell. Due to this, when a battery is nearly fully charged, the charger will put very little current into it.

Batteries usually have stickers on them that say what the cell count and capacity is. One trick to determine the cell count is to count the wires in the balancing connector. There will be 1 wire for the ground of all the cells. Each additional wire is for each individual cell. For example, if a balance connector has 4 wires, it means the battery is a 3-cell. It is possible to use a voltmeter to see each cell's voltage by connecting it to the balance tab or battery ground and to each cell's positive wire.

The next important component is the electric motor, an example of which is shown in Figure 3.8. Here, a large electric motor is mounted to a 6-axis sting in a wind tunnel. There are DC motors that only need two wires to power them. These kinds of motors

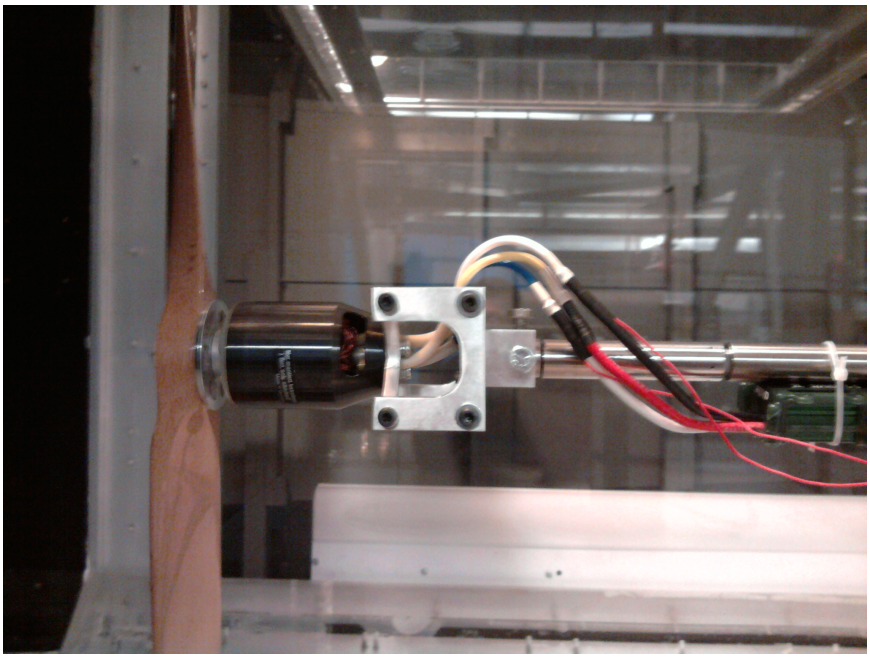

Figure 3.8: Electric motor and speed control mounted in a wind tunnel.

can be connected directly to a battery. These motors often have brushes in them that cause the current to switch in the proper way in order to cause a rotation in the shaft. Most modern RC electric motors are brushless. There are two kinds: inrunner and outrunner, as was discussed. Motors will have a kV rating wich is a measure of how fast the motor will spin for a certain voltage since kV stands for RPM per volt. Lower kV means that the motor will make higher torque and can turn a larger

propeller. High kV motors can be used with high RPM ducted fans or small high RPM propellers. Motors will be rated in terms of the maximum current they can use. They will also be rated for a certain number of cells in a battery. It is the users option as to what capacity battery will be used and how many cells to use, as long as the cell count is within the specified range. Increasing the cell count will increase the power output of the engine, but extra cells are heavier. Generally when less cells are used, larger propellers can be used. If the cell count is increased, a smaller propeller will usually have to be used. Otherwise, the motor will draw too much current. The current draw is checked with an in-line Amp meter, and this will be discussed for the combined power plant.

The next important component is the ESC. The ESC is directly connected to the battery and motor, and it delivers the battery power to the motor. ESCs are rated for the voltage they can receive and the maximum current they can draw. It is best to choose an ESC that has a higher maximum current than the maximum current draw of the motor. This way, the ESC will not overheat or stop from drawing too much current. The ESC has three wires that attach to the motor. The ESC pulses current into these three wires in order to cause the motor to spin. The ESC uses back electromotive force (back EMF) to time the pulses to the motor properly. When the throttle is increased, the ESC simply switches the battery on for longer times as the motor rotates so that each pulse puts more energy into the motor. ESCs for DC motors cannot be used with brushless motors because they only have two wires and do not use back EMF to spin the motor. The ESC is controlled by a pulsed width modulation (PWM) signal that comes from an RC receiver. The RC receiver is controlled by an RC transmitter. There are many such systems available, but the key components are the transmitter, receiver, and servos. The servos are used to move control surfaces on an aircraft, for example. Most ESCs will provide power for the receiver and servos by use of a battery eliminator circuit (BEC) that is part of the ESC. The BEC reduces the main battery voltage to a lower voltage that servos can use, usually in the 4.8-6 Volt range. There are servos that are high voltage that can directly use the voltage from a 2-cell LiPo. These servos do not need a BEC if used with a 2-cell battery. Many high power ESCs do not have a built in BEC, and a separate BEC must be used for the servos. There are many ESCs available, but Castle Creations ESCs are fairly common. These ESCs are programmable from a computer. Castle Creations ESCs allow the rotation of the motor, voltage cutoffs,

amperage limits, battery type, and many other settings to be easily changed. Many of the new Castle Creations ESCs can store data, such as RPM, voltage, Amp draw, throttle setting, ESC temperature, and many other parameters. In this way, the power plant performance can be monitored easily.

Table 3.1 shows suggested power requirements for different types of model aircraft [11]. The suggested way to power models in Table 3.1 is a good starting point. It is possible

Watts per Pound	Performance Desired
50-70	Lightly Loaded Slow Aircraft
70-90	Training and Slow Aircraft
90-110	Mildly Aerobatic
110-130	Highly Aerobatic
130-150	3D Aircraft
150-200+	Extreme 3D aircraft

Table 3.1: This table shows suggested power per pound in model aircraft for a desired performance.

to reduce the watts required if more efficient power plants are designed. Most RC flyers expect very good performance from the power plants. The 3D setups are for airplanes that can hover on the propeller pointing straight up. The highest power airplanes can accelerate very rapidly going straight up. This kind of performance is not needed for the average UAV, however. Most of the time, some trial and error testing is required to find the optimum setup. It would be better to be able to choose an electric power plant without trial and error testing. It is usually best to choose a system that overpowers the airplane. This way, the airplane will fly well, and the throttle settings can be reduced. This project aims to develop a tool that can predict the overall performance of any kind of power plant without having to test every setup.

To choose an electric motor, ESC, and battery, the main things that must be compatible are the voltages and Amps. The ESC must be able to supply the Amps the motor needs without over heating. The battery also needs to be rated to supply those Amps. The motor will be rated for some cell count. Therefore, a battery or batteries must be chosen to meet this cell count. The ESC must then also be able to use the cell count or voltage of the battery. There are many high voltage setups that need special ESCs, so it is important to check the specifications of each component. Basically, the motor, ESC, and battery must be chosen together or at least with the other components in mind because each component affects the others.

Once the motor, ESC, and battery are chosen and installed in an aircraft, the propeller can be sized. The propeller to be used will often be known before hand, but it is important to check the power plant performance to verify the propeller choice. This is accomplished with the use of an in-line Amp meter. To test the Amp draw, the battery is connected to the in-line Amp meter, and the Amp meter is connected to the ESC. The power plant is then run at full throttle while monitoring the Amp draw. The Amp draw must be less than the maximum recommended levels for each component. If the Amp draw is low, a larger propeller or one with more pitch can be used to cause the power plant to use more power. Propellers will be discussed in detail in the following chapter.

A sample power plant sizing will be shown next, based on Table 3.1. As an example, suppose there is an 8 lb aircraft. The aircraft is to be highly aerobatic and needs 110 Watts of power per pound. Therefore, 880 Watts of power are required. If a 3-cell battery is used, the nominal voltage of 3.7 Volts per cell can be assumed. Therefore, $3 \times 3.7 = 11.1$ Volts. $880/11.1 = 79.3$ Amps. If a 4000 mAh battery is used with a 20 C continuous rating, the battery can supply $4 \times 20 = 80$ Amps, so the Amp draw requirement is met. The flight time at 80 Amps will be $4(Ah)/80 = 0.05(h) = 3\ minutes$. This may seem like a short flight time, but many aircraft fly at a quarter to half throttle most of the time. A 10 minute flight time could perhaps be expected for this setup. If longer flight times are required, two batteries can be wired in parallel, and this will double the flight time. The batteries can be wired in parallel as many times as needed to extend the flight time. Another option would be to use a battery with a larger capacity. If a larger cell count is used, the Amp draw will be less because the voltage will be higher. If a 4-cell battery is used, the Amp draw will be 59.5 Amps. With the same 4000 mAh capacity, the flight time will be 4 minutes. The flight time increase is therefore minimal. This brief example shows that there are compromises to be made in choosing the motor, ESC, and battery. The flight time, power required, and power plant weight are all factors that must be considered. Lastly, it is not recommended to mix batteries of different cell count or capacity when wiring them in series or in parallel.

The goal of this project is to develop a tool that will predict the power plant performance in terms of the thrust produced, not the input Watts to the motor. There will be a significant loss in power as it passes from the battery and produces shaft horsepower on the output shaft of the electric motor. There will be a further loss in

efficiency as the shaft power is converted into thrust by use of a propeller. A more sophisticated analysis will be required to predict the thrust vs. velocity performance.

Chapter 4

Modeling Power Plant Performance

4.1 Theory

The most advanced method developed to estimate propeller performance is based on vortex lattice models [12]. This method is similar to a lifting surface model of a finite wing. There are other similar methods that use a combined blade element-momentum theory that are not as accurate but are simpler to calculate. The vortex method requires a significant amount of computing power, and with improved computers can compute predictions quickly. The vortex theory takes into account the induced velocities due to the propeller and is thus more accurate than other methods.

4.1.1 Vortex Propeller Theory

This project uses the method described in reference [13] in implementing the vortex equations into MATLAB® code. This code can accurately calculate the useful data for any propeller given that the parameters for the airfoils used are specified at all of the operating conditions. The code described in this paper is further improved because it calculates the data for many propellers and takes into account scaling effects depending on the size of the propeller, the operating condition, and induced velocity effects. The combined code is called Vortex Propeller code, or VP code.

The VP code first needs non-dimensional propeller geometry calculated from the

quantities shown in Figure 4.1. The chord, c, thickness, h, and pitch are found by measuring the propeller at a radial station, r. These measurements are conducted at small intervals from the center of the propeller to the tip, but the values could be arbitrarily specified if a new design is being evaluated.

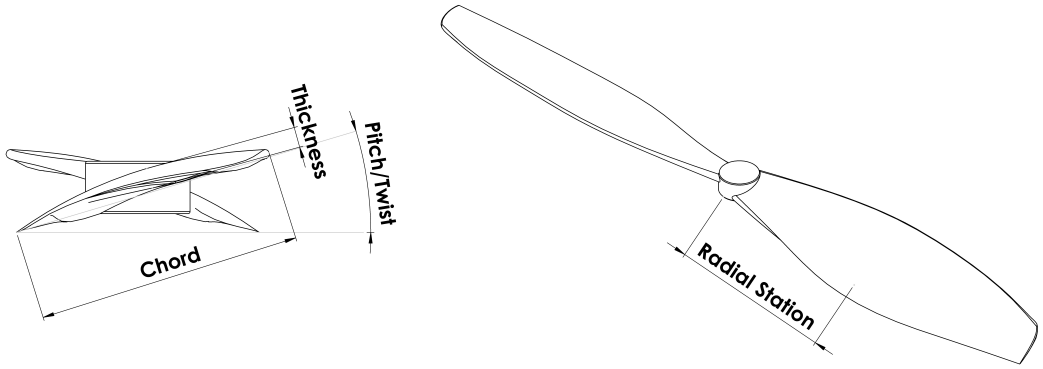

Figure 4.1: Chord, thickness, and pitch at a radial station.

After the propeller dimensions from Figure 4.1 are known, they are non-dimensionalized. The non-dimensional radial position, x, is found by,

$$x = \frac{r}{R} \tag{4.1}$$

where the radial station is r and the radius at the tip of the propeller is R. The non-dimensional chord to diameter ratio, c_D, is defined by,

$$c_D = \frac{c}{D} \tag{4.2}$$

where the station chord, c, is divided by the propeller diameter, D. The non-dimensional thickness to chord ratio, h_c, is,

$$h_c = \frac{h}{c} \tag{4.3}$$

where the thickness of the blade section, h, is divided by the section chord, c. The pitch or twist of the propeller is usually specified in degrees and is not non-dimensionalized. Propellers are generally labeled by their diameter, D, and pitch in degrees specified at $0.75r$. So a 26 by 16 propeller has a 26 inch diameter and 16

degree pitch three quarters of the way out from the axis of rotation.

At each non-dimensional radial station, x, the propeller has a certain shape or airfoil section, shown in Figure 4.3. This shape will determine how much differential upwards lift, dL, is made at each radial station, x, depending on the angle, α, that it is inclined to the relative incoming flow, shown as the vector V_E in Figure 4.3. If an airfoil at a particular station is making lift, in general it must make some differential drag, dD. How much lift or drag is made are characteristics of the airfoil and depend on the Reynolds number, Re, given by,

$$Re = \frac{\rho\, V x_{RE}}{\mu} \tag{4.4}$$

where ρ is the density of the fluid that the airfoil is passing through, V is the velocity of the fluid passing over the airfoil, x_{RE} is the characteristic length which in the case of the propeller or wing is the chord, c. μ is the absolute viscosity coefficient. It varies with temperature but can be assumed to be $1.7894 \times 10^5 kg/(m)(s)$ corresponding to standard sea level conditions. Airfoils perform differently depending on the Reynolds number, which varies largely due to velocity or characteristic length changes as seen from Equation 4.4. To evaluate an airfoil, its lift and drag performance is non-dimensionalized into the lift and drag coefficients $C\ell$, and Cd, respectively by,

$$C\ell = \frac{L}{1/2\rho\, V^2 S} \tag{4.5}$$

$$Cd = \frac{D}{1/2\rho\, V^2 S} \tag{4.6}$$

where L is the lift, D is the drag, ρ is the air density, V is the velocity of the air moving towards the airfoil, and S is the area of the specimen being tested. An example of how the Reynolds number effects airfoil performance is shown in Figure 4.2. It is clear from Figure 4.2(a) that the lower Reynolds number flow produces poor performance of the Clark Y airfoil above 10 degrees of angle of attack because the airfoil has stalled and the flow across the top of the airfoil has separated. The airfoil also achieves lower lift coefficients, $C\ell$, for the same angle of attack and produces far more drag in the linear range below 10 degrees angle of attack at a Reynolds number of 60,000 compared to a Reynolds number of 400,000. This airfoil is representative

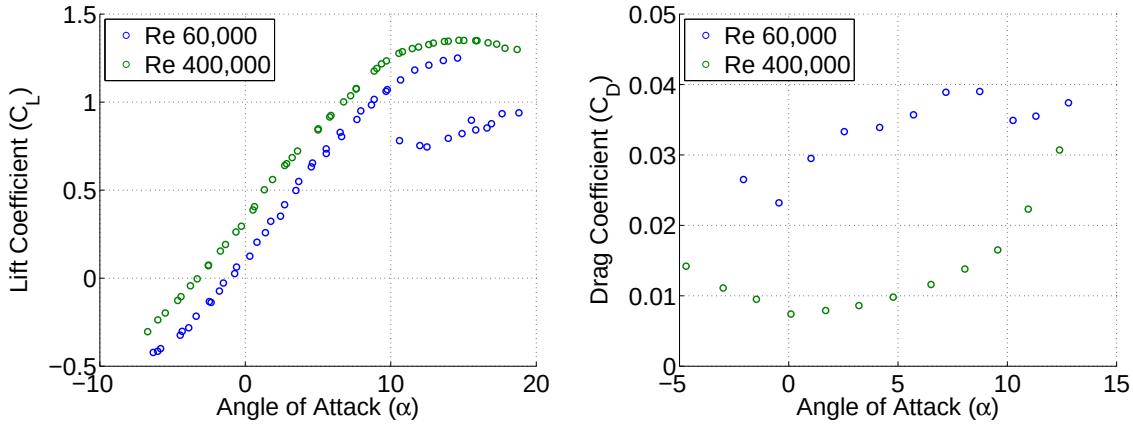

(a) C_L vs. α (b) C_D vs. α

Figure 4.2: Clark Y airfoil performance at Re = 60,000 and 400,000.

of a large number of wooden propellers used both for model and large aircraft. This type of performance change in the airfoil will occur on a propeller because the width of the propeller and velocity due to rotation at each radial station will change the Reynolds number.

Figure 4.2(a) also shows hysteresis effects for a Reynolds Number of 60,000. When the angle of attack is increased, the lift coefficient increases to its highest value, about 1.25 (shown in blue). It then quickly drops to about 0.9 and stays there as the angle of attack is increased. When the angle of attack is then decreased, the lift coefficient stays at about 0.8-0.9 until it jumps back up to the original curve at an angle of attack of about 10 degrees. This type of behavior makes it difficult to predict airfoil performance when the airfoil is stalled. Stall often occurs when the propeller is traveling through the air slowly or during static conditions, such as during takeoff. For this project, the linear range of the lift curve is approximated by a straight line with a slope, a. The stall region of the lift curve is approximated by a second-order polynomial. The drag coefficient curve is in general approximated by a second order polynomial, but for lower Reynolds numbers a higher order would more be accurate. When calculations are performed involving the angle of attack and lift coefficients, the VP code is written such that it will choose the proper slope depending on the Reynolds number, and then it will choose the linear region or stall region depending on the angle of attack. The VP code also chooses the proper slope for the drag coefficient curve depending on the Reynolds number. In this way, each radial station, x, will be analyzed with proper airfoil data.

Using the the forward velocity, V, and the rotational velocity, $\omega_{rot}r$, the relative velocity that the propeller at a radial station, x, sees is the vector V_R at an angle ϕ, shown in Figure 4.3. As the propeller turns it will cause a rotating induced velocity, ω, at an angle α_i, which can be decomposed into an axial component, ω_a, and a tangential component, ω_t. When the forward velocity, V, the rotational velocity, $\omega_{rot}r$, and the induced velocity, ω, are added together vectorially, the resulting incoming velocity is the vector V_E.

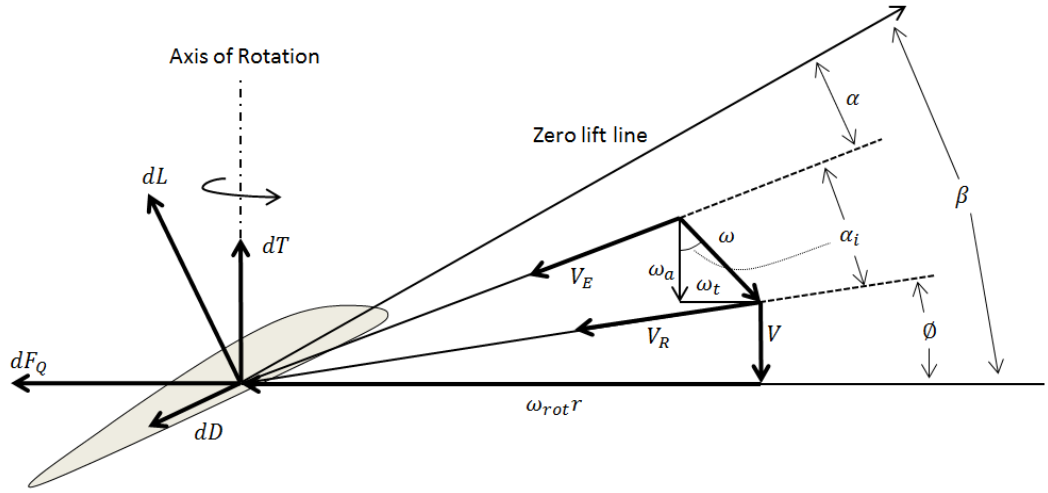

Figure 4.3: Forces and velocities acting on a blade section at radius r.

From a basic understanding of Figure 4.3, some limitations of propellers can be seen. If a given power, P, is to be absorbed by a propeller at a given velocity, V, a larger propeller will do it by accelerating a large mass of air a small amount, whereas a small propeller will have to move a small mass of air very fast. Therefore, the smaller propeller will generate a larger induced velocity, ω, reducing the velocity of incoming air, V_E, by approximately $\omega \sin(\alpha_i)$ and will reduce the effective angle of attack, α. So the smaller propeller will need larger built-in twist, β, to get sufficient angle of attack, α, to make differential lift, dL. As the built-in twist, β, is increased, the lift vector, dL is tilted farther from the direction of thrust, dT, making it less efficient as the component of lift producing thrust is reduced by $\cos(\beta)$. Even if the induced velocity, ω, is minimized by using a larger propeller, increasing forward velocity, V, will cause the effective angle of attack, α, to be reduced until no thrust, T, is produced. This can be compensated for by twisting the propeller more, but this will reduce the thrust at lower speeds. Also evident is that increasing the rotational speed will increase the

effective angle of attack, but this can only be done until the tip velocity approaches the speed of sound, given by,

$$a = \sqrt{\gamma RT} \tag{4.7}$$

where the heat capacity, γ, equals 1.4 for air, the gas constant, R, equals 287 J/kgK for air, and T is the temperature in degrees K. When the tip velocity, V_{Etip}, approaches the speed of sound, a, the tip Mach number, M_{tip}, given by,

$$M_{tip} = \frac{V_{Etip}}{a} \tag{4.8}$$

approaches one. Shock waves will be produced anywhere the local Mach number is equal to or greater than 1, and this will occur generally on the top of airfoils because the local velocity is greatest due to the curvature of the airfoil [14]. On small RC model aircraft, the tip velocity must be kept below about $M_{tip} = 0.75$ to reduce tip noise and inefficiencies from shock waves. Large propeller driven aircraft sometimes operate with tip Mach numbers near one but are very loud because of this. It is assumed that the $M_{tip} = 0.75$ constraint must be satisfied for any propeller/engine combination and shows that a larger propeller must turn at slower RPM compared with smaller propellers because $\omega_{rot}r$ is the dominant velocity in Figure 4.3.

As is common in aerospace engineering, the propeller performance is non-dimensionalized so that the results can be used for many different propellers. All useful RPM and expected velocities of the propeller must be characterized. These can be non-dimensionalized into the advance ratio, J,

$$J = \frac{V}{nD} \tag{4.9}$$

where n is the RPM converted into revolutions per second (RPS), and D is the diameter of the propeller. The thrust produced and power absorbed is non-dimensionalized into the thrust coefficient, C_T, and power coefficient, C_P,

$$C_T = \frac{T}{\rho\ n^2 D^4} \tag{4.10}$$

$$C_P = \frac{P_{req}}{\rho\ n^3 D^5} \tag{4.11}$$

where T is the thrust, P_{req} is the power absorbed or power required, ρ is the air density, n is the rotational speed in RPS, and D is the propeller diameter. The efficiency is then defined as,

$$\eta = \frac{C_T J}{C_P} \tag{4.12}$$

where the thrust and power coefficients, C_T and C_P, corresponding to a certain advance ratio, J, are used.

To summarize, the VP code uses the non-dimensional propeller geometry, Reynolds number dependent airfoil performance data at each radial station, and the expected RPM and forward velocity to produce thrust and power coefficient data. The Reynolds number at each radial station and tip Mach number are also calculated for each combination of RPM and velocity. The thrust produced, T, and power required, P_{req}, are found for each combination of RPM and velocity using Equations 4.10 and 4.11. These data describe the useful parameters for a propeller.

4.1.2 Experimental Propeller Data

It is also possible to gather real data for the propellers of interest instead of predicting the propeller performance using the VP code. To gather the same data as produced from the VP code will require that the propeller(s) of interest be tested in a wind tunnel or with another suitable testing device. The propeller will have to be moved through the air at the range of velocities for which it will be used. At each velocity, the propeller will have to be run at a range of RPMs, and the torques and power required for that particular RPM and velocity will have to be recorded. This data will be more accurate than that predicted using the vortex code and can be used for more accurate combined power plant performance predictions. The following example analysis, however, uses the VP code to make power plant performance predictions, though the procedure is exactly the same if real data is used for the propeller.

4.1.3 Theory of Combining a Propeller and Power Source

The different powers shown in Figure 4.4 are now defined. P_{output} is the power that is available directly on the output shaft of a power source. If the engine is geared, there may be some loss of power through the gearing, denoted by P_{lost}. The power available after gearing is denoted by P_{input} where $P_{input} = P_{output} - P_{lost}$. It will

always be assumed that the propeller is driven by the input power, P_{input}, and that the propeller absorbs this power to create thrust. Therefore, $P_{absorbed}$ will denote the power that the propeller is using to create thrust. If there is no gearing, it can be assumed that there is a 1:1 gear reduction that is 100% efficient, so that the output power of the engine equals the input power of the propeller, ($P_{output} = P_{input}$). After the propeller has absorbed the input power, it will create useful power, P_{useful}, that the aircraft the engine is mounted to will use. This useful power can also be thought of as the useful thrust of the power plant, T_{useful}.

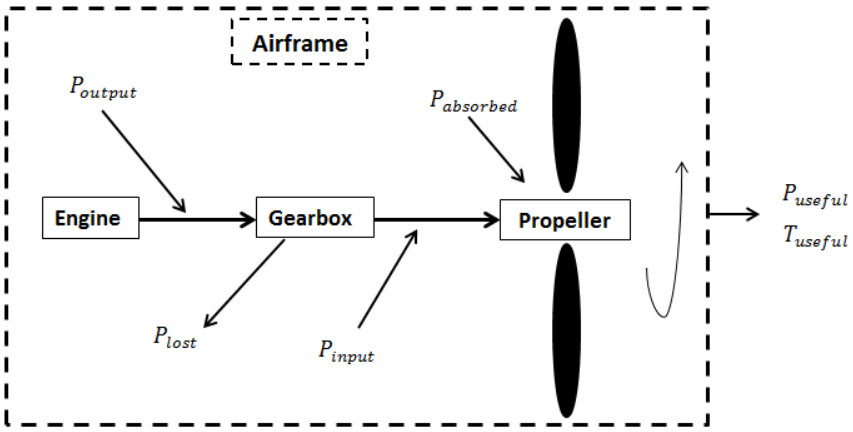

Figure 4.4: Flow of power through a power plant.

Fundamentally, for any system to reach a steady state condition, the inputs must equal the outputs. This is the first assumption that is made about the power source's output torque and power and the propellers absorbed torque and power. This is shown in Figure 4.4. The power source can be an electric motor, an internal combustion engine, or anything that can spin a shaft. Most power sources can spin an output shaft at varying RPM, and they will likely produce different torque and power characteristics. Therefore, any load can be applied to the power source that absorbs the power at the RPM of the power source. Matching the RPM of the power source and RPM of the load is the governing constraint on the system. For an ICE, it may be desirable to run the engine at high RPM because ICEs make the most torque and power at high RPM. If a load in the form of a propeller is to be put on an engine, it must absorb the power output of the engine at the engine RPM. This means a small propeller must be used because only small propellers absorb power at high RPM. This is the reason direct drive high RPM engines are not very efficient in aircraft applications, though they can fly fast and are simple. If only the power output of the engine (or

power input from a gearbox) and the power absorbed by the propeller must match, steady state could be reached, but the RPM of the engine and propeller would not be the same. Therefore, gearing is used to convert the RPM of the engine to the desired RPM of the propeller or vice versa. The gear reduction will introduce a slight inefficiency of about 15% depending on the gear sizes and lubrication, but will be more than offset by the available combinations of engine and propeller. This will allow for the selection of any engine or power source as long as it can be made to drive the propeller through some kind of gear mechanism.

An example of the benefit of gearing is the LRP ZR 0.3 cubic inch RC car engine. It was found to produce about 2.25 HP at 28,000 RPM and weighs only 350 grams, not including the muffler and gear reduction parts. A similarly sized direct drive RC airplane engine such as the O.S. 0.65 cubic inch 65AX produces 1.73 HP at 16,000 RPM and weighs 497 grams without a muffler. This comparison is not entirely fair as the RC airplane engine is designed for long life and extended full throttle operation, while the RC car engine is designed for bursts of power at full throttle. The engines are also different with regards to the air cooling arrangement. However, the RC car engine could be modified to power an aircraft and would provide much improved performance for its weight. Because RC airplane engines are in general direct drive, they have been made such that they produce power at an RPM that a propeller could absorb. The following Engine Propeller Matching code (EPM) allows the designer to choose the optimum motor or engine, run it at its best RPM with regards to fuel efficiency or power, and match it to the optimum propeller for the aircraft being designed.

The ideal implementation of the EPM code would be to have power vs. RPM data for all power sources that are of interest. Manufacturers do not generally provide this data; they only usually provide the maximum power and RPM, which makes it difficult to estimate the power curve. Accurate power plant performance predictions require that the power sources that could potentially be used be tested to give the power vs. RPM curve for each power source.

Generally, this could be done by mounting the power source to a bearing that will allow it to rotate around the same axis as the output shaft, putting a load on the power source at various RPM, and measuring the RPM and reaction torque using an arm attached to the swiveling power source. The horsepower, HP, produced is found

using,

$$HP = \tau_b(2\pi n) \tag{4.13}$$

where τ_b is the brake torque in pound-feet and n is the revolutions per second. Most engines are given horsepower ratings, so Equation 4.13 is preferable, but the American units can be converted into Watts for calculations. However, there are many ways to find the power curve such as using a water brake, generator, or eddy-current absorber; all of which are known as dynamometers. All of the aforementioned methods use Equation 4.13 in some form to calculate the power curve. An approximate curve with the peak power and RPM can also be created for each engine of interest. Once the power curves are found, a strategy must be used to choose the desired operating RPM of the engine. The goal could be maximum power, fuel efficiency, minimal engine wear, heat rejection, etc., but an RPM will need to be chosen corresponding to the desired engine operating condition. Because the engine will be used in an airplane, one must also have knowledge of what the airplane is being designed for. This project assumes that fixed pitch propellers will be used. This means that the power plant can only be optimized for one velocity because of having to compromise between low speed and high speed performance as described in Section 4.1 4.1.1. Good performance can be still be found at slow and fast speeds, but choosing the optimization velocity, V_{OPT} is essential to being able to find the gear ratio, as will be shown.

The engine power curve has the same units and axes as the power curves for the propeller. This will allow the engine's power curve (P_{output} vs. RPM) to be plotted with the propeller's power absorbed, ($P_{absorbed}$ vs. RPM) curves. Figure 4.5(a) shows a hypothetical engine curve similar to an RC car engine and a TopFlite 24 inch by 10° pitch propeller power absorbed curve at a velocity of 13.1 m/sec (about 30 miles/hour), without any gear reduction. This engine power output curve is assumed to be the power produced at full throttle at the RPMs shown. The propeller power absorbed curve shows what is expected for a propeller. If a propeller is moving through the air at a given velocity and RPM, it will require power to spin at that RPM. As the RPM is increased, the propeller absorbs the increased power, though there is a non-linear increase in power absorbed for a linear increase in RPM.

It is convenient to convert all units to metric for calculations; this is the reason the engine power output data is in Watts. This hypothetical engine produces a maximum

power of about 3.5 HP at 22,000 RPM, which is about 2615 Watts. The RPM range between 3,000 and 33,000 RPM is realistic for an RC car engine. The lower limit of 3,000 RPM represents the fact that the engine could only idle at that speed.

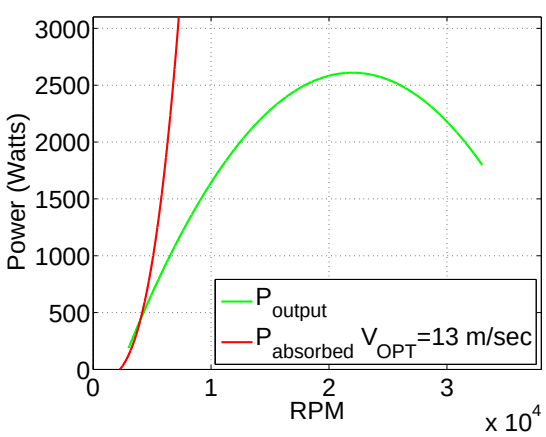

(a) Power available from the engine and power required by the propeller at a velocity of 13.1 m/sec.

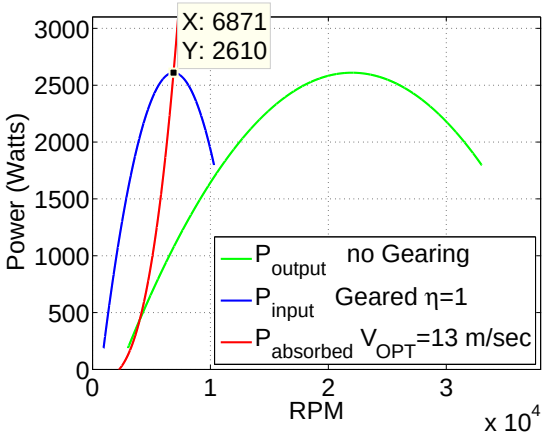

(b) Power available from the engine and power required by the propeller at a velocity of 13.1 m/sec, with gear reduction. The steady state operating RPM and power is 6871 RPM and 2610 Watts respectively.

Figure 4.5: Figures showing the effect of adding gear reduction to the system.

If the power output of the engine can equal the power absorbed of the propeller, it will be marked by the intersection of the engine power output curve and the propeller power absorbed curve. Figure 4.5(a) shows that there is basically no way that the power output of the engine could equal the power absorbed of the propeller, except for at about 4000 RPM. This means that if the propeller was mounted to the engine without gearing, and run at full throttle, it would reach a steady state RPM of about 4000 RPM at a flight velocity of 13.1 m/sec. If the engine power output curve can be moved so that the maximum power of the engine intersects the power absorbed by the propeller, shown in Figure 4.5(b), the system will be optimized for maximum power, and the result should be maximum thrust at the optimization velocity chosen. At this point, the engine power output has been converted to be the power input to the propeller, shown in Figure 4.4, though ($P_{output} = P_{input}$) because 100% efficiency is assumed through the gearbox. Any engine operating condition can be chosen, but for simplicity the goal in this example will be to extract maximum power from the engine at the chosen optimization velocity. In practice, it is best to optimize the power plant over a range of velocities and choose the best overall performance, but

the analysis will continue as if 13.1 m/sec is the ideal velocity for optimization.

To optimize the system, the engine power output curve, P_{output}, is searched to find its maximum power output and the corresponding RPM, RPM_{eng}, which is 2610 Watts and 22,000 RPM respectively. Next, the propeller power absorbed curve, $P_{absorbed}$, shown in Figure 4.5(a) and Figure 4.5(b), is searched to find the RPM of the propeller, RPM_{prop}, when its power absorbed matches the available maximum power output of the engine. Figure 4.5(b) shows that the maximum power output of the engine equals the power absorbed of the propeller at 2610 Watts and a propeller RPM of 6871. This RPM_{prop} for the propeller is then used to find the thrust produced at that velocity, shown in Figure 4.6.

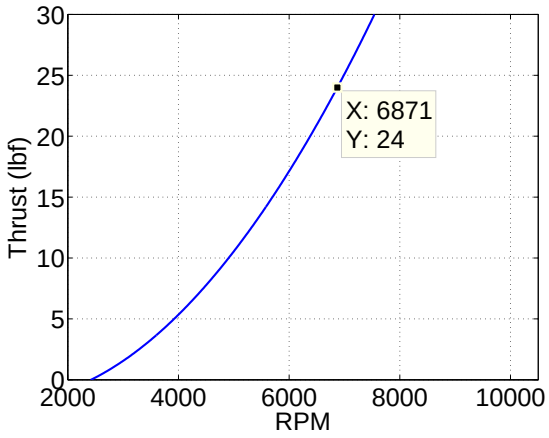

Figure 4.6: Thrust vs. RPM at a velocity of 13.1 m/sec. 24 lbf of thrust is produced at 6871 RPM.

Next, the RPM of the propeller, RPM_{prop}, is divided by the RPM of the engine, RPM_{eng},

$$G = \frac{RPM_{eng}}{RPM_{prop}} \tag{4.14}$$

and this produces the correct gear ratio, G, 3.2019:1 in this case. An important consideration is that gears will only have an integer number of teeth, so the available gear ratios are not infinite. Once the power plant analysis is complete, research must be conducted as to what gear ratios are available. The available gear ratios must then be used instead of the optimization velocity, and the analysis can then be completed for each gear ratio to see which is best. The optimization velocity was only used to force one of the power absorbed curves to intersect the power input curve at some

desired RPM. If the gear ratio is specified, then the intersection of the power input curve with the power absorbed curves may not be ideal, but it will be close to ideal assuming the original gear ratio is close to the available gear ratios. Once the gear ratio is chosen, the engine RPM, RPM_{eng}, which corresponds to the power output of the engine, P_{output}, can be divided by G to convert the engine RPM into the propeller RPM, shown by Figure 4.5(b) (it is assumed that the gearing is 100% efficient). Now the power output of the engine will equal the power input to the propeller, but the RPMs have changed.

It is clear from Figure 4.5(b) that the gear reduction has dramatically narrowed the engines power curve. In practice, it has proven more effective to move the propeller's power curves by varying the pitch of the propeller. However, variable pitch propellers may be overly complex and unnecessary for the average UAV or model airplane since these aircraft will usually be optimized for one task, and therefore one operating condition.

Once the gear ratio is chosen, the procedure for finding the power, RPM, thrust, and torque vs. velocity can be summarized by the following steps:

1. Find the intersection of the power absorbed curve with the power input curve. The intersection gives the steady state RPM that the system will operate at for some particular velocity.
2. Optional: Take the RPM and Power intersection found at that particular velocity and calculate the torque produced using Equation 4.13.
3. Take the RPM found and find the thrust produced at that particular velocity at that RPM.
4. Save and plot the power intersection found, RPM at the power intersection, torque and thrust at the RPM, all at some velocity.
5. Repeat for all velocities.

Now, the engine power input curve can be plotted with all of the power absorbed curves for the propeller. There is interesting behavior of the movement of these curves with forward velocity, shown in Figure 4.7(a). Starting at zero velocity, the curves move to the left, until about 6 m/sec, and then they move to the right with

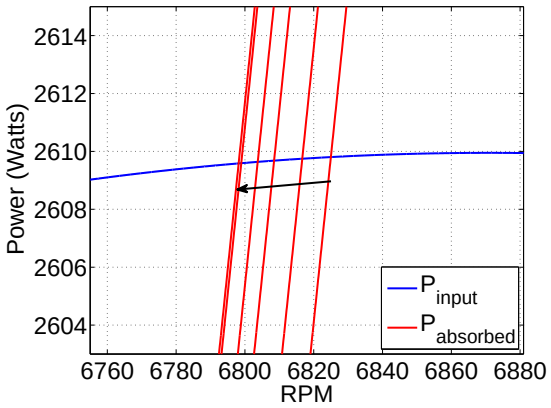

(a) Movement of power required curves with increasing velocity from zero to 6.1 m/sec.

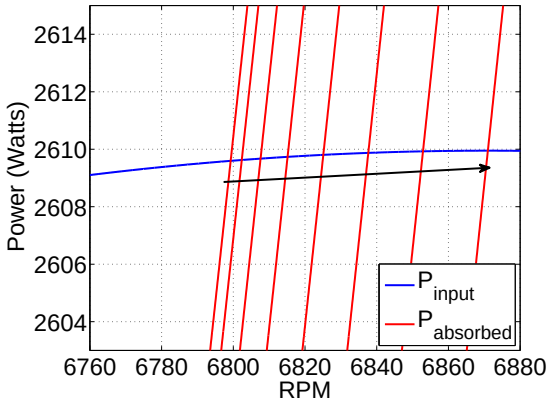

(b) Movement of power required curves with increasing velocity from 6.1 to 13.1 m/sec.

Figure 4.7: Figures showing the movement of the power required curves with increasing velocity.

increasing velocity, shown in Figure 4.7(b) and 4.8(a). These trends help the low speed performance of the power plant because the power absorbed curves for the propeller do not immediately move to the right. The geared engine's power input curve has a negative parabolic shape, though it could be a different shape. For the engine curve shown, it is desired to stay at the peak power output of the engine. If the RPM of the engine is increased from the RPM of peak power, the engine will produce less power. As described, the intersection of the engine's geared power input curve with the propeller power absorbed curves denotes the steady state operating point. If these intersections happen at higher RPM than the RPM of the engine at peak power, it will mean the engine is producing less power. It would be possible to place the peak of the engine power curve such that higher RPM, and thus higher power, is reached at higher velocities. This could be done with the engine power curve shown in Figure 4.5(b) by gearing the engine such that the intersection of the power input curve intersects the propeller power absorbed curve for 13.1 m/sec at a lower ungeared engine RPM. This basically means that the gear ratio would be smaller than 3.2:1, and the intersection of the power absorbed curve for 13.1 m/sec with the power input curve would happen on the steep part of the power input curve closest to the origin. Thus, as the velocity is increased, the power intersections would move up the engine power curve. More power would be produced as the velocity is increased until the intersections come to the peak of the power input curve, and increasing velocity further would cause the power to decrease again as the RPM is increased. In this

case, the propeller power absorbed curves basically traverse the peak of the engine power input curve twice. This means that the engine will be allowed to develop near maximum power at static conditions because the power is being absorbed by the propeller near the RPM where the engine develops maximum power. Because of the movement of the power absorbed curves, the engine will produce maximum power at the optimization velocity and slightly higher and lower velocities. Since maximum power from the engine is being absorbed, it can be seen that this will result in the maximum thrust produced at those velocities. This is apparent from Figure 4.6, which shows that higher RPM of the propeller produces more thrust, and higher RPM can only be achieved by absorbing more power, shown by Figure 4.5(b). The choice of the gear ratio then depends on what kind of performance is desired. However, choosing an optimization velocity and using fixed pitch propellers may not be a great limitation in relatively low speed flight because of these trends. Clearly, if high speed flight is required, smaller gear ratios can be used, but the engine will not be able to develop maximum power until those higher flight velocities because it can not develop maximum power until its RPMs are increased. So there is a trade off between low speed performance and relatively fast performance. Figure 4.8(a), for example, shows many propeller power absorbed curves. The farthest to the right corresponds to a flight velocity of 54m/sec (120 miles/hour). If this power absorbed curve was chosen to optimize the power plant, it is clear that the engine wouldn't produce maximum power until those faster speeds are reached because most of the power absorbed curves would be on the left side of the peak at lower power values. One hundred twenty miles/hour isn't considered very fast relative to many large propeller driven aircraft. If even faster speeds are desired, the low speed performance will be sacrificed even more. It is interesting that the trade off is not necessarily a design flaw of the propeller or engine. It is simply the movement of the power intersections that causes the power, and thus the thrust, to be reduced at either low or high velocities depending on the optimization velocity or gear ratio.

It is also of interest to note that the propeller can capture power, as shown in Figure 4.8(a) by the negative values of the power required curves. This could be used to capture power on a descent, for example, in a hybrid style power plant. Most aircraft use flaps, spoilers, landing gear, air brakes, etc., to produce drag to slow down in a descent. It may be possible to use the propeller instead. However, this could only be done effectively at higher velocities, shown by the trends in Figure 4.8(a),

so there would be some limitations to this idea. Another problem is that for the propeller to capture power, the angles of attack must be generally negative, and the lift coefficient and drag coefficients used in the VP code were not accurately approximated for negative angles of attack, nor did they account for a negative stall region at negative angles of attack. If actual propeller data is used, additional testing of the propeller would be required so that it produces drag in addition to thrust at the range of RPM and velocities of interest.

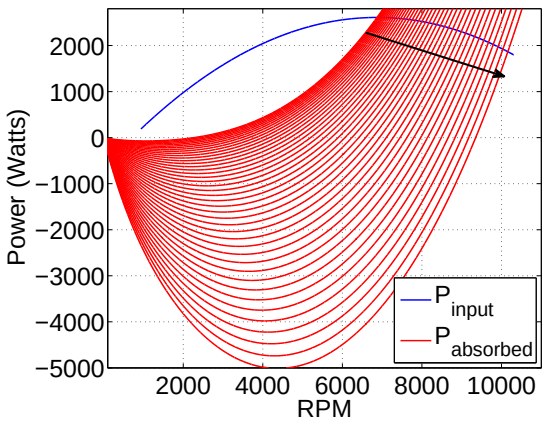

(a) Movement of power required curves with increasing velocity from 13.1 - 54 m/sec

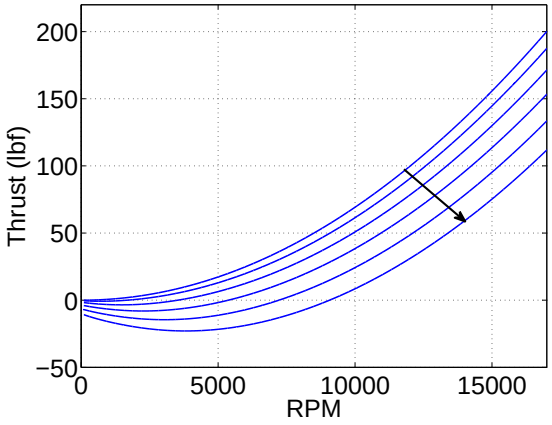

(b) Thrust (lbf) vs. propeller RPM for Velocity of 1, 10, 20, 30, 40, 50 m/sec from top to bottom.

Figure 4.8: Figures showing the movement of the power required and thrust vs. RPM with increasing velocity.

The thrust vs. RPM curves at each velocity are shown in Figure 4.8(b), and the curve shown in Figure 4.6 could be plotted in Figure 4.8(b). A sampling of curves is shown at every 10 m/sec, but in general, the curves shift down and to the right less when the velocity is near zero. As the velocity is increased, the thrust produced vs. RPM curves shift down more rapidly. The behavior of the thrust curves means that as velocity is increased, less thrust is produced for a given RPM. One could for example require that constant thrust would be produced across the flight envelope. To achieve this, the RPM would have to be increased in a non-linear fashion. This can be seen by looking at where each thrust vs. RPM curve produces 50 pounds of thrust. Because the thrust vs. RPM curves are moving down and to the right, it can be seen that non-linear increases in RPM will be required to continue producing 50 pounds of thrust as the velocity is increased linearly.

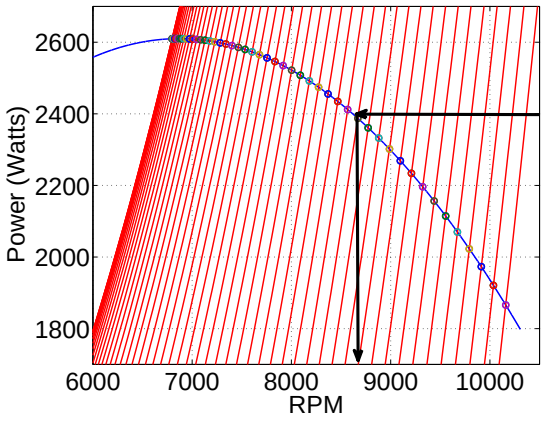

(a) Intersections found using the error function.

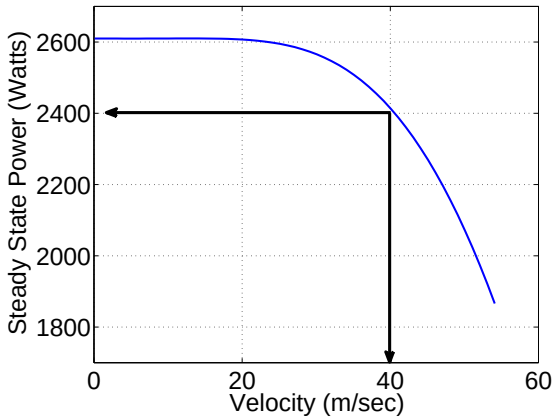

(b) Operating power stored from the intersections and corresponding velocity.

Figure 4.9: Figures showing how the error function was used to find the intersections of the curves and plotting those intersections vs. velocity

To find the thrust at each velocity, the intersection of the power input curve with each power absorbed curve needs to be found, shown in Figures 4.7(a), 4.7(b), 4.8(a), and 4.9(a). This is implemented by using an error function and is the same procedure as described above. The gear ratio, G, was used to divide the engine RPM, meaning that the power input and power absorbed y-coordinates could be plotted against the same x-coordinates. This way, a single x-coordinate corresponds to y-coordinates from either the power input or power absorbed curves. The error function is implemented by subtracting each element in the power input curve from each element in the power absorbed curves. The resulting vectors will be composed of positive and negative numbers.

The intersection of the power input curve with any given power absorbed curve will be marked by a change in sign of the error vectors, assuming only one intersection point. The index of where the sign changes in the error vectors will be the same index in either the power input, power absorbed, or RPM vector. Using the index, the steady state power and RPM is found for each velocity, shown in Figure 4.9(b). The black arrows show that at 40 m/sec, the propeller will absorb about 2400 Watts and spin at about 8700 RPM. Figure 4.11(a) shows that about 8 pounds of thrust are produced at 40 m/sec, and this means that the power absorbed curve, shown in Figure 4.9(a) by the black arrows, is the power absorbed curve for 40 m/sec.

Figure 4.10(a) shows how the RPM decreased slightly as explained in Figure 4.7(a)

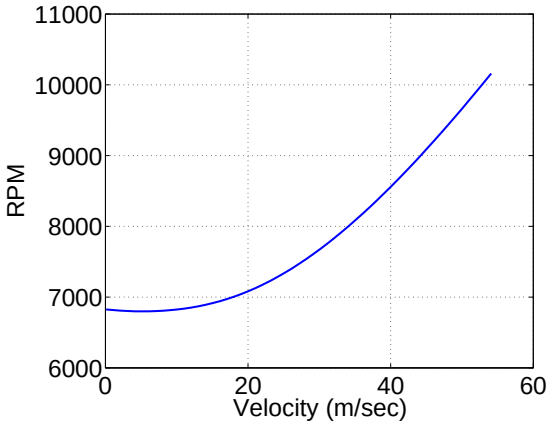

(a) RPM corresponding to the operating power vs. velocity.

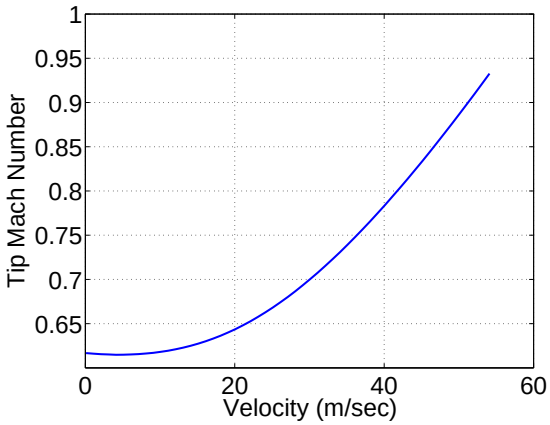

(b) Tip Mach number vs. velocity.

Figure 4.10: Figures showing the increase in RPM with velocity and resulting tip Mach numbers.

and then steadily increased again. This is different than the behavior of the operating power curve shown in Figure 4.9(b) in that the RPM begins rising well before the operating power drops off. This is because the engine power remains relatively constant at the maximum power while the RPM steadily increases once the power absorbed curves begin moving to the right. The tip Mach number follows the RPM very closely with increasing velocity. As was described, the tip Mach number is the limiting factor in how fast any particular propeller driven power plant can propel an aircraft. From Figure 4.10(b), about 37 m/sec is the practical top speed with regards to noise. If the velocity is increased much further, there will be shock waves on the propeller, and this will limit the thrust produced. The data for the airfoils is only accurate for the incompressible region of velocity [3], so the higher RPM and tip Mach numbers at high velocities indicate that the results are not exact [15]. Because it is not desired to fly at such high tip Mach numbers, this is not cause for concern, but the code could be modified to select airfoil data based on whether or not the flow is incompressible. This would require significant testing for the airfoils involved, however. It may be possible to choose a propeller such that high tip Mach numbers are not encountered even if the airplane is to fly fast. This could be done by using a smaller propeller or one with higher pitch. This would avoid the need to conduct more airfoil testing. The useful top speed of the power plant would occur when thrust is no longer produced, shown in Figure 4.11(a) by extending the linear trend to the x-axis, at about 58 m/sec (120 miles/hour). The power plant could go faster than

this, but it would produce negative thrust. The drag from the aircraft increases as the velocity squared at high velocities, due to parasitic drag [3], so the velocity where the power plant produces zero thrust may not be attainable because the airframe drag will be non zero. Therefore, it is important to consider the high speed drag of the airframe when designing the power plant because the thrust required to overcome drag at high speeds grows quickly.

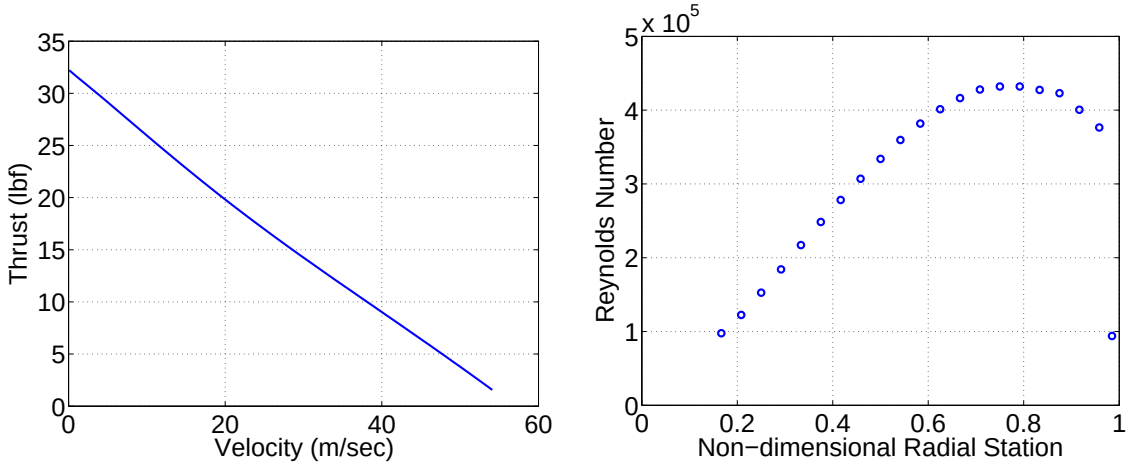

(a) Thrust (lbf) vs. Velocity (m/sec).

(b) Reynolds number vs. radial station x at the optimization velocity, V_{OPT}.

Figure 4.11: Figures showing the thrust vs. velocity curve and the Reynolds number vs. radial station.

The Reynolds number at each radial station is also found. Only the station Reynolds numbers at the optimization velocity are shown in Figure 4.11(b) because many graphs would be required for all the velocities. Figure 4.11(b) shows that it would be incorrect to assume that the Reynolds number increases all the way to the tip in a steady fashion. Even though the velocity due to rotation is steadily increasing, the chord becomes smaller at the blade tip causing the Reynolds number to decrease. The propeller tested in the following graphs has an angled tip; this is the reason for the sudden drop in the Reynolds number at the tip at $x = 1$. Figure 4.11(b) also shows that there is indeed a large variation in the Reynolds number along the length of the blade, and it is of benefit to take these variations into account in selecting the proper slopes for the lift and drag coefficients, as was done in the VP code.

4.1.3.1 Geared vs. Direct Drive

For comparison, an 11 by 6 Zinger propeller is simulated as being attached to the engine without a gear reduction unit, using the EPM code. The system is optimized at a velocity of about 41 m/sec, meaning that the engine's peak power is positioned to intersect the 41.1 m/sec power required curve. From Figure 4.12(a) it is shown that the power curve is much wider. The operating power can be maintained for a larger range of velocity, as shown by Figure 4.12(b), compared to the large TopFlite 24 by 10 propeller.

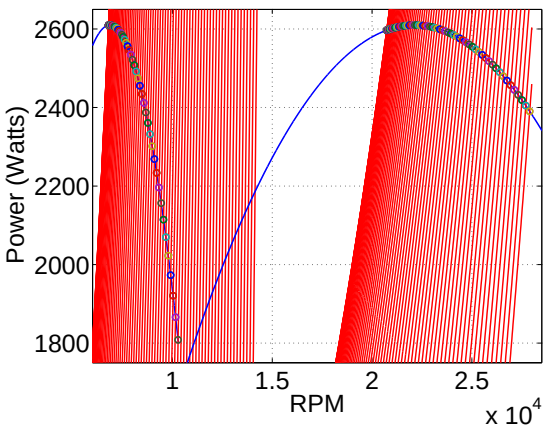

(a) Intersections found using the error function for two propellers. The TopFlite intersections are on the left, and the Zinger intersections are on the right.

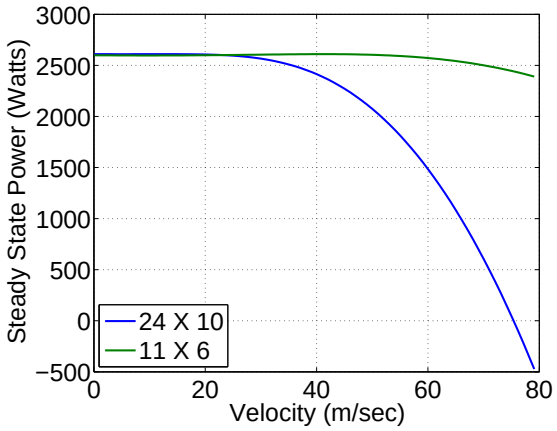

(b) Operating power stored from the intersections and corresponding velocity for two propellers.

Figure 4.12: Figures showing how the error function was used to find the intersections of the curves and plotting those intersections vs. velocity. The TopFlite propeller is geared 3.2:1 and the Zinger propeller is direct drive.

If the power plant was set up using the Zinger 11 by 6 propeller, the tip Mach number is always too high, shown by Figure 4.13(b). This is due to the propeller spinning very fast as shown by Figure 4.13(a). This setup could perhaps work, but it would be very noisy and therefore unacceptable in most applications. The airfoil data used to generate these curves is also for low speed flows, so the results are not accurate, but they do show the limitations of using a very high RPM engine with a direct drive propeller.

The airfoil data used to generate the curves should be reasonably accurate up to a Mach number of approximately 0.9 as there will likely not be strong shock waves on

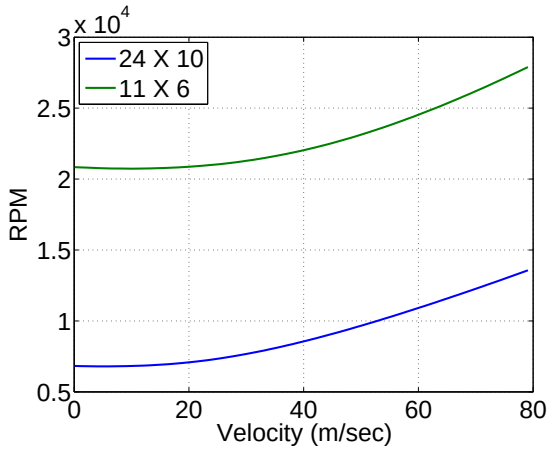

(a) RPM corresponding to the operating power vs. velocity for two propellers.

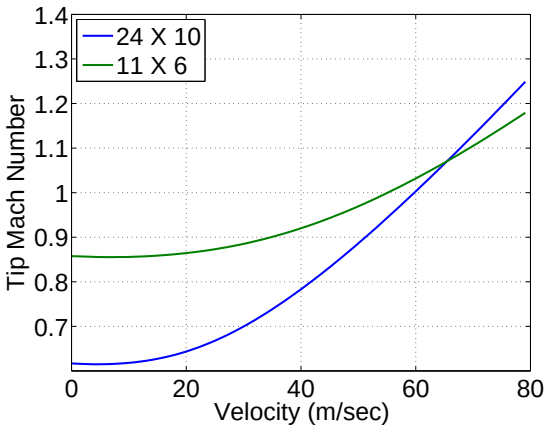

(b) Tip Mach number vs. velocity for two propellers.

Figure 4.13: Figures showing the increase in RPM with velocity and resulting tip Mach numbers.

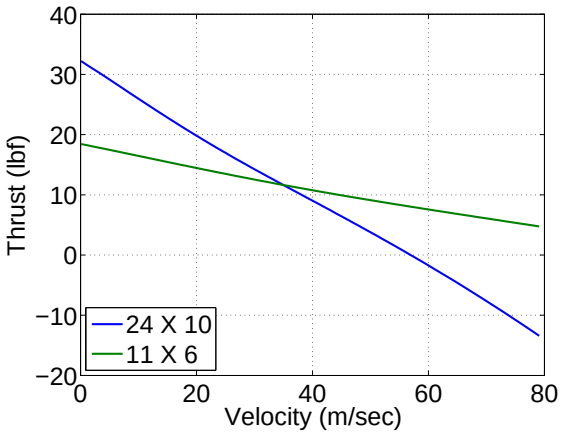

(a) Thrust (lbf) vs. Velocity (m/sec) for two propellers.

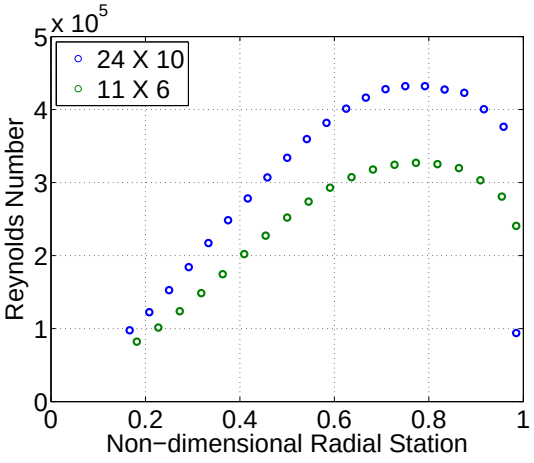

(b) Reynolds number vs. radial station x at the optimization velocity, V_{OPT}, for two propellers.

Figure 4.14: Figures showing the thrust vs. velocity curve and the Reynolds number vs. radial station for two propellers.

the blade yet. Full scale testing in 1944 found that once the Mach number exceeds 0.91, the efficiency drops significantly [15]. It would be reasonable to assume the same limit for small propellers. This corresponds to about 40 m/sec in Figure 4.13. Assuming the validity of the airfoil data, the small, high RPM propeller has just begun to produce more thrust than the large propeller, as shown by Figure 4.14(a). The small propeller would in theory produce more thrust at higher speeds, as shown,

but the tip Mach number would be entirely supersonic, and the performance shown would not occur. Figure 4.14(a) does show that high RPM configurations can perform better at high speeds, as was expected. It is interesting that the Reynolds numbers on the smaller propeller at the optimization velocity of 41 m/sec are less than the large propeller at a slower speed of 13 m/sec, shown in Figure 4.14(b). Clearly, the chord of the blade sections and overall diameter have a large effect on the station Reynolds numbers. Several studies have been performed for large propellers, which can be consulted to push the limits of the tip Mach number and to reduce propeller noise. [16] [15] [17]

Due to the high tip Mach numbers, using direct drive with this hypothetical RC car engine would not work. If the high power to weight ratio of such engines is to be utilized in aircraft, gear reduction will have to be used.

4.1.3.2 Validity of Non-dimensional Propeller Coefficients

The non-dimensional thrust and power coefficients are a very useful way to represent propeller performance data, shown by Figures 4.15(a) and 4.15(b). In these figures,

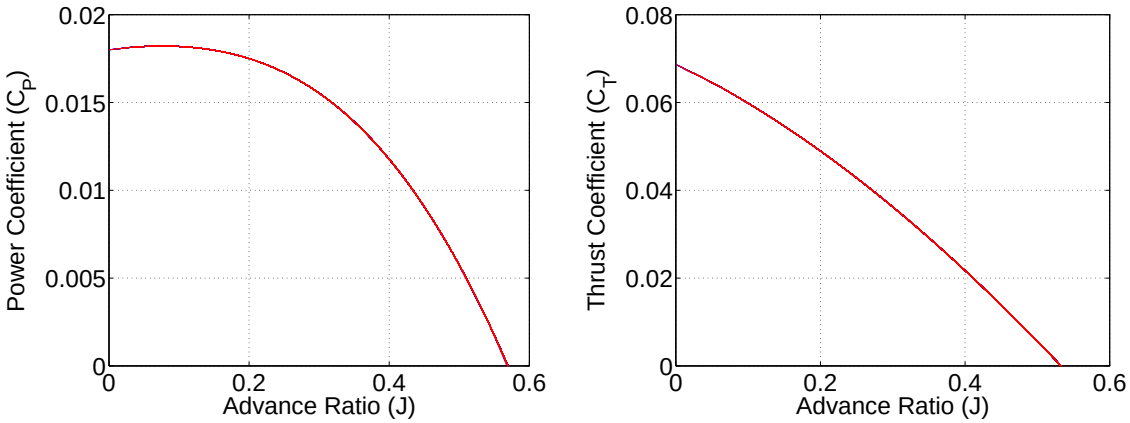

(a) Power coefficient C_P vs. Advance ratio J.

(b) Thrust coefficient C_T vs. Advance ratio J.

Figure 4.15: Figures showing the non-dimensional Power and Thrust coefficients. The non-dimensional geometry for a TopFlite 24 by 10 propeller was scaled to a 12 by 10 and a 48 by 10 propeller and all three results are plotted.

the non-dimensional data was scaled from the original 24 inch TopFlite propeller to a 12 inch and 48 inch propeller. The results are plotted on the same figure and are not labeled since the lines are on top of one another. This shows that even though the Reynolds numbers are different, the performance can be non-dimensionalized.

This means the results from one propeller could be used to predict the performance of another propeller, and one design could simply be scaled to produce the desired thrust. However, several tests have been conducted on RC airplane propellers, and the non-dimensional coefficient curves were found to be different depending on the RPM of the propeller [18]. This brings into question whether propeller performance should be scaled using the non-dimensional propeller coefficient data.

Even if the non-dimensional propeller data is deemed accurate enough, the average UAV builder likely is not interested in designing and manufacturing propellers. To scale or change the performance, a larger or smaller propeller would most likely be purchased and tested, not manufactured. Having measured several propellers from the Zinger line of propellers, it was clear that none of them had the same non-dimensional geometry. This means that every propeller will likely be different, so all propellers of interest would have to be measured and run through the VP code to get the non-dimensional performance coefficients, or tested in a wind tunnel as previously described. Another limitation of the thrust and power coefficients is that there is no information about the tip Mach number. For example, the tip Mach number curve shown in Figures 4.10 and 4.13, is essential to understanding what the top speed of an aircraft could be with a particular power plant. Lastly, there is no intuitive way to plot an engine performance curve with the non-dimensional propeller data. The simplest way to understand what the non-dimensional propeller parameters mean for a power plant is to use the dimensions from the propeller that created the non-dimensional data with the VP code and produce all the relevant plots that have been shown.

Chapter 5

Experimental Validation of Power Plant Models

In this chapter, we will compare the performance predicted by the models described in Chapter 3 to results obtained from experiments. To this end, we will provide a detailed description of the propeller and engine testing apparatus' that were built to perform these experiments. Following, we will present the results of the experiments done to validate the models developed in Chapter 4.

The EPM code was used to design a power plant for the 2013 SAE Aero Design competition. In this competition, the engine size is limited to a maximum displacement of 0.46 cubic inches. The highest power, 0.46 cu in, direct drive RC airplane engine is advertised as producing 1.63 HP and this is much less than RC car engines. Therefore, a high power, high RPM RC car engine was chosen. There are several brands and sizes, but the LRP 0.3-0.32 engines listed the highest power, around 4 HP, at the time of the search. The LRP ZR.32 engine had higher power at a lower RPM, but weighed slightly more due to a pull starter, so the LRP ZR.30X Competition engine was chosen. The LRP ZR.30X engine has a listed maximum power of 4.21 HP and a maximum RPM of 38,300. The rules did not limit the airframe configuration, but an airframe weight less than 8 lbs and total weight of 26 lbs would maximize the score. Additionally, there had to be a live video feed and altitude reporting, and a payload dropping system, which would add to the empty weight of the airframe. Therefore, it was of great importance to design a high thrust, yet light power plant. The propeller size and gear ratio is not limited, however. As was described, larger propellers are

more efficient at producing thrust, so the largest RC electric propellers were chosen. The reason for choosing electric propellers is that they have thinner cross sections and are the lightest. Electric motors have a smooth application of power and do not need to accept the high peak torque values of large direct drive ICE's. Because the RC car engine would be running at very high RPM, the peak torque values should be relatively low. Also, the RC car engine would be geared through a large gear ratio, and have a centrifugal clutch to allow for slippage if a resonance occurred, so it was deemed safe to use an electric propeller. It was chosen to experimentally test all available XOAR 26 inch propellers, as was described in Section 4.1.2. The available XOAR propellers are 26 inch by 8, 10, 12, 14, and 16 pitch. The reason for testing all 5 propellers experimentally is that it was not yet understood which one would produce the greatest thrust for a given gear ratio or optimization velocity. It was also unknown which airfoils were used on the propellers. Therefore, there wasn't any airfoil data to use with the VP code. It would be much faster to use the VP code rather than extensively test each propeller if that was a possibility.

5.1 Propeller Testing Apparatus

Electric motors are ideal for use in a wind tunnel because they have reasonably repeatable performance assuming the battery and ESC do not get worn out. The University of Minnesota UAV Lab has two fairly large UAVs. One of these UAVs has a high power, low torque, German made Actro 40-6 motor and Castle Creations high voltage 80 Amp ESC. This motor is not designed for 26 inch propellers, but because of its high quality, it can spin them for short bursts long enough to characterize the propellers. For this reason, the UAV labs power plant was used to test the five XOAR propellers. Figure 5.1 shows the Actro 40-6 motor, the Castle Creations HV 80 speed control, the RC equipment, a combined volt and amp meter, and two large Thunder Power 25C 5400 mAh 5 cell batteries which were used in series. When testing, this setup could draw near 80 Amps at 42 volts, which is a relatively large amount of electrical power. The RC equipment mentioned above included a Spektrum AR7000 receiver, a TM 1000 telemetry unit, and a 2 cell 1000 mAh Turnigy battery. This RC equipment was used with a Spektrum DX8 transmitter, shown in Figure 5.2, so that the telemetry data, including all battery pack voltages, and motor temperature could be monitored on the transmitter. Additionally, the RPM sensor was hooked up to the motor and telemetry unit but it was found to be unreliable. The temperature

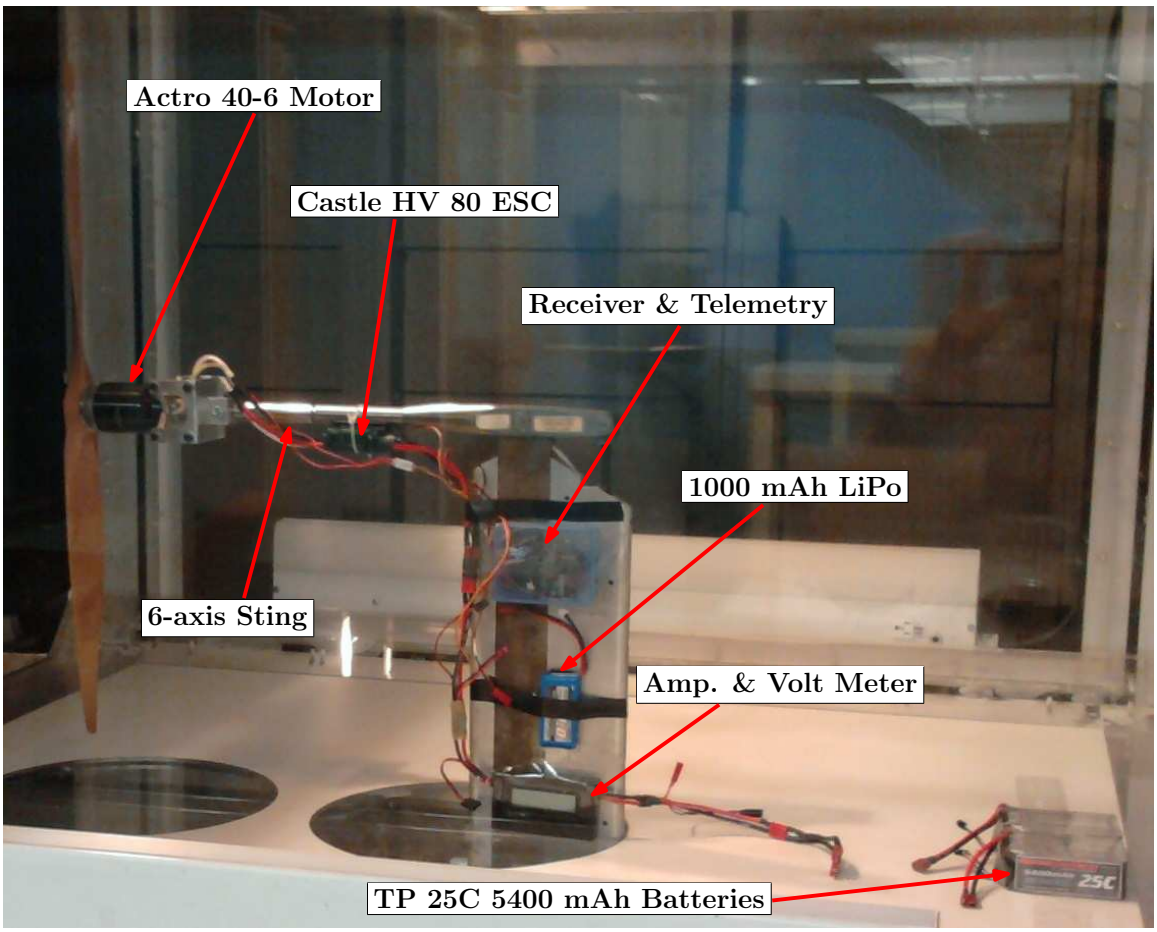

Figure 5.1: This figure shows a side view of the propeller testing apparatus. An Actro 40-6 motor, Castle Creations HV80 Speed Control, 6-axis sting, amperage and volt meter, plastic box with RC receiver and telemetry module, 1000 mAh 2-cell battery, and two Thunder Power 25C 5400 mAh 5-cell batteries are shown.

wire was strapped to the aluminum plate that the motor was mounted to. This gave an indication of the motor temperature though the flow of heat was slightly delayed. The Actro 40-6 motor has a maximum rated temperature of 100 C, and this could be easily reached if the motor wasn't periodically cooled. This is the reason for the relatively large distance between the RPM peaks in Figure 5.3(a), where the index is a measure of the sampling frequency of the ESC. The ESC's built in data logging system was used instead of the telemetry to record the motor RPM, shown in Figure 5.3(a). For the tests, the highest sampling frequency was used, and only the RPM was stored in order to allow for the longest testing time possible before running out of storage on the ESC and having to clear the ESC data. The ESC software reports that about 10 minutes of data can be stored when only storing RPM at the highest

Figure 5.2: This figure shows the DX8 transmitter.

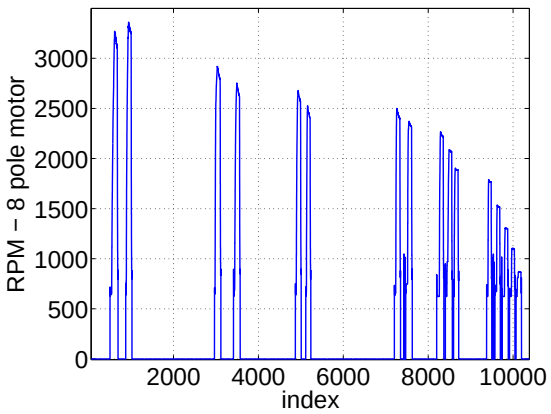

(a) RPM vs. storage index in Speed Control

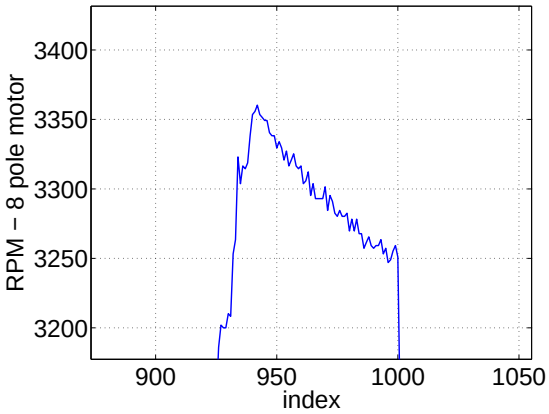

(b) RPM for the second peak in Figure 5.3(a).

Figure 5.3: Figures showing an example of RPM values stored in the Speed Control at a velocity of 0 m/sec.

sampling frequency, but longer times are possible if the motor is off for long periods of time. For this reason, it is unknown how long of a test can be done, but it is best to keep them under the maximum time.

To characterize the thrust and power absorbed by each propeller at some RPM and velocity, the torque, thrust, and RPM must be collected at the same operating point. Figure 5.1 shows a 6-axis sting which is able to record forces and moments in all directions, though only thrust and torque about its axis are important for this experiment. The sting is unable to collect RPM data. For this reason, the sting, and associated software and hardware were used to collect the thrust and torque data. The ESC was used to collect the RPM data. This creates a problem in knowing what RPM corresponds to which sting torque and thrust readings. For this reason, short bursts of power were used so that there would be countable peaks in the RPM data. This was accomplished by using the DX8 transmitter to quickly go from the motor being stopped to some desired throttle setting. The sting data was taken as soon as

the desired throttle setting was reached, and then the motor was immediately shut off after the thrust and torque data was collected. Three samples of thrust and torque were taken for each data point, using the sting. The DX8 has the option of displaying the position of the control sticks as percentage of movement. This was used to have repeatable throttle settings for the motor. The sting has a torque limit of 25 in-lbf (2.1 ft-lbf) which was possible to exceed with high throttle settings. For this reason, a slightly lower throttle setting is used first, and then the limit is incrementally approached, as shown by the peak torque in Figure 5.4(a).

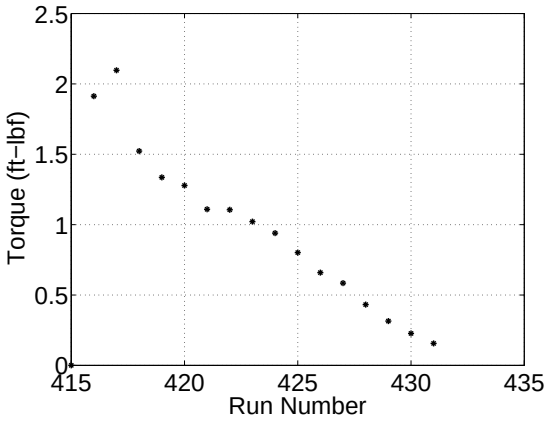

(a) Torque (ft-lbf) corresponding to each RPM in Figure 5.3(a) vs. run number.

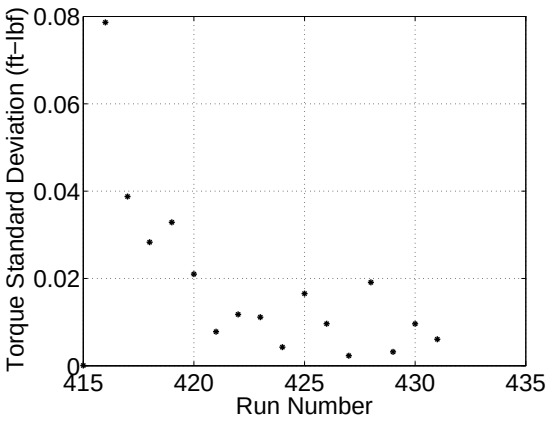

(b) Standard deviation of each torque value in Figure 5.4(a).

Figure 5.4: Figures showing the torque produced and standard deviation for the values of RPM in Figure 5.3(a), comparing values left to right in all figures.

Unfortunately, the electric motor, ESC, and batteries can not hold a constant RPM with a constant throttle setting. To hold a constant RPM, a governor or other controller which takes into account the propeller RPM would have to be used. Figure 5.3(b) shows the steep decline in RPM for the first RPM peak. The RPM readings used for each data point are those between the maximum RPM and the minimum RPM of the slowly declining region in each peak. The portions of the RPM data where the slope is very steep are not included in the RPM reading. To get an RPM data point, the RPM readings are averaged. It is assumed that the sting readings were taken at the beginning, middle, and end of the RPM peak. Because of the linear trends, the average of the thrust, torque, and RPM readings should be almost as accurate as if the RPM was held constant and not declining. A possible reason for the declining RPM is that the motor is getting hot, but most likely it is because the voltage in the batteries is dropping. It may be possible to achieve a more steady RPM

at high power settings using a large capacitor in line with the batteries. The standard deviation in the thrust and torque due to the declining RPM can be seen in Figures 5.5(b) and 5.4(b). It is clear that at lower throttle settings, the thrust and torque readings are more consistent. This further supports that the battery voltage declining could be the cause of the declining RPMs, since less current was being drawn at the lower throttle settings.

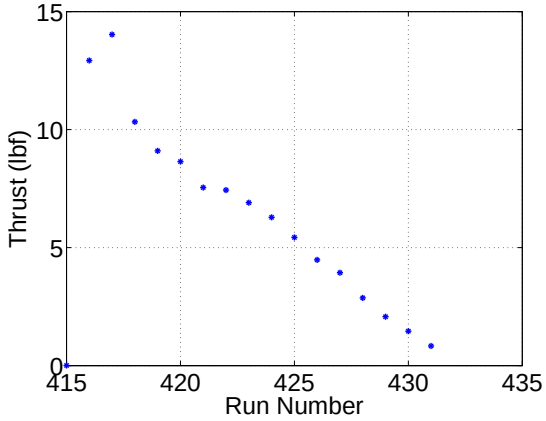

(a) Thrust (lbf) corresponding to each RPM in Figure 5.3(a) vs. run number.

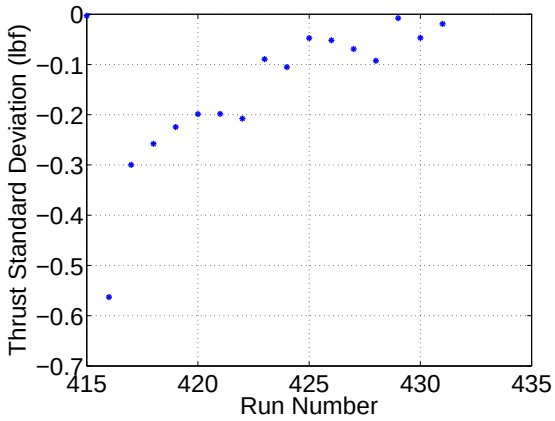

(b) Standard deviation of each thrust value in Figure 5.5(a).

Figure 5.5: Figures showing the thrust produced and standard deviation for the values of RPM in Figure 5.3(a), comparing values left to right in all figures.

Another concern is that the heat produced by running the electric motor was transferred directly to the aluminum mount holding it, and this heat was then transferred directly to the 6-axis sting. The 6-axis sting is constructed using strain gauges. These are known to be affected by temperature. These effects were mitigated somewhat by zeroing the readings from the 6-axis sting several times in each data set, but it is unknown what affects there could be because of this.

The propellers were each tested in this way in 2 m/sec increments up to a maximum of 30 m/sec for the XOAR 26x16 propeller. The XOAR 26x8 propeller was tested to 24 m/sec, the XOAR 26x10 propeller was tested to 26 m/sec, the XOAR 26x12 propeller was tested to 28 m/sec, and the XOAR 26x14 propeller was tested to 28 m/sec. The reason for increasing the maximum speed is that the propellers with larger pitch continued to produce thrust at the higher velocities, where the lower pitch propellers made almost no thrust with the power the electric motor could supply at 24 m/sec.

5.2 Engine Testing Apparatus

To test the LRP ZR.30 X engine, a suitable testing stand was needed that could also be used for testing the combined engine and propeller power plant. The 6-axis sting is too delicate to have a vibrating engine with the associated fuel and oil leaking from it. The requirements for the stand were that it could measure thrust and drag up to

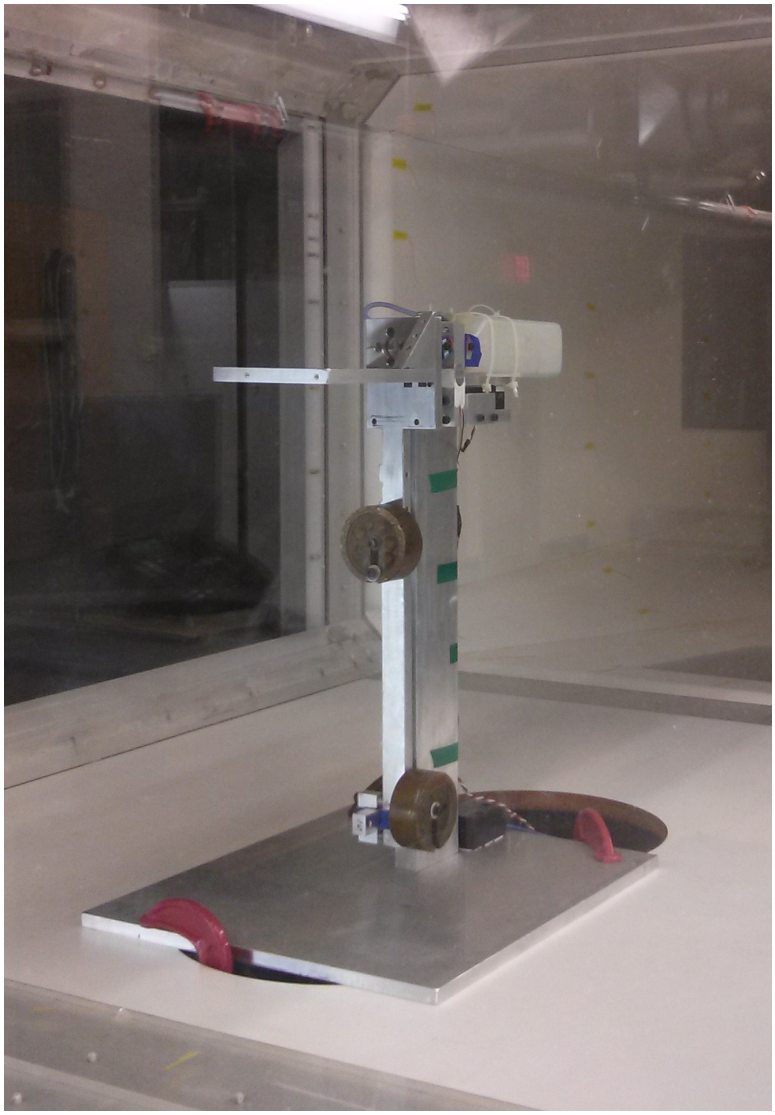

Figure 5.6: This figure shows an instrumented thrust and torque stand set up for small RC glow engines, mounted in a closed return wind tunnel.

at least 20 pounds of force and torque up to about 5 ft-lbf. These were estimated values from the expected performance of the power plant. The engine was first tested on a very simple stand that only allowed the engine to rotate about the axis it spins

the propeller around. A simple lever was then attached to the rotating part of the stand and caused to engage the top of a scale. In this way, the engine was tested using a range of propellers, to be discussed in detail in Section 5.3.2. Based on this data, performance predictions were made using the preliminary engine data and all the propeller data found using the electric motor. It was assumed that the LRP ZR.30 X engine would be relatively smooth running and that it would have relatively low vibration and peak torque values because of its high RPM. This proved to be entirely not true, as will be discussed in detail in Section 5.3.2. The stand was designed to have a large degree of flexibility to accommodate any necessary design changes that could be necessary. The preliminary engine testing revealed that the lever arm attached to the engine would essentially bounce on top of the scale as the engine ran. Depending on where the scale was positioned, the readings would change as well. If the lever arm attached to the engine was held, the torque spikes could be felt in the fingers, and it was rather unpleasant. For these reasons, some design features were needed to address the potential vibration problems of the engine.

The first design feature incorporated is a large pendulum type lever arm to measure the torque of the engine, shown in Figure 5.6. The lever arm was made as long as possible in case the engine produced large torque spikes. Additionally, locations for mounting weights to the lever arm were included in order to damp out vibrations.

To measure the thrust and torque, it was desired to use strain gauges with Wheatstone bridges to measure the voltages. However, strain gauges can be fairly expensive, so a cheap alternative was sought. As an experiment, two kinds of digital scales were purchased from Harbor Freight in order to see how they were designed, one of which is shown in Figure 5.7. Upon disassembling the scales, it was discovered that there were

Figure 5.7: This figure shows the 70 lb digital scale from which the strain gauges were removed.

aluminum bars with strain gauges on either side of them, shown in Figures 5.8(a) and 5.8(b) by the red arrows. There may even be a third strain gauge on the aluminum bars in order to provide some temperature compensation, but the white plastic coating was never removed to investigate, shown in Figure 5.8(a). The strain gauges shown both came from the same scale, but originally a smaller scale's aluminum bar with strain gauges was used for the torque readings. This smaller scale's aluminum bar was more sensitive, but it could not handle the engines peak torque values, as will be discussed in Section 5.3.2.

The next design feature is a bearing assembly, shown in Figure 5.8(a) by the green arrow, to allow the engine to cause a rotation. The rotating motion is constrained by clamping the aluminum bar with the strain gauges on it to the bottom of the pendulum, shown in Figure 5.8(b). The green arrow points to a block of aluminum, but inside of the block are two large angular contact bearings that are pre-loaded by a bolt on the end of a shaft. The circular metal piece next to the aluminum block on the left connects to a shaft that runs through the aluminum block, shown by the green arrow, and the end of the shaft is threaded to allow a bolt to pre-load the bearings, as described. This allows the entire assembly left of the aluminum block to rotate freely if not constrained by the torque sensor, which is the aluminum bar with strain guages on either side of it shown in Figure 5.8(b).

To measure the thrust, the entire rotating torque assembly, which includes the pendulum, bearing assembly, engine mounting plate on the front of the pendulum, and the aluminum plate under the bearing block, is allowed to slide forward and backward on the black linear bearings shown in Figure 5.8(a) by the yellow arrow. The forward and backward sliding motion is constrained by the thrust sensor, which is the aluminum bar with strain gauges on it shown in Figure 5.8(a). The thrust sensor is mounted to a block which is rigidly mounted to the long, rectangular, aluminum bar extending from the base of the stand which is clamped to the wind tunnel. The configuration of the thrust and torque sensors is such that the linear bearings do not have to resist any torques; they only support up and down forces and allow the assembly to slide. Only the torque sensor receives the torque of the engine, and only the thrust sensor measures the thrust or drag produced. One downside to the configuration is that as thrust is produced, the entire pendulum assembly is pulled forward relative to the torque sensor, as the torque sensor is also rigidly attached to the long rectangular bar extending from the base of the stand. Testing revealed that metal

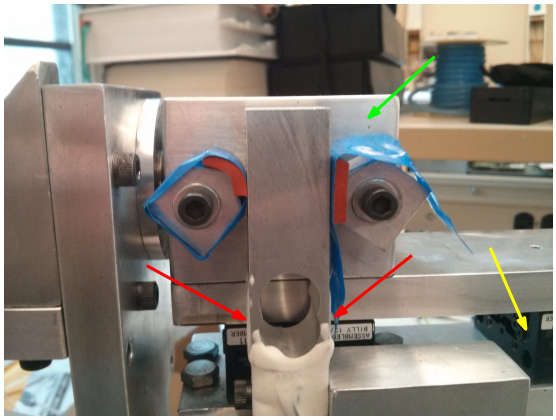

(a) A figure with the thrust strain gauges shown by red arrows, one of the two linear sliders shown by the yellow arrow, and the bearing assembly shown by the green arrow.

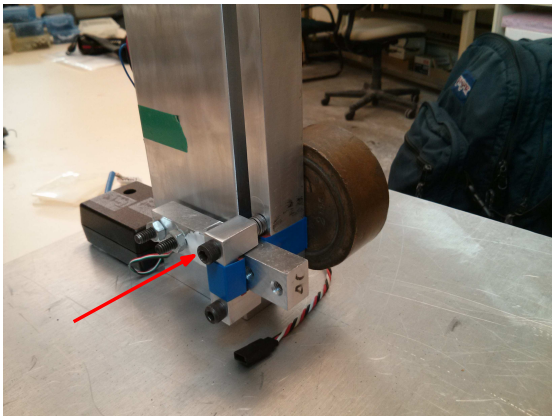

(b) A figure with the one of the two torque strain guages shown by the red arrow.

Figure 5.8: Figures showing the thrust and torque strain gauges.

to metal contact points between the thrust and torque sensors would not work, as engine vibration would widen the gap and wear out the aluminum. For this reason, rubber pads were installed between the thrust and torque sensors, shown in Figure 5.8(a). This can create problems because the rubber will allow for actual movement of the pendulum assembly, whereas the knife edge contact points would in theory allow almost no movement. This creates the possibility of the thrust of a power plant pulling on the torque sensor, by pulling the pendulum forward in such a way that the thrust induces a torque. This is somewhat compensated for by the clamping of the rubber pads being somewhat loose and by the fact that the engine vibrates so much that the assembly moves to a new position because of the vibration. This was the best compromise found, though miniature linear sliding bearings or other kinds of linkages could be used to constrain the movement and make the measurements more precise.

The engine test stand also incorporates several mounting holes that are used to mount the LRP ZR.30 X and the combined power plant, shown in Figure 5.9(a). The aluminum engine or power plant mounting plate is also fairly large so new holes can be drilled to mount a variety of engines and power plants. The engine test stand can also be configured to mount things with different heights shown in Figure 5.9(b) by the red arrows. The reason for this is that it is best to have the centerline of the propeller in line with the rotation axis of the pendulum. By definition, a pure

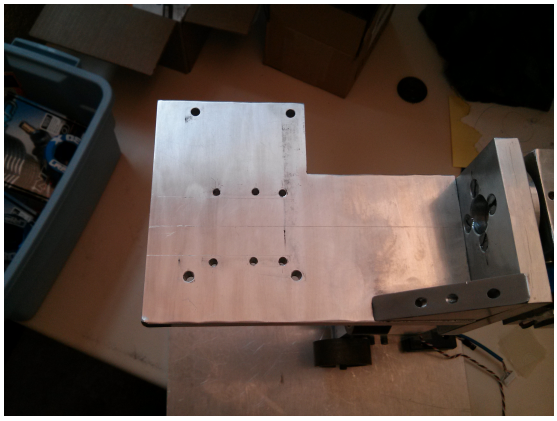

(a) Engine or power plant mounting holes.

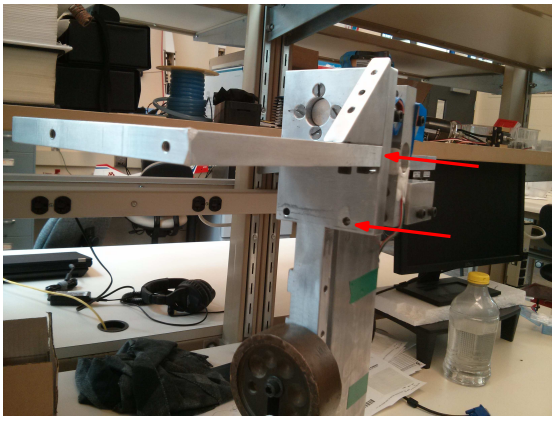

(b) A figure showing the two possible mount posistions of the engine/power plant mounting plate.

Figure 5.9: Figures showing the possible locations of the engine/power plant support plate and its mounting holes.

moment applied somewhere can be moved such that it is applied about some arbitrary axis perpendicular to the same plane, so if the centerline of the propeller shaft is not exactly centered on the axis of rotation of the pendulum, the results should still be accurate. It is important to realize what is exerting a torque on the engine test stand. Clearly, it is the propeller which is pushing against the air which causes a reaction torque to be measured by the stand. The engines torque is then transmitted to the propeller. To measure the thrust and torque, the sensors must be wired to Wheatstone bridges and connected to measuring equipment, to be discussed next.

5.2.1 Wiring

To measure the voltage output from the thrust and torque sensors, two operational amplifier (Op Amp) circuits were constructed and mounted inside the black box shown in Figure 5.10. The output from the thrust and torque sensors is in the millivolt range,

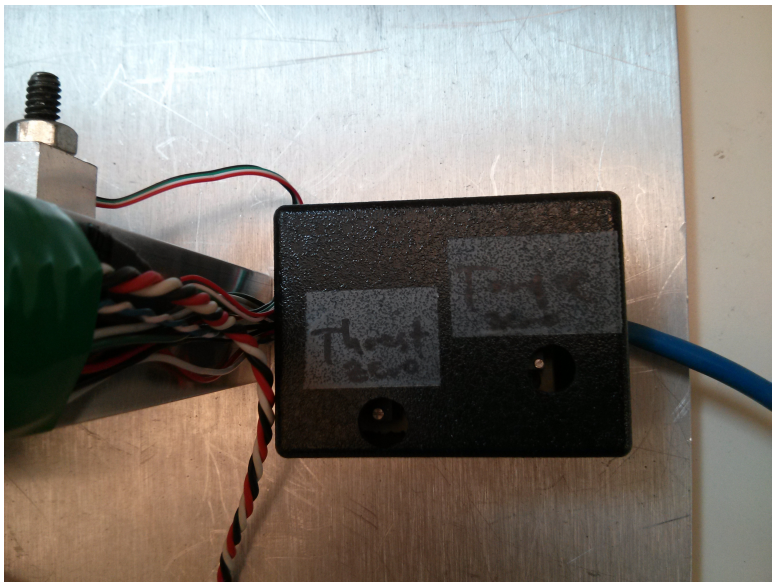

Figure 5.10: This figure shows a black box with a pair of Wheatstone bridges and potentiometers in it to zero each bridge for the thrust and torque strain gauges.

so it would be hard to get reliable voltage readings unless the voltage is amplified. The two amplifier circuits each use two Op Amps in series to step up the voltage. There are also variable potentiometers (POT) that allow the voltage output to be manually zeroed before doing any testing. It was possible to get within about 0.2 volts of 0 volts when manually zeroing the Op Amps. There is significant voltage drift over time, however, so it is not critical to manually zero the Op Amps with the POTs because the voltage drift is subtracted digitally in the measured data.

The Wheatstone bridges on the thrust and torque sensors are powered using -7.5, 0, and 7.5 Volts from a power supply, shown in Figure 5.11(a). This power also goes to the Op Amp circuits. It is possible to increase or reduce the voltages, but the main concern would be overheating the strain gauges. The wires for the power and voltage outputs all pass through solid core Ethernet cable. Three of the wires are for the negative, ground or 0 voltage, and the positive voltage. These three wires run forward to the Op Amp circuit and also power the strain gauges and Wheatstone

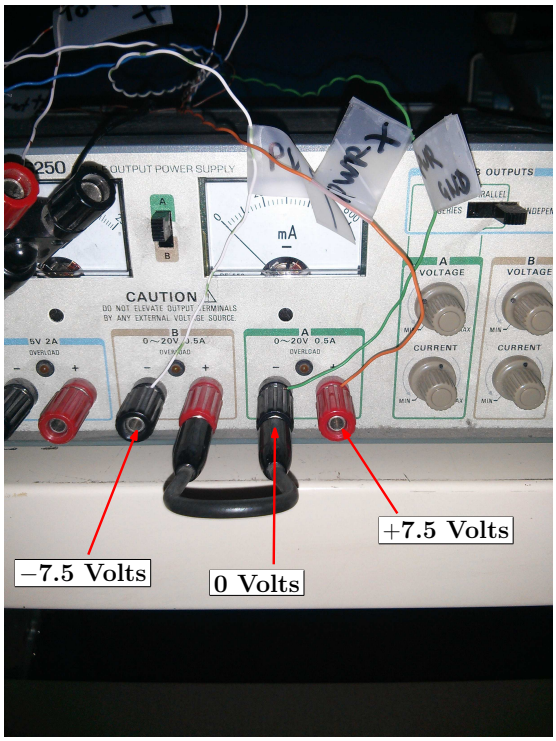

(a) A figure showing the -7.5, 0, and +7.5 Volt hookups, on a power supply, for the Wheatstone bridges.

(b) A figure showing the zero reading on a voltmeter for the thrust strain guages.

Figure 5.11: Figures showing the power supply hookups and the zero reading of the thrust and torque strain gauges.

bridges. The output from the Wheatstone bridges is then passed to the Op Amps which then pass the amplified signal back through the Ethernet cable up to a junction box, shown in the top left of Figure 5.11(b) where the junction box has the leads from the red voltmeter in two of the ports.

The junction box is connected to a Texas Instruments data collection tool which is used with a program called crtunnel. The program communicates with the Texas Instruments device and allows for several options in the data collection. With two outputs being measured, the sampling rate could be as high as 50,000 Hz, and this was used for most of the tests. When more channels on the Texas Instruments device are used, the sampling rate can not be as high. For this reason, it is desirable to reduce the number of channels being measured, if possible.

Originally, it was planned to use a dedicated sensor to measure the RPM of any motor mounted to the engine test stand. This required a third channel and forced

the sampling rate to be reduced to 20,000 Hz. The RPM sensor was a sensor that would sense the passing of a ferrous metal, such as the crankshaft on an engine. This sensor would output 0 volts except for right when the metal object passed, where it would output over 2 volts. Because of the extremely fast engine RPMs, 30,000 or more, the data collected only had 4 data points for each peak in the RPM signal, for RPMs around 30,000. The RPM data gathered was good enough to characterize the engine, but better accuracy was desired. It was discovered that an FFT of the torque signal could be used instead of an RPM sensor, which will be discussed in detail. For this reason, only two channels are used with the engine stand, but the wires are available in the Ethernet cable to hook up the RPM sensor if something with a weak or non-periodic torque signal is tested on the engine stand. An important point with the RPM sensor is that it does not get power from the power supply; it gets power from the telemetry unit which is connected to the RC receiver. If something is going to be tested that does not use an RC receiver and telemetry unit, a separate power supply or battery will have to be used for the RPM sensor. In order to convert the measured voltages from the Op Amps to thrust and torque data, the engine test stand must be calibrated. This is discussed next.

5.2.2 Calibration

The engine test stand must be calibrated before any useful data can be gathered from it. A lesson learned from testing the LRP ZR.30X, however, is that it may make more sense to run the engine on the stand and collect a sample of data before calibrating the sensors. Before testing, it was unknown that the engine would produce so much vibration and high peak torque values. There may be resonances in the entire system that cause the torque signal to be so high. This will be discussed in detail in following sections. The important point is to test the engine of interest and look at the signal. Originally, a smaller torque sensor was used which was not at the end of the pendulum. This made the sensor much more sensitive to torques because of a smaller lever arm and because it was designed for smaller forces up to 11 lbs. When looking at the data from those first tests, it was discovered that there was severe clipping of the sinusoidal output signal. For this reason, a test should be conducted to find the maximum torque and thrust voltages that can be reported by the Op Amp circuit. This can be found by loading the sensors until the voltages do not change with increasing torque or thrust. A test can then be conducted with the engine of interest. The peaks in the data from the engine test should not come close to the maximum measurable voltages, or there may be clipping of the data at some operating condition. If the peaks do get clipped, more damping in the form of weights can be attached to the pendulum or more rubber can be used between the sensor contact points. If these tweaks do not work, the Op Amp circuit must be re-designed to amplify to a higher voltage. The sensor location may also have to be changed or a larger sensor can be used.

To calibrate the sensors, known forces and torques must be applied to the engine test stand. The corresponding output voltage must then be recorded. Then, using this data, a calibration curve can be constructed. It was assumed that the engine stand would only measure forward thrust and positive torques. It was found that this was true for the mean thrust and torque values, but the output shows that the voltages and thrust and torque values were negative a large percentage of the time. For this reason, the engine test stand should be calibrated in both directions for both sensors if more accurate results are desired. The output from the thrust and torque sensors was essentially linear, so it is probably not a large source of error, but it is unknown what the calibration is for the negative directions.

For these calibrations, the power plant is mounted to the engine test stand so that the Op Amp circuits could be zeroed with the power plant on the stand. The calibrations could be conducted with the power plant or engine off of the stand in the same way. To calibrate the thrust sensor, a stand was set up as shown in Figures 5.12(a), 5.12(b), and 5.13(a). On top of this stand is a pulley. A string is then attached to something

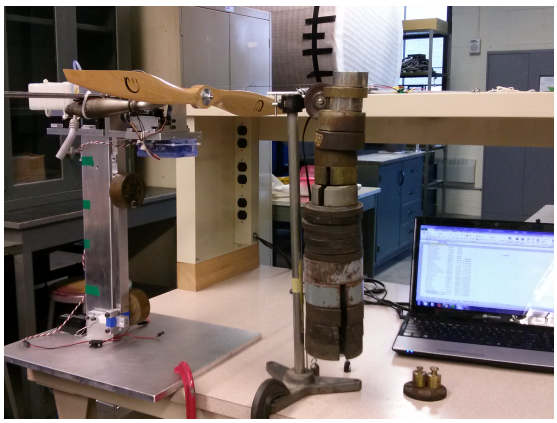

(a) Thrust calibration.

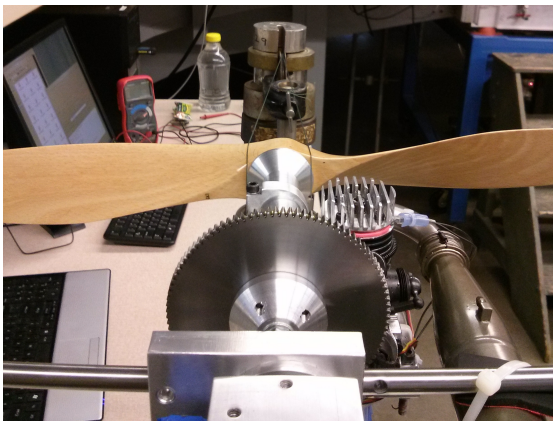

(b) In-line string for thrust calibration.

Figure 5.12: Figures showing the maximum weight used for calibrating the thrust readings and the positioning of the string holding the weights.

on the engine test stand and put on the pulley so that the gravitational force of the weights causes a simulated thrust force. In this case, the string is wrapped around the propeller hub and attached to the power plant. The string in this case was braided fishing line that was looped around several times so that it could support the large amount of weight shown. It is important to place the string and pulley so that the string is directly in line with the line of action of the thrust force of the propeller, shown by Figures 5.12(b) and 5.13(a). Weights are then hung on the string in incremental steps to calibrate the thrust sensor. Figure 5.12(a) shows the maximum weight used for calibrating the thrust sensor, which was about 40 lbs.

To calibrate the torque sensor, weights are hung from the metal bar attached to the rotating part of the engine test stand, shown in Figure 5.13(b). The metal bar is sized so that the hanging point for the weights is almost exactly 1 foot from the centerline of the axis of rotation. The holes drilled in the metal bar were done on a mill with rather high precision. Figure 5.13(b) shows the maximum weight hung on the metal bar, which was about 26 lbs, which means the maximum torque applied was 26 ft-lbf. An error source is the fact that the metal bar bends significantly when the 26 ft-lbf

is applied, shown in Figure 5.13(b). This was not accounted for in the calibration because the angle that the bar bends to is about 5 degrees. The results of the thrust

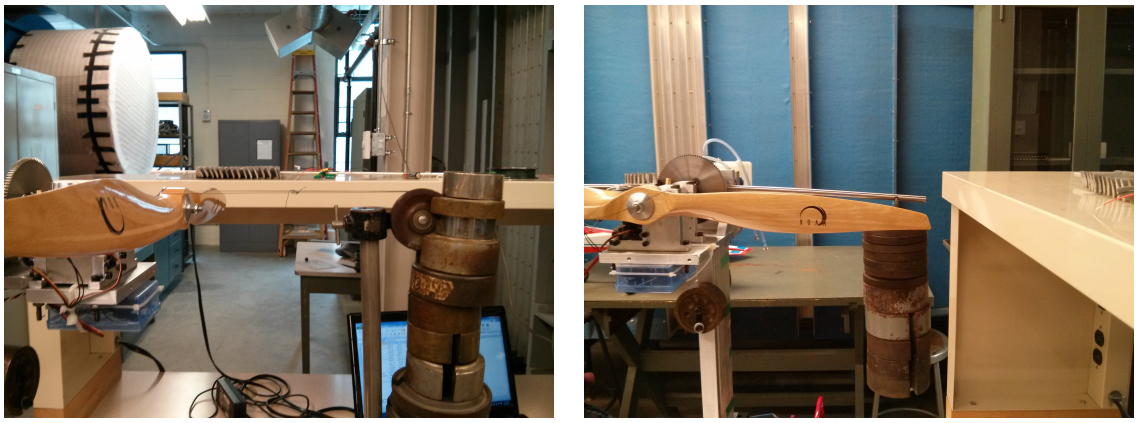

(a) In-line string for thrust calibration. (b) Torque calibration.

Figure 5.13: Figures showing the string and weights for the thrust calibration and the maximum weight used for the torque calibration.

and torque calibration are shown in Figures 5.14(a) and 5.14(b). Clearly, the trends are very linear, though the torque values appear to be more linear. The thrust at high values is some times above the linear trend, and sometimes below it. This introduces a slight error when converting from voltage to force, but the error is small. It would be possible to use a linear interpolation function to connect the data points, but this was not done for simplicity.

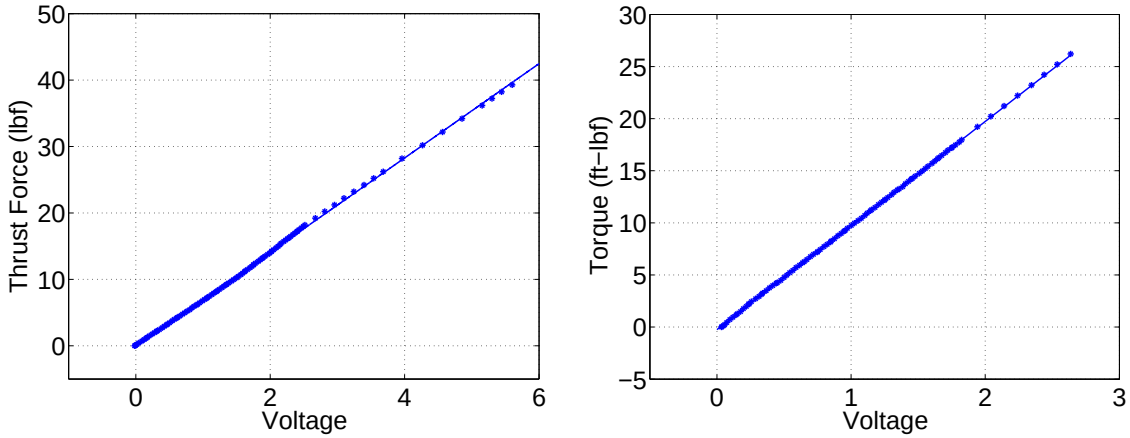

(a) Thrust force (lbf) vs. thrust voltage. (b) Torque (ft-lbf) vs. torque voltage.

Figure 5.14: Figures showing the thrust and torque readings vs. voltage.

Only the slope in Figures 5.14(a) and 5.14(b) is of importance and this is what is used to convert voltage to force or torque. A non-zero y-intercept doesn't have much effect because the sensors must be zeroed often to remove any voltage drift.

Lastly, there are several error sources with this setup that have not been quantified. The voltages on the power supply have to be manually adjusted to be as close to plus or minus 7.5 Volts as possible. After the voltages are set, the calibration of the sensors is conducted. The power supply was found to drift by about 0.1 Volts from the desired reading over time. It is unknown what affect this has on the calibration of the sensors.

5.2.3 Wind Tunnel Thrust Compensation

Because of the large frontal area of the test stand, a relatively large amount of drag is produced at higher velocities. This must be taken into account when characterizing any power plant mounted to the test stand. This was accomplished by running just the engine test stand in the wind tunnel through the expected range of velocities for the power plant. Some of the velocities were tested twice, but most were tested only once. The tests were conducted by first taking voltage readings at 0 velocity, then setting the tunnel speed to 2 m/sec, 0 m/sec, 4 m/sec, and so on using 2 m/sec increments. This way, there is a zeroing between each data point. Figure 5.15(a) shows the measured voltages of the thrust sensor vs. velocity. The grouping of data points on the y-axis at 0 velocity shows the zero readings. The reason for the voltage

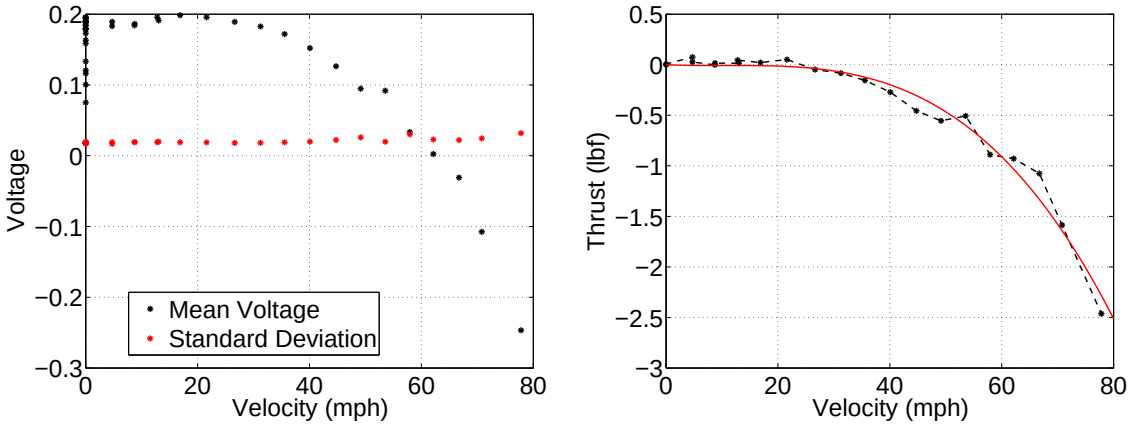

(a) Mean thrust voltage and standard deviation in voltage vs. velocity.

(b) Measured thrust in black vs. velocity and a line of best fit.

Figure 5.15: Figures showing the mean thrust voltage, standard deviation, and corresponding thrust vs. velocity.

drift of the sensor is likely friction effects in the setup, but temperature effects are possible as well. For these tests, the parts of the engine test stand that clamped the thrust and torque sensors were loosened so that friction from the clamping force could not bias the measurements as much. This is a known error source because it is unknown if the vibration of the engine allows pendulum to move as thrust is produced, as discussed. Also, after the engine had been run for a significant amount of time on the engine test stand, it was noticed that the linear bearings stick at a particular location in their range. It is believed that the vibration of the engine has caused this, so more robust linear bearings may be required. The zero readings at 0

velocity, between each velocity step, show that as velocity was increased and returned to 0, the thrust sensor measured increasingly negative forces. The largest zero reading was just over 0.1 Volts, and this is an error or bias of about 0.7 lbs, as can be seen from Figure 5.14(a). After the test was finished, a voltmeter was connected to the thrust output on the junction box. The engine test stand was then lightly tapped, and the voltage jumped back to its original zero reading. This indicates that there is something that is sticking in the setup. It is assumed that the engine vibration keeps these sticking effects to a minimum, but the error caused by this is unknown.

Figure 5.15(b) shows the computed drag vs. velocity of the engine test stand. The black data points include the effects of the zeros, meaning that each zero is taken as the reference for the next data point. This has the effect of reducing the measured drag at high velocities, which could bias the measured data for a particular power plant by about 1 lb. To accurately characterize the drag of the stand, more tests would have to be conducted where the stand is lightly tapped, as well as zeroed between each velocity.

The line of best fit through the data points shown in Figure 5.15(b) is what is used to compensate the measured thrust of the power plant in the following sections.

5.2.4 Wind Tunnel Torque Compensation

It was assumed that the torque readings would not be affected by increasing forward velocity. This was found to be true for the aerodynamics of the engine stand, but not for the torque sensor. To test the torque vs. velocity characteristics of just the stand, a voltage reading was first taken at 0 velocity. The tunnel speed was then set to 2 m/sec, 0 m/sec, 4 m/sec, and so on using 2 m/sec increments, the same as for the thrust sensor. In fact, the thrust and torque characteristics of the engine stand were found at the same time. Figure 5.16(a) shows the recorded torque voltages vs. velocity. The gathering of data points on the y-axis shows that as the velocity was

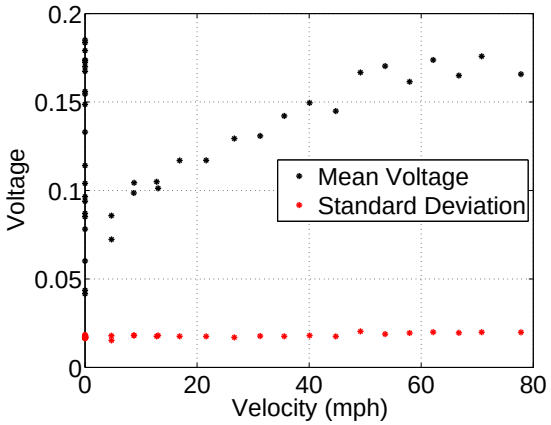

(a) Mean torque voltage and standard deviation in voltage vs. velocity.

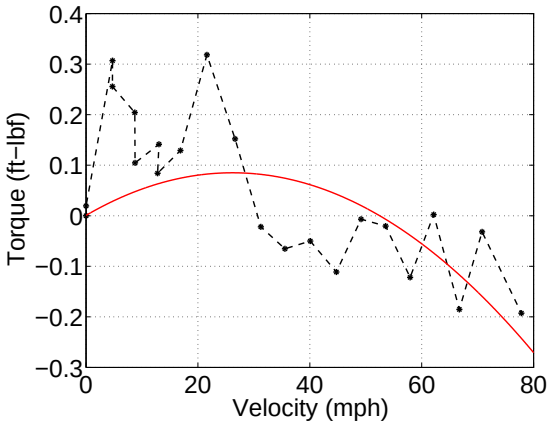

(b) Measured torque in black vs. velocity and a line of best fit.

Figure 5.16: Figures showing the mean torque voltage, standard deviation, and corresponding torque vs. velocity.

increased, the voltages with the tunnel off and on were increased. This rise in voltage appears to be because of temperature changes in the torque sensor. The engine stand was inspected, and the bearings supporting the entire rotating assembly were found to allow smooth rotation. Tapping on the stand after the test did not cause the zero voltage to change either. The voltage drift of the torque sensor is on the order of 0.15 Volts. The temperature affects are likely due to the fast airflow quickly cooling the aluminum sensor. The thrust sensor has a similar voltage drift of about 0.15 Volts, but after tapping on the thrust sensor, the voltage went back to the original reading from before the test began. A known problem with the torque sensor setup is that the mean torque desired to be measured is about 3 ft-lbf. This corresponds to a voltage of about 0.25 Volts. This means that the torque readings will be affected much more by

voltage drifts and setup issues in the engine test stand. This is necessary to capture the peak torque values of over 2.5 Volts, which corresponds to a torque of 26 ft-lbf. Before the large weights were attached to the pendulum, the peak torque values were over 5 volts, which means the peak torque was above 50 ft-lbf. This means that the peak values of torque are plus or minus more than 10 times the average torque values.

The thrust readings are not affected as much by voltage and/or setup issues because the thrust force of interest is on the order of 20 lbs, which is about 2.75 volts. Compared to the measured thrust voltages, small errors will not bias the results very much. The thrust voltages also have high peak values like the torque signal, as will be discussed in the following sections.

The severity of the torque voltage drift can be seen in Figure 5.17 where only a zero reading was taken at the beginning of the test and not in between each velocity increment. The bias in torque is then about half of the expected torque, in the worst

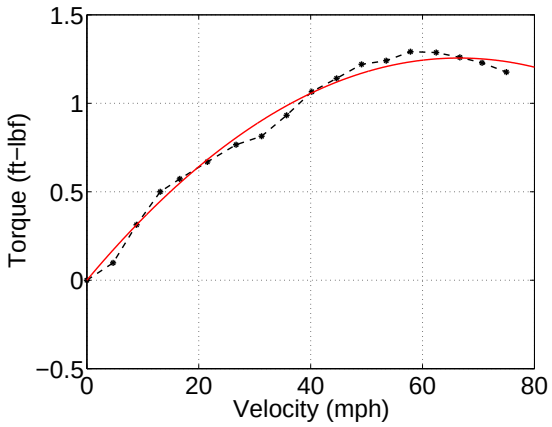

Figure 5.17: This figure shows what happens if the torque reading is not zeroed between each data point. The measured torque is in black, and a line of best fit is in red.

case, which would affect the results significantly. It is then very important to zero the voltages between each data point or as often as possible. This makes any testing more time-intensive, but is necessary in order to get the best data possible. It would be possible to build an insulated box around the torque sensor to shield it from the airflow in the wind tunnel, but tests would have to be conducted to verify the results.

5.3 Experimental Data Collection

5.3.1 Example Thrust and Torque Voltages

As was described, the sampling frequency was 50,000 Hz. This allows for capturing a large, detailed amount of data for the thrust and torque signals. It is important to see how noisy the thrust and torque signals are when there is no airflow, and the engine test stand is not being moved. Figure 5.18(a) shows a sample of the thrust voltage signal with the engine off. Figure 5.18(b) shows that there is very little frequency dependent noise that could bias the readings. Figure 5.19(a) shows a sample of the

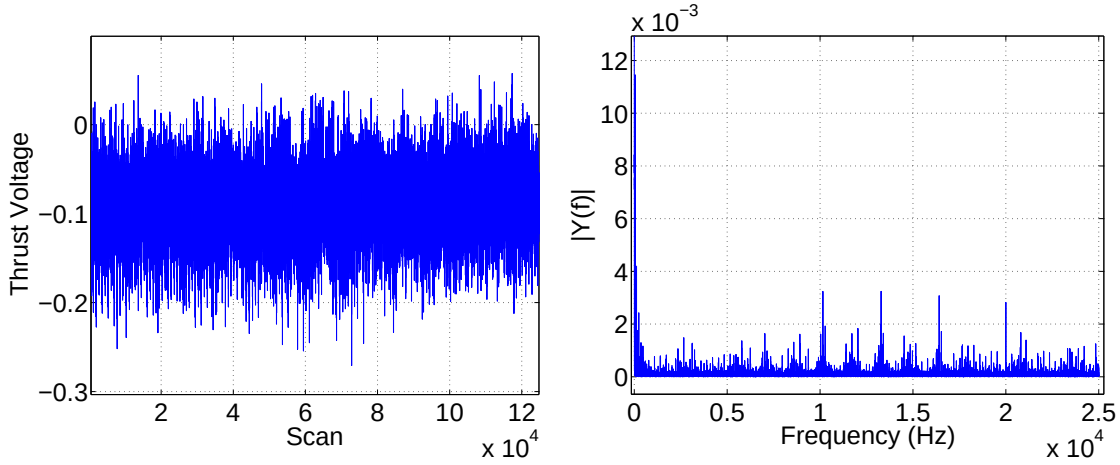

(a) A sample of the thrust voltage output with the engine off.

(b) An FFT of the thrust signal with the engine off showing little frequency content.

Figure 5.18: Figures showing a sample set of thrust voltage and an FFT of the same data, with the engine off.

torque voltage signal with the engine off. Figure 5.19(b) also shows that there is very little frequency dependent noise that could bias the torque signal. This is important because the FFT of the torque signal is to be used to calculate the RPM of the engine. If there was strong, frequency dependent noise, it could affect the RPM data.

The following figures are samples of thrust and torque voltages taken when testing only the LRP ZR.30 X engine, not a combined power plant. These are shown to give some idea of the severe thrust and torque fluctuations due to the engine. Figure 5.20(a) shows a sample of thrust voltages. Clearly, the engine is causing the readings to fluctuate very fast. Figure 5.20(b) shows a closer look at the voltages in Figure 5.20(a). The thrust signal is periodic and the engine is able to affect the thrust signal

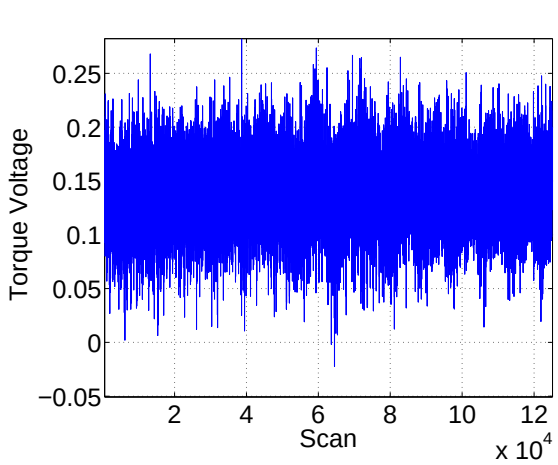

(a) A sample of the torque voltage output with the engine off.

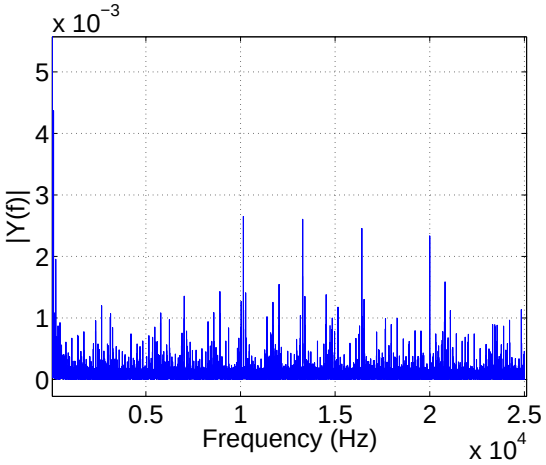

(b) An FFT of the torque signal with the engine off showing little frequency content.

Figure 5.19: Figures showing a sample set of torque voltage and an FFT of the same data, with the engine off.

almost as much as the torque signal, even though it would seem most of the torque fluctuations would go into the torque sensor.

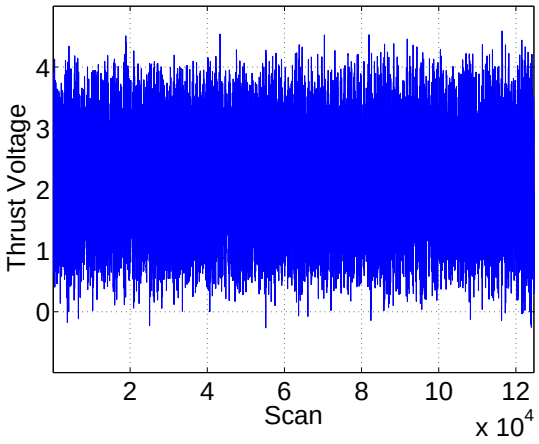

(a) A sample of the thrust voltage output with the engine on.

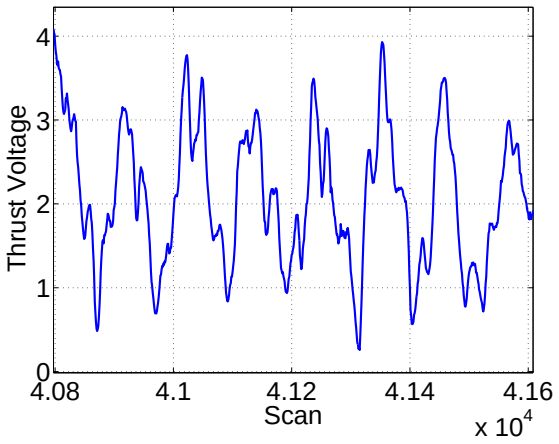

(b) A zoomed in sample of the thrust voltage output, with the engine on, in Figure 5.20(a).

Figure 5.20: Figures showing a sample set of thrust voltages with the engine on.

Figure 5.21(a) shows a sample of torque voltages. These voltages oscillate about as much as the thrust voltages. Figure 5.21(b) shows a sample of the voltages in Figure 5.21(a). This signal is very periodic, which shows the effect of combustion in the engine. It is unknown if there are resonance effects in the engine stand causing the

high torque fluctuations, or if it is really the engines torque.

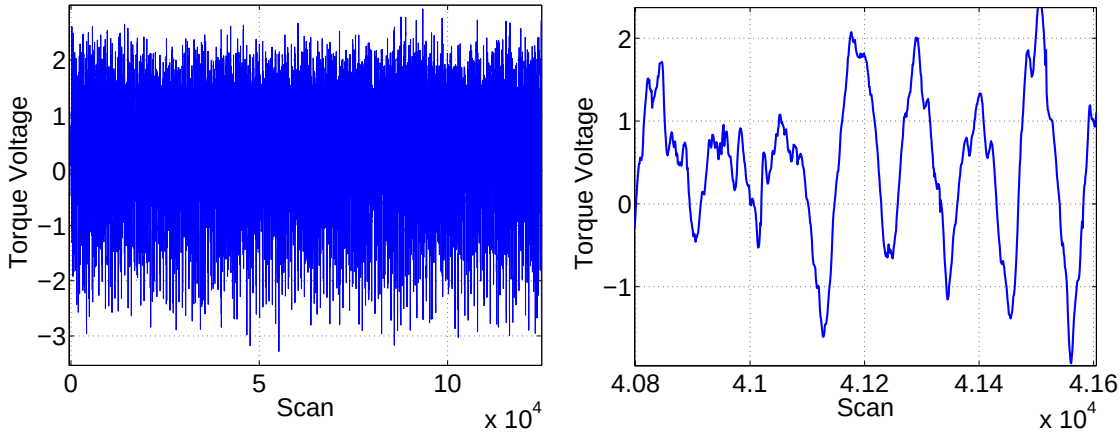

(a) A sample of the torque voltage output with the engine on.

(b) A zoomed in sample of the torque voltage output, with the engine on, in Figure 5.21(a).

Figure 5.21: Figures showing a sample set of torque voltages with the engine on.

Clearly, some of the torque signal must be because of the engine because it is periodic, shown by the strong peak corresponding to the engine RPM in the FFT in Figure 5.22. The RPM is found from the FFT by multiplying the frequency in Hz by 60,

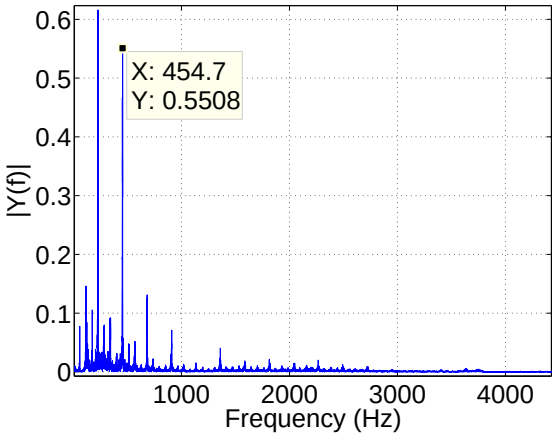

Figure 5.22: An FFT of the torque signal, with the engine on, showing two strong peaks.

which gives 27,282 RPM in this case. The other peak corresponds to a resonance effect in the engine test stand. This resonance could be heard even though the engine was very loud, and earplugs were being used. Because of the possibility of more than one peak, it is necessary to visually pick the peak corresponding to the RPM for each data point. Many of the FFTs of the torque signals only had one strong peak

corresponding to the RPM, but because of the possibility of having multiple peaks, it is necessary to visually confirm the frequencies in each FFT. There was never a case when multiple peaks were near the same frequency. If that were to happen, it would be hard to chose the proper RPM of the engine. Even though the Texas Instruments device was not connected to the magnetic RPM sensor, the DX8 and telemetry unit were used to visually note the approximate RPM of the engine. This aids in picking the proper peak in the FFT. Figure 5.22 shows that there are other peaks in the RPM data. These could be because of resonance effects, or because of the engine dynamics, but it is generally not understood what these peaks correspond to.

5.3.2 Thrust and Torque of Engine

The LRP ZR.30 X RC car engine seems like a small, harmless device with limited potential, based on its small size and weight, shown in Table 5.1. When looking at the maximum reported HP, however, the performance is extremely impressive. The engine uses several design features to achieve this high power. Figure 5.23(b) shows the piston and sleeve of the engine. Usually, two-stroke engines of this nature have 1 exhaust port and 3 intake ports. This engine has 7 intake ports and 1 large exhaust port. The exhaust port is seen on the left side of the brass sleeve. Technically, the engine has 5 intake ports. Two of them are the long slender vertical slots, one of which is shown in Figure 5.23(b). Two of the intake ports have a larger horizontal slotted shape, shown on the right of the sleeve in Figure 5.23(b). The 5th intake port is on the far right of the sleeve in Figure 5.23(b) but is not visible. It has the same shape as the two larger horizontal intake ports described. The extra two intake ports, which bring the total to 7, are the small square holes in the bottom of the sleeve. These holes allow the fuel-air charge to flow through small holes in the side of the piston. These extra two ports are an unusual feature and show the extreme measures taken to get maximum performance from this competition engine. The crankshaft also has some shapes called scoops, shown on the left end of the crankshaft in Figure 5.23(c). These are supposed to aid the flow out of the crankshaft. The flow of fuel and air through the crankshaft starts on the top, in the middle, and then exits the left end. There are certainly some complicated flow characteristics involving the connecting rod and crankshaft in the "scoop" area.

(a) LRP ZR.30 X (b) Piston and sleve [19] (c) Crankshaft [20]

Figure 5.23: Figures showing the LRP ZR.30 X Engine, piston, sleeve, and crankshaft.

Figure 5.24 shows the engine mounted to the engine test stand in the approximate configuration used. The muffler is not rigidly attached to the engine and the RC

Displacement	4.92 cc (0.30 cu in)
Bore	19.20 mm
Stroke	17.00 mm
Number of Ports	7 transfer, 1 exhaust
Max Power Output	4.15 HP
Max RPM	38,300
Weight	350 g
Weight w/o cooling head	254 g
Approximate Length	107 mm
Approximate Height w/o cooling head	68 mm
Approximate Height w/cooling head	114 mm
Approximate Width w/o cooling head	43.5 mm

Table 5.1: This table shows the specifications of the LRP ZR.30 X engine.

electronics are not shown, but otherwise everything is shown as it would be during testing. The aluminum pipe directly behind the engine had to be machined from aluminum bar stock because the original header was U shaped. To set the length of the

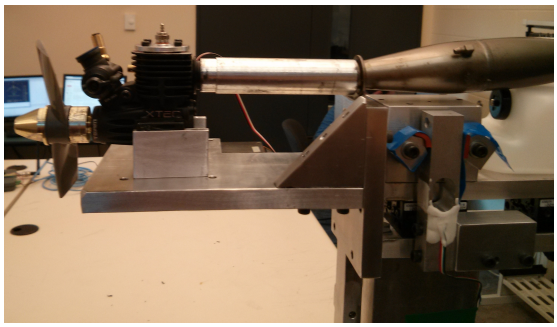

Figure 5.24: This figure shows an LRP ZR.30 X engine mounted to the engine test stand. The engine is not ready for testing in this figure, only the basic configuration is shown.

aluminum pipe, the inner and outer distance of the U shaped header were measured, and the average was taken in order to set the length of the aluminum pipe. This could potentially introduce some errors in characterizing the engine performance because the performance of small two stroke engines, like the one tested, are greatly influenced by the length of the header or pipe and the design of the muffler. The header or pipe connecting the engine to the muffler and the muffler are often called a tuned pipe. Tuned pipes increase the performance of two-stroke engines by reflecting the exhaust pulse, from when the exhaust port open, off of the back of the muffler as previously described. The length of the header and the shape of the muffler are therefore critical

in timing when the reflected pulse should arrive back at the engine. The reflected pulse increases the performance by increasing the pressure in the combustion chamber, which increases the density of the charge. This in turn allows more fuel to be burnt, which leads to more power. There are many tuned pipes available, but they are generally categorized as low speed or high speed pipes and they cause the engine to produce highest power at low or high RPM.

Because RC car engines are not optimized for extended full throttle operation, it was chosen to operate the LRP engine at a relatively low RPM of about 28,000. Also, it was anticipated that the engine would not be run at full throttle for extended periods of time except for takeoff, so a low RPM tuned pipe was chosen to assist the engine at the anticipated operating condition. Therefore, Reedy 2035 Tuned Exhaust System with a 3-chamber muffler and advertised linear power band was chosen.

The LRP ZR.30 X engine is to be used with RC car fuel. Most RC engine fuels contain nitro in some percentage ranging from about 10-40 %. There is also castor and/or synthetic oil in the fuel. There is much discussion on what kind of oil is best, but most fuels use a blend of castor and synthetic oil in the range of 18%. The rest of the fuel is composed of methanol. Methanol is a relatively cool running fuel, and this contributes to the high power to weight ratio of model engines, since less needs to be done to cool the engine, as previously described.

The option of maximum power of the power plant was desired, and engines produce more power with higher nitro content. Therefore, the highest recommended nitro fuel was used, which is 30% nitro. There are several fuels with 30% nitro, but there are mixed reports about all of them. For this reason, Thunder Power 30% Sport fuel was chosen. This was the cheapest kind but was still over $35 per gallon. A limitation of 30% nitro fuel is that the engine isn't supposed to last as long. This wasn't considered a problem because the flights at the competition are rather short. Additionally, the engine would be run with rich fuel-air mixtures to keep the engine cool and to ensure proper lubrication. Also, sport fuel had higher percentages of oil compared to available racing fuels. After frequent testing and use at the competition, the engine was still running well, so it is unknown what the longevity of a power plant would be using an LRP ZR.30 X engine. Depending on the application, it would be possible to use less nitro because the power plant produced more thrust than expected, and reducing the nitro content may not significantly impact the performance.

As was described, model engines use glow plugs to ignite the mixture in the combustion chamber. Glow plugs work similarly to a diesel engine in that there is not a timed ignition event; it happens because of the compression of the fuel-air charge. The glow plug has a coil of platinum in it that is initially heated with a 1.5 Volt battery or other power supply. The glowing element ignites the mixture, and the burning of fuel keeps the glow plug element hot after the 1.5 Volt battery is removed. The timing of ignition can be controlled by the gauge of the coil and by how big the hole is surrounding the glow plug element. "Colder" plugs have larger gauge elements, smaller holes around the element, and are used with high nitro fuels.

The LRP ZR.30 X engine has shims between the crankcase and the cylinder head. These are used to set the compression of the engine. The thickness of shims is different depending on the nitro content. For 30% nitro, 0.016 inches of shims were specified, and this is what was used. It may be possible to optimize the power output and fuel consumption of this power plant by trying a range of nitro contents, glow plugs, shim thickness, and tuned pipes. Clearly, this would require significant testing, but it is an area for optimization.

RC car engines usually have large cooling heads because there is little airflow around the engine most of the time. When the LRP ZR.30 X engine was used with propellers, it ran much cooler than recommended by the manufacturer. This is because of the fast airflow over the engine due to the propeller. Different amounts of cooling were tested by wrapping the engine in various amounts of aluminum foil in order to achieve the proper operating temperature. Eventually, the cooling head was removed completely because the engine ran at the proper temperature without it. The temperature was monitored using a sensor wrapped around the cylinder head of the engine, which was plugged into the telemetry unit. The temperature could then be seen on the DX8 screen.

The initial perceptions about the engine's small size were completely proven wrong on numerous occasions. The engine would vibrate bolts loose, break RC servos, wear out parts of the engine test stand, and make an incredible amount of noise. It was reported that the engine could be heard across campus when ran outside. This was not known about the engine when it was first tested on a simple test stand. The preliminary test stand only had the ability to measure torque. It was constructed using the same bearing block used in the final engine test stand, but instead of a

pendulum, it had a lever arm that would engage the top of a digital scale. It was possible to bolt the lever arm to the rest of the stand so that no torque could be measured. This was done to break the engine in.

Breaking in an engine consists of running it in a prescribed manner where fuel-air mixtures are rich, and the temperature and RPM are relatively low, as was described. This is done for about six tanks of fuel, where a tank is considered about 3 fluid ounces for RC cars. In between runs the engine is allowed to cool completely with the piston at BDC. The LRP ZR.30 X engine uses ABC cylinder liner construction, so getting the engine temperature reasonably high while also having a rich mixture is important.

An engine's performance is very dependent on the fuel-air mixture. With two-stroke engines, the fuel provides the lubrication. If the mixture is leaned out too much, it can damage the engine. Maximum power is only found by leaning the engine out, however. Therefore, there is a balance between getting maximum power and not damaging the engine. Racing fuels use less oil so that more methanol and nitro can be burned. With these fuels, the danger of running too lean is even greater, which is why sport fuel was chosen. Leaning out an engine means turning the high speed needle in until maximum RPM is reached. If the mixture is leaned further, the RPM will drop or the engine can quit. With the LRP ZR.30 X setup, there is another factor: the engine temperature. As the mixture is leaned, the engine gets hotter. The manufacturer recommends no temperatures higher than 260 degrees Fahrenheit. Therefore, when approaching maximum power with the LRP ZR.30 X, the RPM is monitored as well as the engine temperature. Because the engine produced more power than needed, it was usually only leaned out a little and allowed to run rich. Very rich mixtures produced much more smoke, and liquid oil could be seen spraying from the exhaust at times.

After the engine was broken in, it could be run with different propeller sizes in order to get it to reach certain RPM, shown in Figure 5.25. This was done by taking APC propellers in the 10-12 inch diameter range and cutting them down until ever higher RPM was reached. After each propeller was trimmed, it was balanced on a magnetic balancer to ensure the setup would not vibrate. This was an iterative process. The propeller mounted to the engine in Figure 5.25 is a special break-in propeller. The gold colored nut and hub securing it to the engine are specifically made for breaking in RC car engines. Most RC car engines are broken in in the car, but some advocate for

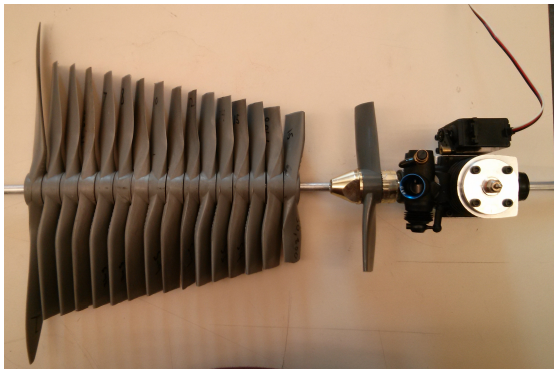

Figure 5.25: This figure shows an LRP ZR.30 X engine next to the shortened propellers used to find the engines power output curve.

using a break-in propeller. The break-in propeller was used as a baseline to establish a starting a diameter for the propellers to be trimmed. The range of propellers shown was created by adding or subtracting 5 mm to the baseline diameter and cutting the propellers down. As the propellers were cut and balanced, they were tested on the engine. Each propeller requires re-tuning the carburetor because the airflow through it at a certain RPM changes drastically. Once the desired RPM range was established and the propellers were ready, the engine performance could be characterized.

Figure 5.26 shows data gathered from initial tests using the simple torque stand described above. The data is fairly inaccurate because the scale readings would jump

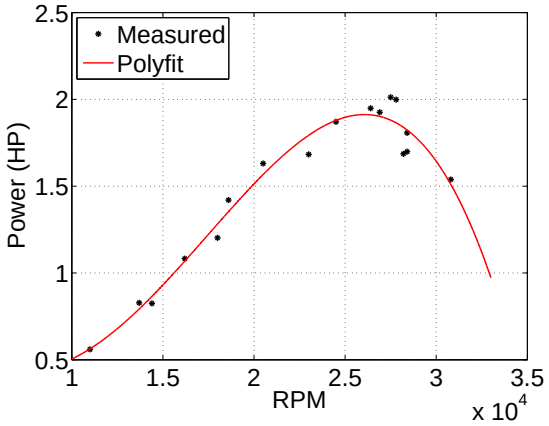

Figure 5.26: This figure shows a preliminary engine power output curve.

around by about 40 grams when the recorded value was on the order of 100-200 grams. The intense torque fluctuations of the engine were not well understood at this point. This is likely the reason for the values on the digital scale jumping around. Also, the

RPM was visually recorded from the display of the DX8 transmitter. These RPM values fluctuated by several hundred RPM. The lever arm attached to the engine would rattle or bounce on top of the scale so a piece of rubber was used to damp out the noise. When testing the engine initially, the lever arm could be supported by holding it, as described. When this was done with the engine running, the strong torque pulses could be felt. The torque produced by the engine was almost painful if the lever arm was held. This initial power curve gave some idea as to what to expect from the engine and gave insights into how to design the final engine test stand. The initial power curve is also what was used with the EPM code to choose the gear ratio for the geared power plant. It was assumed that there would be a loss of power through the gear ratio and it was unknown how reliable the initial power curve data was. For this reason, the curve used with the EPM code was 70% of the curve shown in Figure 5.26.

A more accurate curve was found using the purpose built engine test stand, which was previously described. Figures 5.27(a) and 5.27(b) show the mean thrust and torque voltages and the standard deviations in those voltages vs. RPM of the engine. The voltages and standard deviations can be compared vertically because they occur

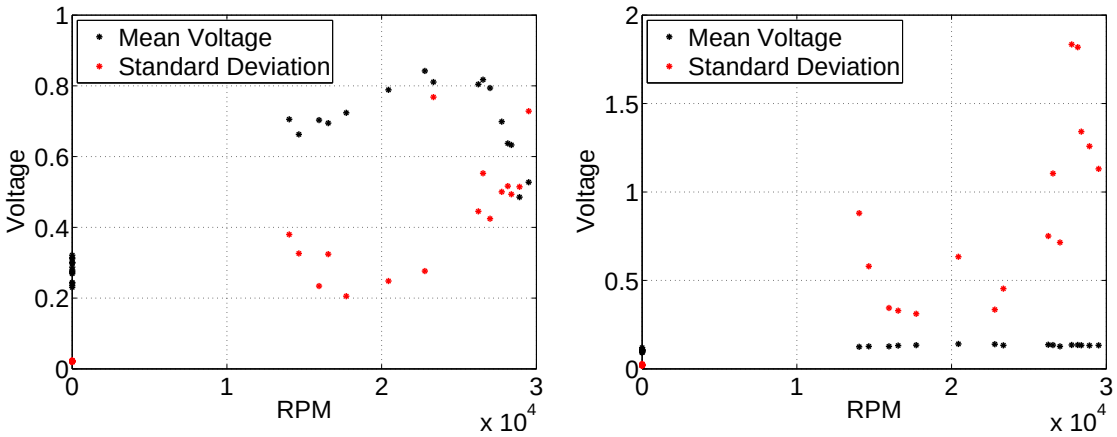

(a) Mean thrust voltage and standard deviation vs. RPM.

(b) Mean torque voltage and standard deviation vs. RPM.

Figure 5.27: Figures showing the mean thrust and torque voltages and standard deviations vs. RPM.

at the same RPM. Figure 5.27(a) shows that the mean thrust voltage is on average higher than the standard deviation. This is not true for the torque signal, shown in Figure 5.27(b), where the standard deviations are much larger than the mean voltage.

The grouping of points on the y-axis in either plot at 0 RPM show the zero readings. This shows that the thrust voltage with the engine off was steadily drifting as the testing continued. The torque zeros did not drift as much. It is clear from Figure 5.27(b) that the mean torque voltage vs. RPM doesn't change much, and this creates a potential for error as was described.

Figures 5.28(a) and 5.28(b) show the thrust and torque computed from the calibration constants and the data shown in Figures 5.27(a) and 5.27(b). This data seems to be

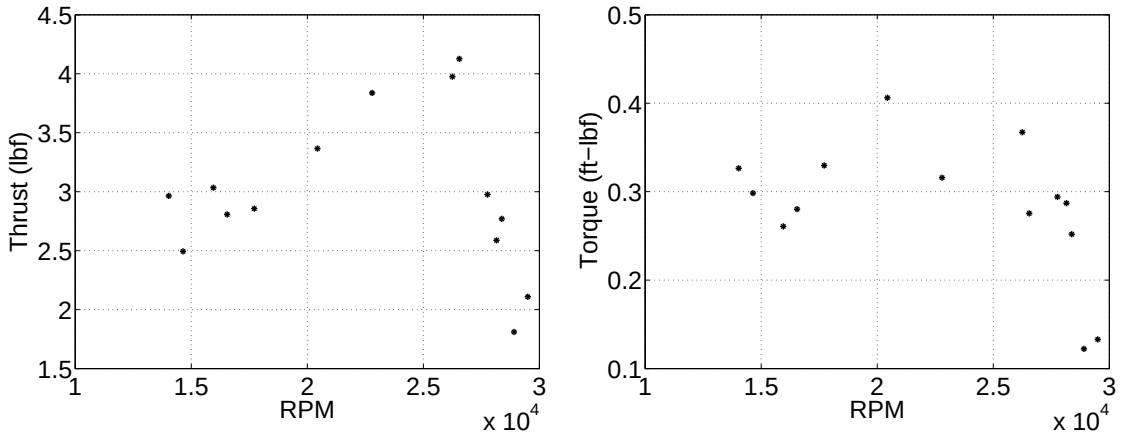

(a) Calculated thrust vs. RPM of the LRP ZR.30 X engine using the shortened propellers shown in Figure 5.25.

(b) Calculated torque vs. RPM of the LRP ZR.30 X engine using the shortened propellers shown in Figure 5.25.

Figure 5.28: Figures showing the thrust and torque vs. RPM of the LRP ZR.30 X engine.

inaccurate because there are no definite trends. This reflects the performance of the engine, however, because the engine would not stay at a particular RPM for long. When the engine was idling, the temperature would decrease. When the engine was run at full throttle with each propeller, the temperature would steadily increase. When the temperature increased, the engine seemed to increase in RPM and run smoother. If the engine was tuned at the higher temperatures, the RPM would change, and there wasn't a way to get repeatable results. Before data was gathered, the engine was run up to speed to try and get the temperature to stabilize, but the high temperatures could only be reached at full throttle. The engine could not be run at full throttle very long in order to not wear it out prematurely. Another factor is that as fuel was used from the fuel tank, the carburetor tuning would change slightly. This is because the fuel level decreasing changes how hard the carburetor has to suck

to pull in fuel. This is somewhat compensated for by the pressure nipple on the muffler which feeds pressure to the tank to help push the fuel to the carburetor. The engine manufacturers warned that RC car engines can't "hold their tune" because they are such high performance engines. This appears to be true, shown by the data in Figures 5.28(a) and 5.28(b). The errors introduced by the engine test stand could also be contributing to the irregular data. An important point about Figures 5.28(a) and 5.28(b) is that the zero data has been factored in when computing the thrust and torque, so these plots will not have the exact same trends as Figures 5.27(a) and 5.27(b).

To get the engine power output data shown in Figures 5.29(a) and 5.29(b), the data shown in Figure 5.28(b) is multiplied by the RPM after it is converted to RPS. Figure

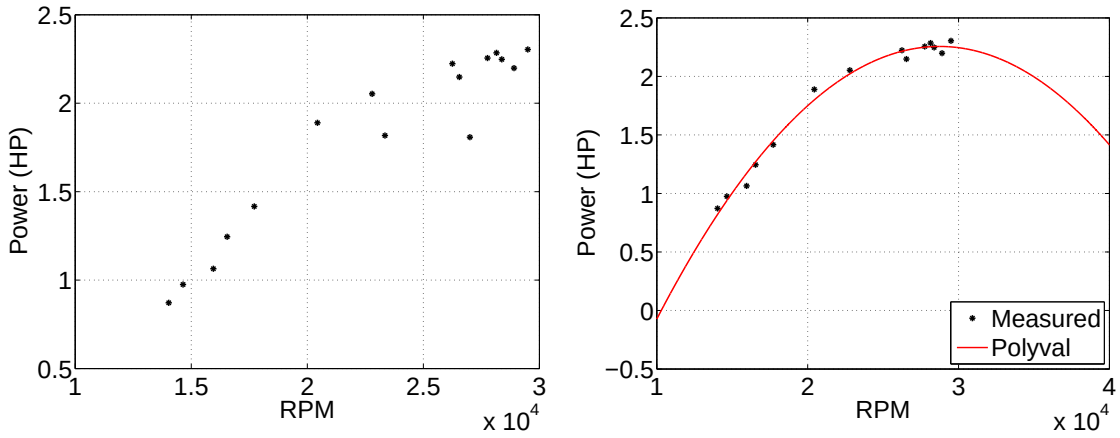

(a) Measured power (HP) vs. RPM of an LRP ZR.30 X engine.

(b) Line of best fit of the data points in Figure 5.29(a).

Figure 5.29: Figures showing the measured power vs. RPM and a line of best fit of the measured data.

5.29(a) shows two data points that seem to be outliers. These data points are not included in the line of best fit shown in Figure 5.29(b). The line of best fit assumes that the engine horsepower will decline after 30,000 RPM. The engines maximum RPM is 38,300, so it is unknown what the horsepower would be at those high RPM. The power seems to be leveling off, so it is possible that the power would remain rather constant. The preliminary engine curve seemed to show a decline in power at high RPM, more so than shown in Figure 5.29(b). The reason for the decline in power in the initial data is probably due to not measuring the torque fluctuations properly. Higher RPM than 30,000 were never reached in testing the geared power

plant, as will be shown, so higher RPM data would not have been of much use in this case.

5.3.3 Original Thrust and Torque Predictions

This section describes how the gear ratio and propeller were chosen for the geared power plant. The performance goal is simply maximum thrust over all velocities. If a compromise needed to be made as to where maximum thrust should be developed, it was desired to have maximum thrust at takeoff velocity and slightly higher, about 12 m/sec or about 27 mph. This is because of the design goals for the SAE Aero Design Advanced class competition. In the competition, if the airplane can takeoff and climb, it can basically do its mission. So high speed flight, and thus high speed thrust, is not a primary goal. It was assumed that propellers with less pitch would produce more efficient thrust at low speeds. This is because less pitch should lead to more of the propeller not being stalled at low speeds. As will be discussed, the highest pitch propeller was the best choice.

To generate thrust vs. velocity curves, the EPM code was used with the procedures previously described. The data needed is the engine power output curve, and each propellers power absorbed curves vs. velocity. The power output curves are then geared, and they become the power input curves to the propeller. The engine power input curves, with the final gear ratio of 100/13, are shown in Figure 5.30(a), where the blue triangles and line of best fit show the preliminary engine data points. The blue line of best fit below the top one is 70% of the top one at all RPM's. This was done so that the engine power input curve would intersect the propeller power absorbed curves, but also because it was unknown how reliable the initial engine power data was. This shows a limitation of using experimentally gathered propeller data because the propeller power absorbed curves may not extend high enough to intersect the desired engine power input curve. This happened because of the limitations of the 6-axis sting and because the electric motor could not spin the large 26 inch propellers any faster. Figure 5.30(a) shows the power absorbed curves for the XOAR 26x16 propeller, because this was the propeller chosen, as will be discussed.

The approach used to find the optimum propeller and gear ratio was to use a range of optimization velocities from 2-24 m/sec. Each propeller was then combined with the engine power output curve using the EPM code for all of the optimization velocities. The results are plotted together. It is not possible to see which optimization velocity corresponds to what line, but it is the general trends that are important. Figure 5.30(b) shows the power intersections found in Figure 5.30(a), except for this was done

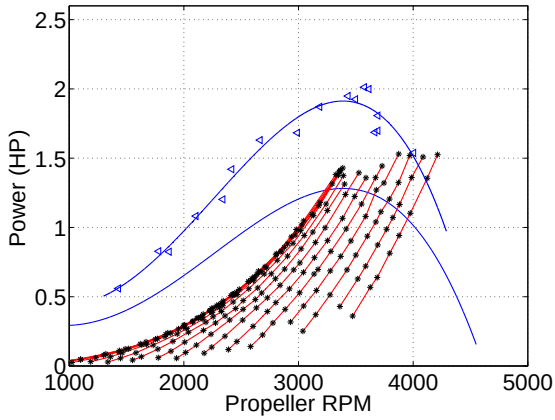

(a) Power (HP) vs. RPM of the propeller power absorbed curves for the XOAR 26x16 propeller and the engine power output curves geared 100/13. The original predictions were made using the lower engine curve, the final engine output curve is shown on top with the measured data points in triangles.

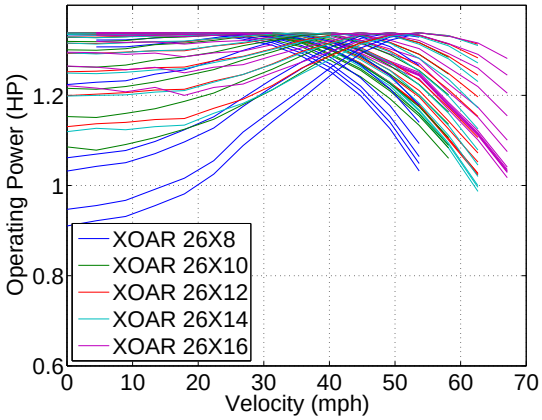

(b) Operating power (HP) vs. velocity for optimization velocities from 2-24 m/sec. This plot shows how the peak power of the engine can be moved such that maximum power is developed at higher velocities.

Figure 5.30: Figures showing the power (HP) vs. RPM and operating power vs. velocity for a range of optimization velocities from 2-24 m/sec.

for all of the propellers over the range of optimization velocities. Figure 5.30(b) shows that as the optimization velocity for each propeller was moved to higher velocities, the peak operating power moved to the higher velocities.

Table 5.2 shows the calculated gear ratio for each optimization velocity and propeller. The trends show that as the optimization velocity is increased, the gear ratio gets smaller. This agrees with what was previously shown, in that the propeller power absorbed curves move to the right as velocity is increased. To get maximum power at high velocities, the engine power input curve also has to be moved to the right. This is done by using smaller gear ratios with the engine power output curve.

Figure 5.30(b) shows that not every propeller has as much reduction in power at certain velocities. For example, the blue lines show the operating power for the XOAR 26x8 propeller. When the optimization velocity is high for this propeller, the low speed power, and therefore thrust, is significantly reduced. The propellers with higher pitch have less of this effect.

Figure 5.31(b) shows the thrust vs. velocity characteristics of all of the XOAR propellers with the range of gear ratios shown in Table 5.2. There is a break in the lines

V_{OPT}	26x8	26x10	26x12	26x14	26x16
2	5.47	6.56	7.33	7.55	7.87
4	5.99	6.54	7.31	7.52	7.89
6	5.95	6.47	7.30	7.50	7.88
8	5.91	6.46	7.30	7.49	7.92
10	5.84	6.41	7.23	7.43	7.88
12	5.72	6.32	7.17	7.36	7.85
14	5.61	6.23	7.07	7.26	7.74
16	4.93	6.11	6.93	7.12	7.66
18	5.32	5.94	6.78	6.97	7.48
20	4.75	5.78	6.59	6.76	7.29
22	4.98	5.61	6.42	6.58	7.12
24	4.80	5.46	6.23	6.36	6.94

Table 5.2: This table shows the optimal gear ratios for the optimization velocities, V_{OPT}, in m/sec, for each XOAR propeller tested.

for the XOAR 26x16 propeller. This is because the power absorbed curve did not extend high enough to intersect the power input curve of the engine. The trend can be extrapolated visually from the purple lines on the left, to the purple lines on the right. Figure 5.31(b) shows that the XOAR 26x16 propeller produces more thrust over velocity than all the other propellers, except for below about 14 mph where the XOAR 26x12 propeller begins to slightly dominate. If the XOAR 26x12 propeller were used, there would be a loss of about 1 lb of thrust compared to the XOAR 26x16 propeller at 50 mph. The XOAR 26x8 propeller is never able to make more thrust than the XOAR 26x16 propeller, which is an unexpected result. These results show that the gear ratio is critical in the design of a power plant. Table 5.2 shows that the gear ratios only changed slightly in the optimizations. For this reason, it would be very hard to find the proper gear ratio by trial and error or making an educated guess. Figure 5.31(b) also shows that many common rules for choosing propellers for engines on RC aircraft do not hold true when the gear ratio can be changed. In general, it is assumed that lower pitch, larger diameter propellers will make more thrust at low speed, and that high pitch small diameter propellers will make more thrust at high speed. Clearly, the choice of propeller is more involved than simple trial and error, as is often the technique used for most RC airplanes.

Figure 5.31(a) shows the RPM vs. velocity for all the XOAR propellers tested. The RPM trends are an interesting result. Basically, as the pitch of the propeller is

increased, the RPM must decrease in order for it to absorb the same power. This requires a larger gear ratio in order to reduce the RPM of the propeller. The benefit is, in general, higher thrust over velocity. There are also many other benefits. By

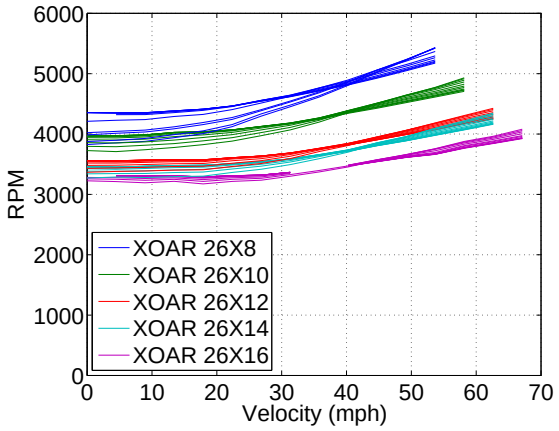

(a) RPM vs. velocity (mph) for optimization velocities from 2-24 m/sec.

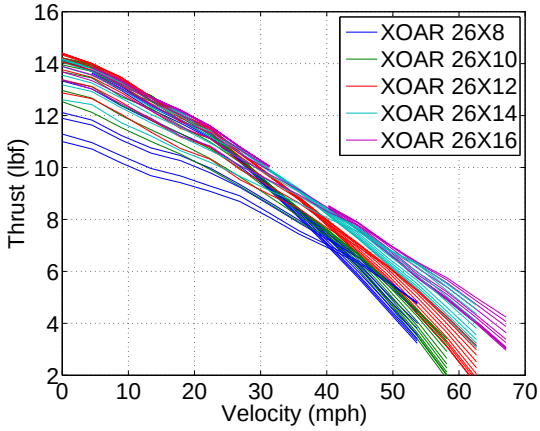

(b) Thrust vs, velocity (mph) for a optimization velocities from 2-24 m/sec. The XOAR 26x16 propeller has the highest thrust over all velocities except for below 10 mph.

Figure 5.31: Figures showing the RPM and Thrust (lbf) vs. Velocity for a range of optimization velocities from 2-24 m/sec.

turning the propeller at a slower speed, the power plant can be quieter because the propeller will be less noisy. Also, the propellers all had about the same mass. This means that the spinning mass of the propeller will have less effect on a propeller shaft, since it would require more torque to turn an object with more angular momentum. This will allow for the propeller shaft to be smaller even though it can spin the same diameter propeller. One drawback to the higher gear ratio is that the gears get much larger. The larger gear can be heavier, but holes can be machined in the gear to lighten it so that it is not a significant penalty. Larger gears can be an aerodynamic problem as well because they have larger frontal area which could be harder to fit a cowling around.

Using the same engine power curve, the overall result is that a propeller with the same diameter, but high pitch, turning at a slower RPM with a higher gear ratio, will produce more thrust at each velocity, compared to a propeller with less pitch. This brings into question several of the limitations assumed for aircraft. If is often said that takoff or low speed performance must be balanced with cruise performance. Perhaps high pitch propellers could produce nearly the same thrust as low pitch propellers at

low speeds if the gear ratio is chosen properly. This analysis was done for relatively low speed flight, however. By extrapolating the trends in Figure 5.31(b), it can be assumed the thrust would be near zero at about 70-80 mph for the XOAR 26x16 propeller. If a propeller with much higher pitch is used, there may be significant loss in thrust at low speeds, but perhaps the low speed thrust would be only slightly less than a low pitch propeller. This would have the result of higher thrust at high speed. The reason for this general rule regarding propellers really comes down to the gear ratio, and the power band where engines produce power. Figure 5.31(a) shows that less RPM is required for a high pitch propeller absorbing the same power. Engines produce more power at high RPM. Therefore, if a high pitch propeller is put on a high RPM motor, the results will show that the combined system performs poorly at low speed because the engine can't achieve the RPM required for high power, and this would cause the thrust to decrease. If high RPM engines with high power are used with no restrictions on the gear ratio, it may be possible to get much better thrust vs. velocity performance from fixed pitch propellers.

5.3.4 Geared Power Plant

Based on the results from the EPM code above, the XOAR 26x16 propeller was chosen with a gear ratio of 100/13 or 7.69:1. This is not exactly one of the gear ratios found by the EPM code, as is shown by Table 5.2, but falls between an optimization velocity of 14 and 16 m/sec. There were some restrictions that led to this choice of gear ratio. The smallest clutch bell gear that could be mounted to the engine was a metric 13 tooth gear with a module of 1, shown in Figure 5.32(a). The clutch bell is an HPI Racing, 13 tooth, surface hardened clutch bell. The width of the clutch bell gear is 6 mm. To make the gears more robust, the large gear should have the same width in order to maximize the contact area for the teeth. There were not many options for the large gear, however, because not many had the proper width and module. The module of the gear teeth must match, or the gears will make noise and fail prematurely. It was desired to use the smallest gear possible for the large gear in order to reduce weight. A 1215c steel, 100 tooth, 6 mm wide gear was the best choice for this reason because they were available without a hub and were the cheapest, shown in many of the following Figures. RC car engines are almost all

(a) Centrifugal Clutch (b) Clutch Shoes [21] (c) Flywheel [22]

Figure 5.32: Figures showing the clutch setup, 3 clutch shoes, and flywheel.

designed to be geared. They also generally use some kind of centrifugal clutch so that the car or truck can be stopped with the engine idling, shown in Figure 5.32(a). Then when the throttle is opened, the centrifugal force causes clutch shoes, shown in Figure 5.32(b), to engage the clutch bell which is connected to the gear on the engine. This makes RC car engines easier to use than RC airplane engines in this case because they are already set up for gearing. The clutch also has the benefit of protecting the system from resonance effects by slipping if a resonance occurs. It would be possible to machine a gear that would bolt directly to the engine. This would be lighter and simpler, but significant testing and analysis would have to be conducted

to ensure the system is safe. Along with the gear on the engine is a flywheel, shown in Figure 5.32(a) by the silver disk behind the clutch bell with a serrated edge, and by Figure 5.32(c). The flywheel bolts directly to the engine crankshaft and always rotates with the engine. The clutch shoes slide on to the pegs on the flywheel. When the engine spins fast enough, the centrifugal force causes the clutch shoes to slide against the inside of the clutch bell. This causes whatever the clutch bell is driving to start spinning. Once the speed of the engine and object being driven equalize, the clutch shoes stop sliding, and the clutch locks together. The force that the clutch shoes push against the clutch bell with is proportional to engine RPM. As the engine produces more power, the clutch shoes clamp harder to transmit the increased power. Figure 5.32(b) shows two different types of springs and some long set screws. The springs have different spring constants which allows for tuning the clutch to engage at a certain RPM. The long set screws can also be used to set when the clutch should engage. Lastly, there are different clutch shoe setups that can be used. There are 2 and 3 shoe setups. Two shoes are said to provide less holding power and softer starts for RC cars, where 3 shoes have a more aggressive engagement. For a propeller, the most holding power is desired, so 3 shoe setups are best. The clutch was eventually set up with the springs pushing the clutch shoes out so that the clutch was always engaged. This was done to provide protection from the clutch slipping at high power, help the engine idle, and to make the clutch shoes last longer. Set up this way, the clutch only provided protection from resonance, and slight protection if there was a propeller strike. Either configuration with the clutch springs worked well, however.

The combined weight of the flywheel, gear, and clutch shoes add inertia to the engine crankshaft which helps the engine idle and smooths out vibrations. If a gear was bolted directly to the engine without a clutch, something would need to be included to give the spinning mass extra inertia. One option would be having a flywheel like disk behind the gear, though the gear and flywheel would be one piece.

Most RC propellers spin in a counterclockwise direction when viewed from the front. It is possible to get propellers designed to spin clockwise as well; these are known as pusher propellers. Pusher propellers allow a standard engine to be mounted facing the rear of the airplane and produce forward thrust. It would be possible to use a pusher propeller in a tractor configuration, but the engine would have to spin in a clockwise fashion. Electric motors can easily be configured to spin in either direction, so most electric propellers only spin counterclockwise. Because an electric propeller was to be

used in this case, it means the propeller shaft would have to spin counterclockwise. The engine also spins counter clockwise. This means the engine would have to be mounted facing the rear, so that the rotation of the engine would rotate the propeller in the right way, shown in Figure 5.33(b) where the power plant has been mounted to the engine test stand. This configuration has some benefits. Most RC car tuned

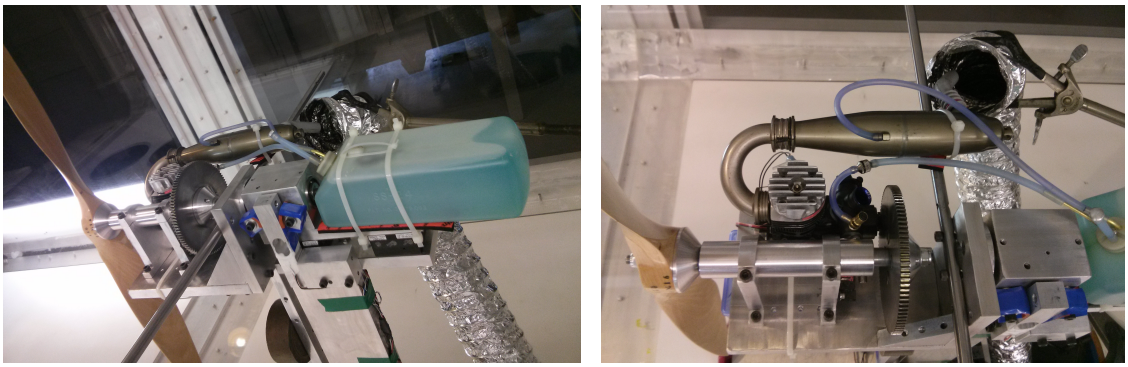

Figure 5.33: Figures showing top views of the geared power plant, mounted to the engine test stand.

pipes have a U bend in the header. This works well with the proposed configuration because the muffler will face the rear as desired. A draw back is that the header comes close to the propeller, and the propeller shaft could be shorter if the header was not in the way. An RC car engine with side exhaust would allow for a more compact setup.

To drive the large propeller, a shaft supported on bearings was needed. The shaft had to be sized to carry the torque forces from the engine and the gyroscopic forces from the propeller. The shaft would also have to carry the thrust produced from the propeller, but this force is small compared to the gyroscopic and peak torque forces. The propeller and shaft are the most dangerous parts of this power plant, so a large safety factor was needed. For this reason, a precision ground 10mm shaft was chosen, made from O1 oil-hardened tool steel with the specifications shown in Table 5.3.

Hardness	Rockwell B89-B96
Maximum Attainable Hardness	Rockwell C60-C62
Heat Treatment	Annealed
Diameter Tolerance	0.013 mm

Table 5.3: This table shows the specifications of the O1 oil-hardened tool steel used for the propeller shaft [23].

To choose this diameter and material, a former mechanical engineer in the mechanical engineering department was consulted who has industry experience designing small ICEs. Based on the size of the propeller and characteristics of the engine, the 10 mm O1 steel shaft was highly recommended.

To support the shaft, at least two bearings were needed. There are several kinds of bearings that could be used. Angular contact bearings can support axial loads as well as radial loads. Radial bearings can only support radial loads. The propeller shaft will have moments put on it by the spinning propeller, perpendicular to its axis of rotation. This will cause the bearings to have to support radial loads, where each bearing will carry some of the load. As the RPM is increased, the propeller will produce thrust, which will cause an axial load in the shaft. This axial load must be carried by the bearing. If radial bearings are used, thrust bearings would have to be used to carry the axial forces. To simplify the setup and reduce the parts required, two angular contact bearings were used, shown in Figure 5.34. These bearings were

Figure 5.34: This figure shows the two angular contact bearings used.

purchased from Boca Bearings and are intended for small jet turbine engines. They are ceramic, high speed bearings, and are described in Table 5.4. They are also fairly

Bearing Material	Stainless Steel 440C
Rolling Element Mat.	Ceramic SI3N4
ID	10 mm
OD	19 mm
Width	5 mm
Max RPM	90,000
Working Temp.	220 C
Weight	4.33 g
Angle Contact	15 deg
Pre-load	light

Table 5.4: This table shows the specifications of the D6800/603C Angular Contact Bearings used for the propeller shaft [24].

expensive, but the SAE team was partially sponsored, so the cost was not as high. The reason for choosing these bearings is that most angular contact bearings are much larger and therefore heavier. These bearings only weigh 4.33 grams each, but they can carry loads well above what could ever be expected. The bearings can only carry axial loads in one direction, however. So the rear bearing would carry the axial thrust produced by the propeller, and the front bearing would carry the loads caused by the gyroscopic loads from turning the propeller. It was discovered that if the bearings were loaded in the wrong direction, dropped, or mishandled, they could fly apart. In one case both bearings essentially exploded. This was due to trying to disassemble the shaft assembly with a pry bar. Once the inner race of one of the bearings began to move it flew off with such force and speed that the ceramic balls went everywhere. After this, the shaft assembly was only disassembled inside of a plastic bag, and the bearings did fall apart on a few occasions after this. A positive aspect of the ball bearings is that even if the bearings fell apart, they could be carefully reassembled by putting the balls in between the races and then snapping the races back together.

As shown in Table 5.4, the bearings need a light pre-load. What this means is that something must push against one of the bearing races so that the play in the bearings is removed, and to prevent them from falling apart as described. This was done by using a small wave spring, shown in Figure 5.35. This wave spring is placed behind

Figure 5.35: This figure shows the wave spring behind the front bearing.

the front bearing so that it pushes on the outer race. In this way, the back bearing carries the thrust force from the propeller, and the front bearing carries any drag forces or the force from a light collision. By putting the wave spring behind the front bearing, the shaft assembly does not move with increasing thrust, and the gear mesh stays the same as well. The bearings pull against each other in this way to take any play out of them. The wave spring can push with about 50 lbs of force when fully compressed, so the dimensions of the shaft and supports for the bearings have to be

sized so that the wave spring is only slightly compressed.

Figure 5.36 shows the propeller shaft. This shaft happens to be the one used on the final design, but the only difference is that this shaft is about 0.7 inches shorter. The shaft has tapered fits on either end of 7 degrees. This is known as a self-locking taper. What this means is that if a hub is bolted to the shaft with the exact same angle, the two pieces of metal will lock together with a great amount of force. Once the hubs are bolted on, the only way to take the shaft apart is with a large clamp or with a hammer. The tapered fit must be machined very precisely. If one of the angles is

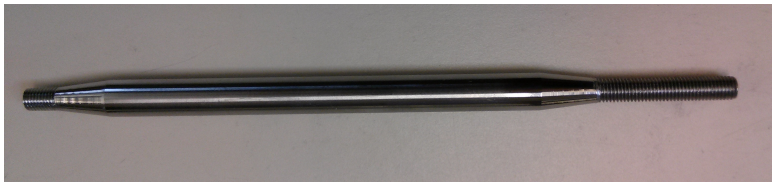

Figure 5.36: This figure shows the propeller shaft.

off, it may not be self-locking. Also, if done improperly, the propeller may wobble as it spins or vibrate. The shaft and hubs were made by several members on the SAE team and required many hours to complete. The hubs are shown in Figure 5.33(b). The first hubs were over designed so that they would be simple. The front hub only supports the propeller. The propeller nut secures the propeller and the front hub to the shaft. The rear hub has 4 tapered holes in it to support the 100 tooth gear. The hub is behind the gear so that the 10 mm hole in the gear can slide onto the 10 mm shaft. This allows the gear to be almost perfectly centered on the shaft.

The gear, hubs, shaft, and propeller all become one assembly when assembled around the tube which supports the two bearings, shown in Figure 5.37. This tube is then clamped by the two vertical aluminum pieces which have a slot cut in them. In this way, the two bolts on top can bend the aluminum so that the propeller tube is secured all along its radius by the clamping force. This also allows for easy forward and backward adjustments of the gear mesh. The engine is then mounted to two smaller vertical pieces, and the entire assembly is bolted together. The gear mesh is supposed to be set with a piece of paper between the gears. This distance was set by carefully measuring where the engine would be in relation to the 100 tooth gear. It is possible to put steel shims under the engine to fine tune the gear mesh.

Once the power plant was assembled, it was mounted to the engine test stand. The

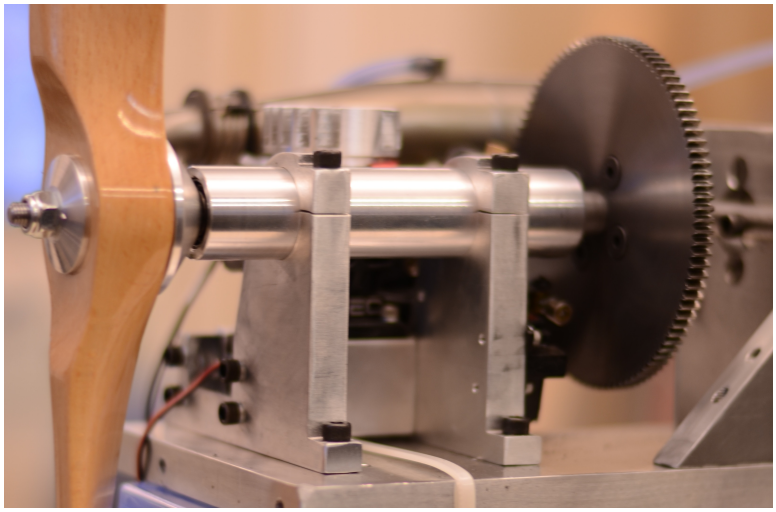

Figure 5.37: This figure shows a side view of the geared power plant.

power plant and engine test stand were then mounted to a table with castering wheels on it. Since the setup was unproven and no similar setups have ever been made that are known of, there was the possibility that something could go seriously wrong. For this reason, it was tested outside first were it could do little damage if it flew apart. It was decided to test the power plant by first starting the engine and ensuring everything was operating correctly. Then the idea was to incrementally increase the RPM until full throttle was reached. At all times no one would be allowed to be in front or to the side of the power plant when it was running since any fragments would likely fly out sideways or forward. At each increment in throttle, the table that the engine test stand and power plant was mounted to would be turned left and right as fast as possible to cause the largest possible gyroscopic loads on the shaft. This was done all the way to full throttle. The power plant was then thoroughly inspected for any damage and everything was found to be working properly.

After the power plant had been tested outside, it was mounted to the engine test stand in the closed return wind tunnel, shown in Figure 5.38 and 5.39. The engine stand was positioned so that the axis of rotation of the propeller was in line with the wind tunnel flow direction. The engine exhaust had to be evacuated from the wind tunnel. This had to be done without changing the exhaust pressure of the engine. Figure 5.33(b) shows the exhaust tube used to capture the engine exhaust. There is a gray plastic extension coming from the engine muffler. The plastic extension was placed so that it was slightly inside the exhaust tube. The exhaust tube is left open

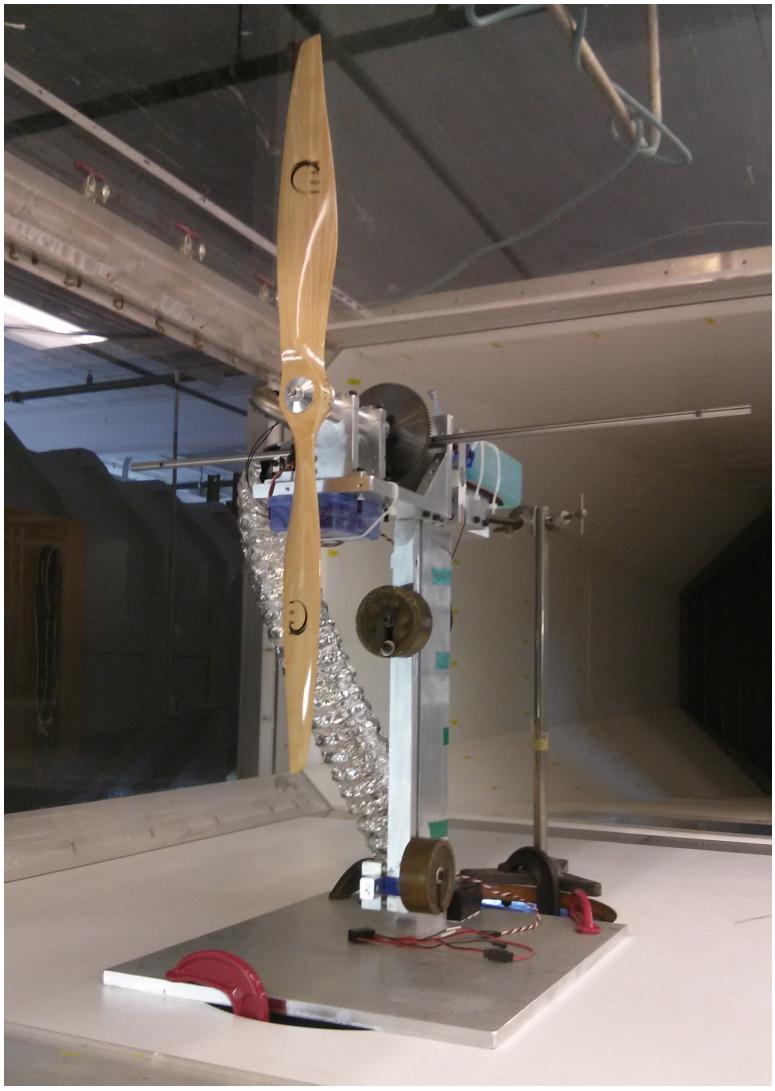

Figure 5.38: This figure shows a geared power plant with a 26x16 XOAR propeller and the LRP ZR.30 X engine, mounted to the engine test stand.

so that fresh air will be drawn in with the engine exhaust and so that the pressure will be almost the same as the engine would see without an exhaust tube capturing its exhaust. A centrifugal electric fan was then attached to the exhaust tube and more tube was attached to the fan to duct the exhaust out a window. Experiments were conducted to determine which end of the tube to place the centrifugal fan. It seemed that if the fan was placed near the engine, it would push more air than if the fan was near the window. This may be due to the centrifugal fan drawing higher pressure air near the engine. If the centrifugal fan was near the window, it would have to pull air over a larger distance and this would force the centrifugal fan to pull a vacuum

in the tube rather than pressurize the tube. A concern with this setup is that the engine exhaust can have fairly large amounts of un-burnt fuel and oil in it. If the mixture was just right, it would be possible for a spark from the centrifugal fan to ignite the mixture. For this reason, the tube openings before and after the centrifugal fan were checked to see if there was any fuel or oil residue. The tubes were found to be completely dry, even after extended periods of engine running. There was a lot of excess air flowing through the tube, so the setup seemed safe. The exhaust tube was held in place by clamps on a stand, which was clamped to the wind tunnel. It was important to check that the exhaust tube did not touch any part of the engine stand as that could skew the results.

As can be seen in Figures 5.38 and 5.39, there are many things behind the engine stand blocking the air flow that could affect the measured results. The thrust and

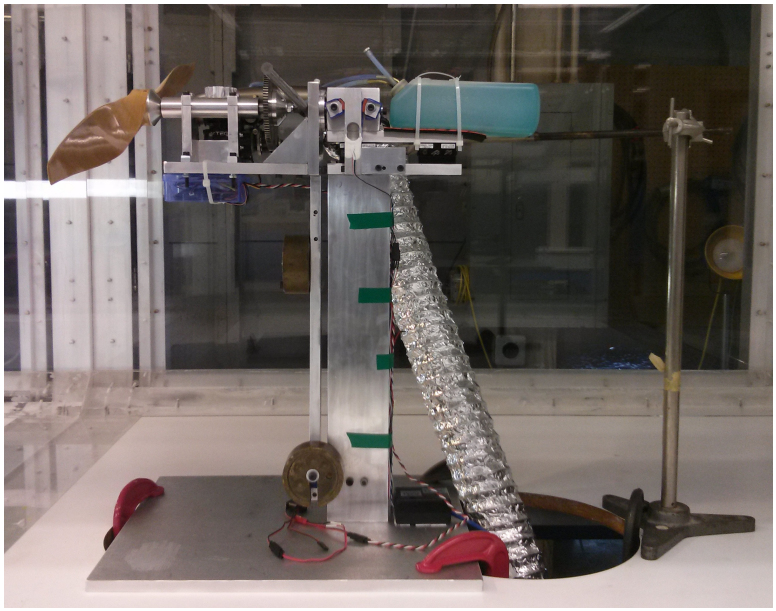

Figure 5.39: This figure shows a side view of a geared power plant with a 26x16 XOAR propeller and the LRP ZR.30 X engine, mounted to the engine test stand.

torque compensation discussed earlier were done without the power plant, exhaust tube, stand holding the exhaust tube, and RC electronics mounted. There is probably a fair amount of drag due to the power plant itself that has not been accounted for in the analysis. To compensate for the drag properly, the propeller testing apparatus should be tested for a range of velocities without the propeller mounted to it. The engine test stand should then be tested with everything set up as if the power plant

were to be tested, as shown in Figures 5.38 and 5.39, except for that the propeller should be removed. In this way, only the propeller performance would be compared, and the drag of everything else would be subtracted.

The following results have some known errors. The thrust compensation discussed previously has been subtracted from the measured thrust data, but it is unclear if some compensation should be done to the torque voltages. A problem with the setup is that it is difficult to start the engine inside of the wind tunnel, so once started, it is best to leave it running. This is the reason for the relatively large fuel tank on the engine test stand. The effects of increasing velocity on the torque sensor voltage were not known initially. The data for the power plant were found by zeroing the engine stand with the engine off, then starting the engine and taking data at each velocity without stopping the engine. As velocity was increased, the torque voltage should have drifted as discussed for the torque compensation. This would affect the torque and horsepower measured for the engine significantly if not accounted for. There were two compensation schemes that could be used for the voltages. One approach was to zero the voltages between each data point. This appeared to eliminate the voltage drift of the sensors as velocity was increased. If the voltage readings were zeroed only at the start, and then the velocity was increased and data was taken, there was a significant drift in torque voltage that needed to be subtracted. Since the engine was started and tested at each velocity without zeroing between each data point, it seems that the torque voltage should have been drifting as the velocity was increased. The measured data for the power plant was gathered as quickly as possible because the engine would wear out faster if run more than necessary. There are probably time dependent characteristics that affect how fast the torque voltage drifts. If the test with the power plant was conducted in a faster manner than the torque compensation tests were, there would likely be errors in the results. Needless to say, the results are not as accurate as they could be and more testing should be done to compensate for the drag of the fixtures and eliminate the voltage drift of the torque sensor. The results from both compensations schemes for the torque voltages are shown below. On the left, the torque voltage drift was not subtracted from the readings, and on the right they were, for the variable of interest.

The RPMs were found from the FFT of the torque signal, and this would not be affected by a voltage bias. Figure 5.40(a) shows the measured engine RPM vs. velocity. The propeller RPM is found by dividing the engine RPM by the gear ratio, shown

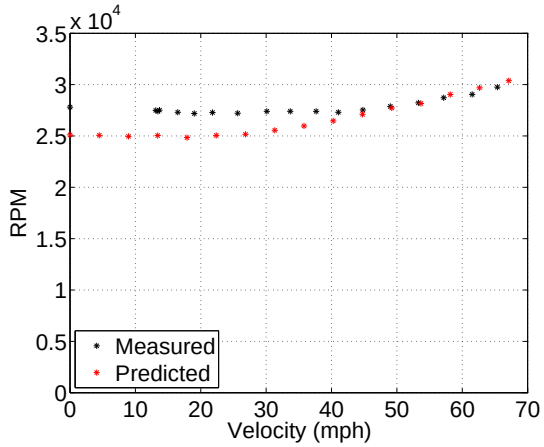

(a) Measured and predicted engine RPM vs. velocity.

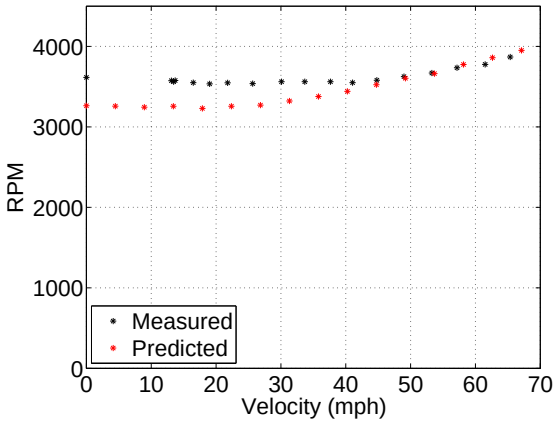

(b) Measured and predicted propeller RPM vs. velocity (mph).

Figure 5.40: Figures showing the measured and predicted engine and propeller RPM vs. velocity.

in Figure 5.40(b). The FFT of the torque signal only has frequency content from the engine combustion and vibration, so there is no way to measure the propeller RPM directly. It would be possible to use a magnetic sensor with the large gear driving the propeller to directly measure the propeller RPM. This could be used to see if the centrifugal clutch is slipping. The predicted RPM using the initial engine power output curve is somewhat lower than the measured RPM until about 50 mph where the prediction is very close to the measured data.

Figures 5.41(a) and 5.41(b) compare the two approaches used to attempt to adjust the torque voltages. Figure 5.41(a) assumes that there has been no voltage drift, and that the tests were conducted fairly fast. Figure 5.41(b) assumes that there has been voltage drift as described in Section 5.2.4. In Figure 5.41(b), the line of best fit used in Figure 5.17 has been subtracted from each torque value at each velocity. In Figure 5.41(a), the torque rises and then drops, where in Figure 5.41(b) the torque only drops. The RPM of the engine is the one known variable. The RPM of the engine slightly drops until about 40 mph, and then it rises. It would seem that the torque should be fairly constant if the RPM is almost constant. For this reason, it seems the proper torque values should lie somewhere in between those shown as measured data points in Figures 5.41(a) and 5.41(b). The torque does drop off with increasing RPM, and this was predicted. There is one data point that can be relied upon more than the others, and this is at 0 velocity. Here, there was no airflow over the torque

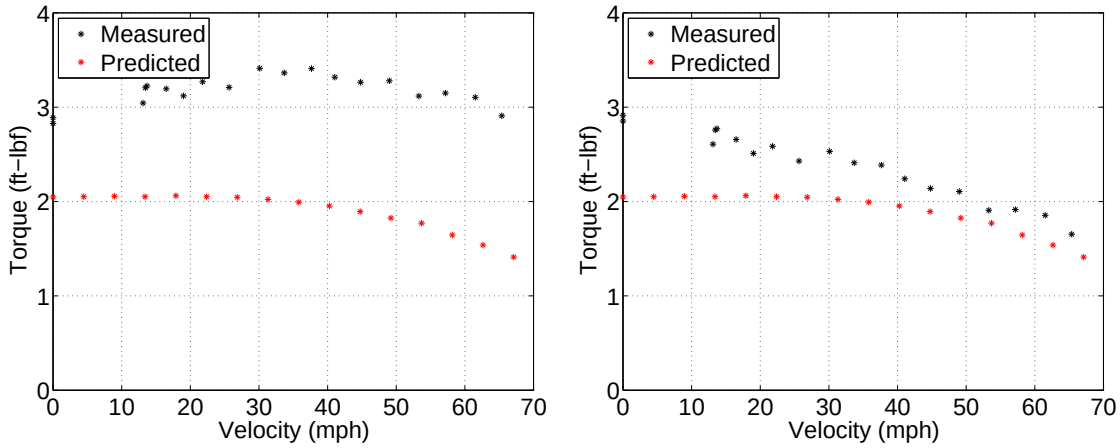

(a) Measured and predicted torque (ft-lbf) vs. velocity (mph).

(b) Measured and predicted torque (ft-lbf) vs. velocity (mph) taking into account voltage drift.

Figure 5.41: Figures showing the measured and predicted torque vs. velocity taking into account the drift of torque voltage.

sensor so the voltage should not have drifted in the short time the data was taken. In both figures, the measured torque is significantly higher than predicted for most of the velocity range, and this is due to the engine producing more torque and power than initially predicted. An interesting point here is that the low torque and high RPM of the engine has been exchanged for much higher torque but reduced RPM. This is the benefit of gearing, which the EPM code takes advantage of.

Figures 5.42(a) and 5.42(b) show the computed power vs. velocity of the power plant. Figure 5.42(a) assumes that there as been no voltage drift and Figure 5.42(b) assumes that there has been voltage drift. These data points show the same trends as the torque data which makes sense because the RPM was almost constant. As far as the engine characteristics go, it does not make sense that the engine would develop more power at full throttle if its RPM was decreasing, which it was up until about 40 mph. For this reason, Figure 5.42(b) seems more accurate. Figure 5.42(b) shows the engine power dropping fairly fast however, and this does not seem right either.

Figures 5.43(a) and 5.43(b) show the computed power vs. propeller RPM of the power plant. The power and RPM data were stored in vectors of the same size and with values in the same order. Therefore, they can be plotted in this manner, even though the data was gathered with increasing velocity. Figure 5.43(a) shows that the power was staying rather constant with RPM, though there are two data points where the

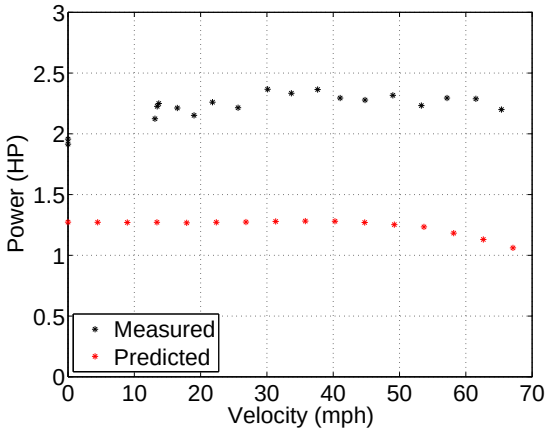

(a) Measured and predicted power (HP) vs. velocity (mph).

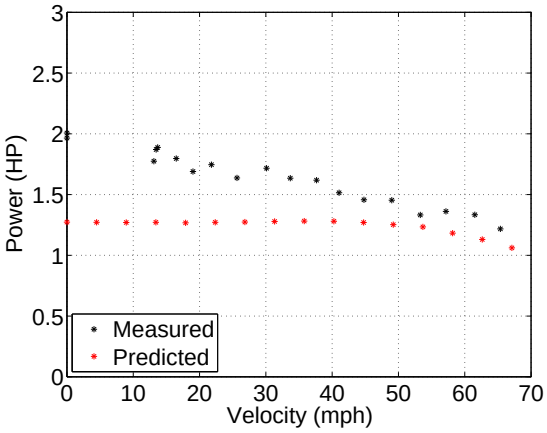

(b) Measured and predicted power (HP) vs. velocity (mph) taking into account voltage drift.

Figure 5.42: Figures showing the measured and predicted power and vs. velocity taking into account the drift of torque voltage.

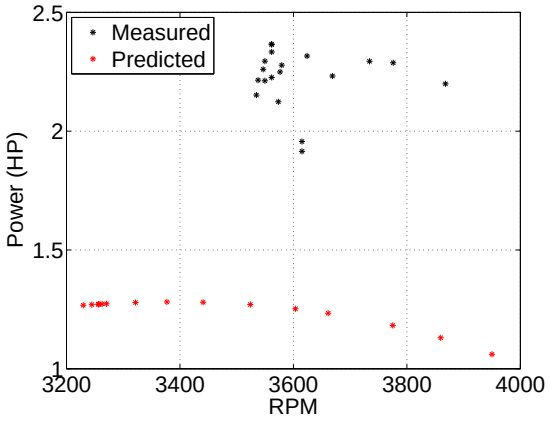

(a) Measured and predicted power (HP) vs. RPM.

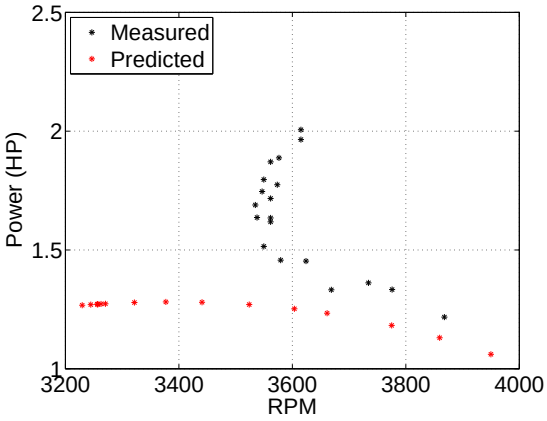

(b) Measured and predicted power (HP) vs. RPM taking into account voltage drift.

Figure 5.43: Figures showing the measured and predicted power vs. RPM taking into account the drift of torque voltage.

engine power has dropped, even though the RPM is the same. Figure 5.43(b) shows that the power of the engine steadily declined at about the same RPM for many of the data points. This could only happen if the torque of the power plant was declining.

From the discussion above, it is clear that nothing definitive can be said about the drifting torque voltages from the data shown. Another way to see if the measured data makes sense is to plot the measured data points from the geared power plant

with the measured data points from the propeller testing. The measured power and RPM at various velocities for the geared power plant should be near the curves found with the propeller testing apparatus. This is shown in Section A in the appendix. There are two velocities missing there, 2 and 4 m/sec, and this is because the propeller pushed the air so much that it wasn't possible to measure those speeds. These curves take into account the voltage drift of the torque sensor. The measured data points lie almost on the power absorbed curves that were initially measured, so it makes sense to subtract the voltage drift of the torque sensor as velocity is increased. Therefore, the figures on the right above are the most correct.

Figure 5.43(b) is then the correct power vs. RPM curve for the geared power plant. This means that the engine's power output was steadily declining at the same RPM. This is likely due to the pressure in the test section of the wind tunnel changing. As the velocity is increased, the pressure should drop by Bernoulli's principle. This will mean less dense air for the engine to burn. It also means that whatever carburetor settings are initially used will be wrong as the tunnel speeds are increased. This is an effect that will only be seen in the wind tunnel and not on a flying airplane. This makes it hard to conduct wind tunnel testing with an internal combustion engine. To get the engine to produce its maximum power as the wind tunnel speed is changed, the carburetor settings would have to be changed. The only way to know how to change them would be to test just the engine in the wind tunnel at all of the speeds and find the optimum carburetor setting at each speed. This would add a significant amount of testing time. It may be best to lean out the mixture as velocity is increased. This could be done by making something that can change the carburetor mixture remotely using the DX8. Then the mixture can be adjusted to give maximum RPM and power for each speed. This could be done when testing the geared power plant, and it would save time.

Figure 5.44 shows the predicted and measured thrust vs. velocity of the power plant. The thrust at low velocity is much higher compared to the original prediction. This is likely due to the engine producing more power. At high velocity, the measured thrust is lower than predicted. The drag of the propeller testing apparatus and combined engine test stand and power plant were not completely accounted for. If the drag of both setups is completely removed from the measured data, it is possible that the measured curve would lie above the predicted curve because the drag of either setup should only have affected the results at higher velocity. Section A in the appendix

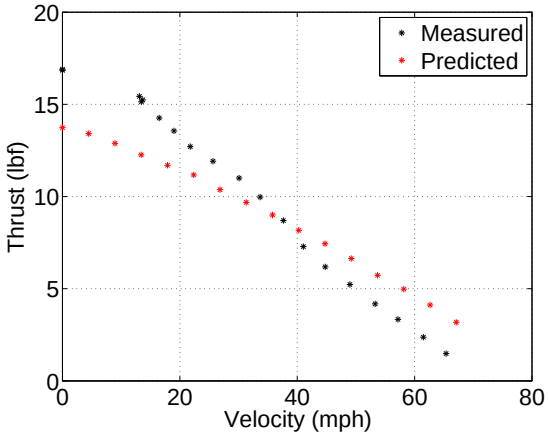

Figure 5.44: Measured and predicted Thrust (lbf) vs. velocity (mph).

shows the measured thrust data found from the propeller testing apparatus. Section A also shows data points found from the geared power plant. There is about 1-2 lbs of thrust difference between the measured thrust for the same RPM. This is likely due to not accounting for the drag of either setup.

For the results shown in this section, the initial engine power output curve was used with the EPM code to form the predictions. The power vs. RPM data shown in Figure 5.43(b) was the most accurate. To see if the EPM code could predict the measured thrust vs. velocity and other parameters, a piecewise engine power out curve was constructed and used with the EPM code, as will be shown next.

5.3.5 Polyval and Offset Thrust and Torque Predictions

Next, it will be shown that the EPM code can accurately predict the measured geared power plant performance if given proper data. To do this, the power absorbed curves found from the propeller testing are offset to intersect the measured data points from testing the geared power plant. This effectively uses the trends in the data from the propeller testing apparatus, but offsets the curves vertically to contain the measured data points. These offset curves are shown by the green curves in Section A in the appendix.

A new engine power curve is needed to represent the performance of the engine in the wind tunnel. The power vs. RPM data measured in the wind tunnel for the geared power plant, shown in Figure 5.43(b), can be used to construct a new engine power input curve. This is done by approximating the first part of the engine curve by a polynomial that is fit to the measured data shown in blue triangles in Figure 5.45 and then offsetting it down to intersect the highest measured power in Figure 5.43(b). This means that there was about an 11% loss in power, even when the engine was running with its optimally tuned carburetor setting at zero velocity. This seems like a reasonable loss in power from gearing. The rest of the engine power input curve is constructed by linearly interpolating between several of the green triangles shown in Figure 5.45. This is a very strange power output curve, but it shows that the EPM code can be used with arbitrary engine power curves. The only constraint is that the power absorbed curves can not be allowed to intersect the engine power curve more than once.

An interesting effect of the power plant in the wind tunnel was that data below about 6 m/sec was not possible to record, as was briefly mentioned. This is because the power plant would move the air in the tunnel at 6 m/sec when at full power. Therefore, the static case was found with the power plant outside the tunnel, and all velocities above 6 m/sec were found inside the tunnel. This is the reason for there not being data for 2 and 4 m/sec, and also contributes to the inaccuracy of the prediction at those velocities. To get data for 2 and 4 m/sec the line of best fit curves were used from the 0 m/sec data. This is also the reason for the lack of figures in Section A in the appendix for 2 and 4 m/sec.

Figure 5.46(a) shows that the power vs. velocity of the predicted and measured data points are in close agreement. The drop in power seems rather abrupt in Figure

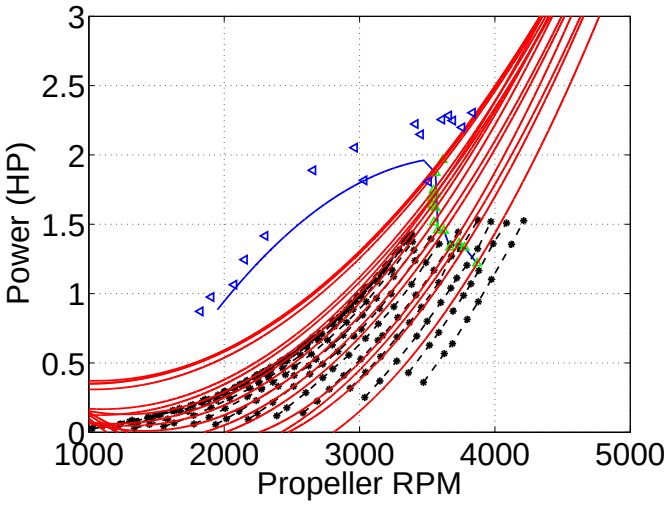

Figure 5.45: Power (HP) vs. RPM of the propeller power absorbed curves for the XOAR 26x16 propeller and the final engine power output curve geared 100/13. The power absorbed curves have been extended using 2nd order lines of best fit.

5.45, but Figure 5.46(a) shows that the power decreases gradually as the velocity is increased. Figure 5.46(b) shows that the RPM vs. velocity is also in close agreement.

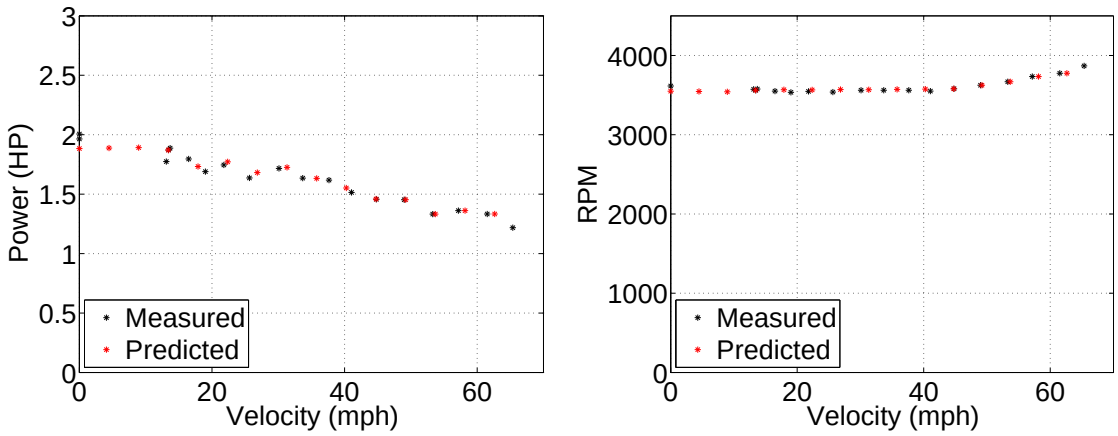

(a) Measured and predicted power (HP) vs. velocity (mph).

(b) Measured and predicted RPM vs. velocity (mph).

Figure 5.46: Figures showing the measured and predicted power and RPM vs. velocity.

The reason for the errors at low velocity is because of the lack of data there, as is the case for the thrust vs. velocity shown in Figure 5.47(a). Figure 5.47(b) shows that the torque vs. velocity is also accurate. In this case, the predicted torque does not have a smooth shape as in previous predictions, and the measured and predicted data

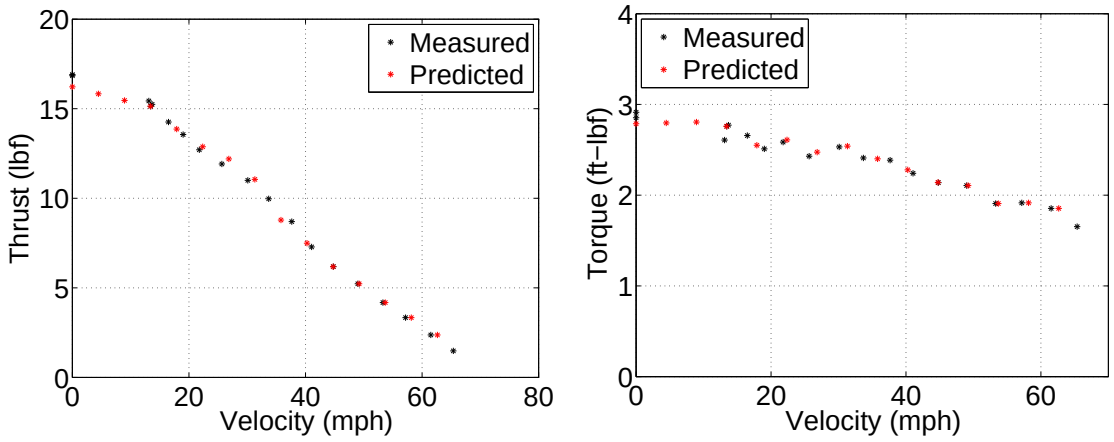

(a) Measured and predicted Thrust (lbf) vs. velocity (mph).

(b) Measured and predicted torque (ft-lbf) vs. velocity (mph).

Figure 5.47: Figures showing the measured and predicted thrust and torque vs. velocity.

points are fairly close. The thrust vs. velocity of the power plant is arguably the most important prediction of the EPM code. The other characteristics are important, but when designing a new aircraft, it is the thrust vs. velocity of a power plant that must be estimated. Figure 5.47(a) shows a reasonably accurate prediction of the measured thrust performance overall, and this proves that the EPM code works well, if good data is supplied to it.

5.3.6 Finalized Geared Power Plant

As was mentioned, the goal was to design a light, powerful power plant for the University of Minnesota SAE Advanced Class airplane, shown in Figure 5.48. The first geared power plant was used to characterize the combined propeller and engine and to test the operation of the shaft and bearings. The first power plant weighed about 3.3 lbs. In order to bring the weight of the entire aircraft down to 8 lbs, the power plant needed to weigh about 2 lbs, which was achieved. The final weight of the airplane was 8.4 lbs, which is very light for a 12 foot wingspan airplane. The airplane had the

Figure 5.48: This figure shows the University of Minnesota SAE Advanced Class airplane with the finalized geared power plant.

most thrust of any airplane at the competition, perhaps 5 lbs more thrust than any of the advanced class airplanes. There was one team that had a geared RC car engine, but they had not done detailed analysis to optimize the gear ratio. It was a very rushed schedule in the weeks before the competition. For this reason, the airplane and systems never got fully tested. The first flight of the power plant and airplane was at the competition. The winds were excessive, at 20-30 mph. Most airplanes hardly moved down the runway after they took off. The UMN airplane took off very fast and flew fast. However, there were some problems with the aircraft design that had not been resolved. The payload was carried in the wings, and the wings were slightly twisted. Each section of wing would have to carry a portion of the payload. Usually the payload is in the fuselage, so the wing twists are not as critical. When the airplane took off, almost full right aileron and rudder were required to keep the

wings level. When the turn was initiated, the airplane could not be righted, and it crashed. The project proved to be much more involved and difficult than anticipated. The power plant, however, performed almost flawlessly and will hopefully be used in future years at the competition. The only issues with the power plant were that it had trouble idling for long periods of time. This is due to the glow plug getting cooled off and oil pooling in the header. Also, if the engine was operating at mid throttle and then brought to idle, the throttle would have to be moved much lower than used for idling. There appears to be two modes of operation for the engine, one of which is slow RPM, and the other which is anything above an idle. Therefore, low throttle settings must be used only when gliding to the runway is possible because the engine may quit. Half throttle and full throttle settings had no problems and could be used until the fuel ran out. As can be seen in the following pictures, the engine was used without a cooling head of any kind. The needle valve settings were then very important to ensure the engine did not overheat. This required the engine to run a little richer than optimal, but it also introduced a safety factor to ensure the engine was lubricated.

Figure 5.49: This figure shows the University of Minnesota SAE Advanced Class airplane with the finalized geared power plant being readied for takeoff.

Figure 5.49 shows the UMN SAE advanced class airplane on the runway being readied

for takeoff. There were significant problems getting the live video feed to work. As a last resort, a cell phone was taped to the airplane and live Google chat was used to broadcast a video feed in order to meet the rule requirements. The cell phone was destroyed in the crash.

Figure 5.50 shows a closer view of the geared power plant in Figure 5.49. Here, the large fuel tank can be seen. Also, the power plant is mounted on a carbon fiber

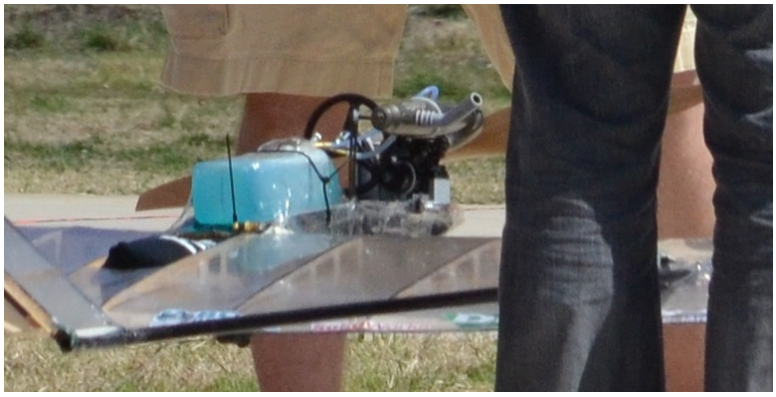

Figure 5.50: This figure shows the University of Minnesota SAE Advanced Class airplane with the finalized geared power plant.

bracket, which is mounted to the wing, shown in Figure 5.51. Here, the relative size

Figure 5.51: Side view of the University of Minnesota SAE Advanced Class airplane.

of the airplane and power plant can be seen.

The following pictures show the geared power plant after the crash at the competition. This is the reason for the dirt on the power plant. To lighten the initial geared power plant, a more compact mount was designed to hold all of the components. The mount had to hold the bearings, engine, and transfer the loads from the power plant to the airframe. As can be seen in the following figures, the shaft is exposed in the center. There are also lightening holes cut in the side of the mount in a triangular pattern, shown in Figure 5.52. The triangular shapes help keep the structure rigid. The large

Figure 5.52: Front and rear view of the finalized geared power plant.

gear was also lightened by milling large holes into it, shown in Figure 5.52. The 3 spoke design was the lightest and simplest design because it only required the hub to have 3 screws to secure the gear to the gear hub. The gear was milled by team members in the UMN Mechanical engineering CNC mill. Two gears were made, which took about 8 hours. The gears were then surface hardened. The first gear used for testing was not hardened, and the teeth had begun to show wear.

The hubs were made significantly lighter by bringing the bolt holes holding the gear to the hubs as close to the propeller shaft as possible. The propeller hub was milled on the sides and drilled from the front. This supported the propeller along its length but not the sides of the propeller. The shaft was made shorter by about 0.7 inches and this saved weight, though the propeller spun very close to the header. The gear mesh was adjusted using steel feeler gauges bought from an automotive store.

The holes for the bearings were precisely measured, but after running the engine for a while, the holes began to widen. The company that donated the engine mount had lightly sand blasted the surface. It is believed that the sandblasted surface wore out

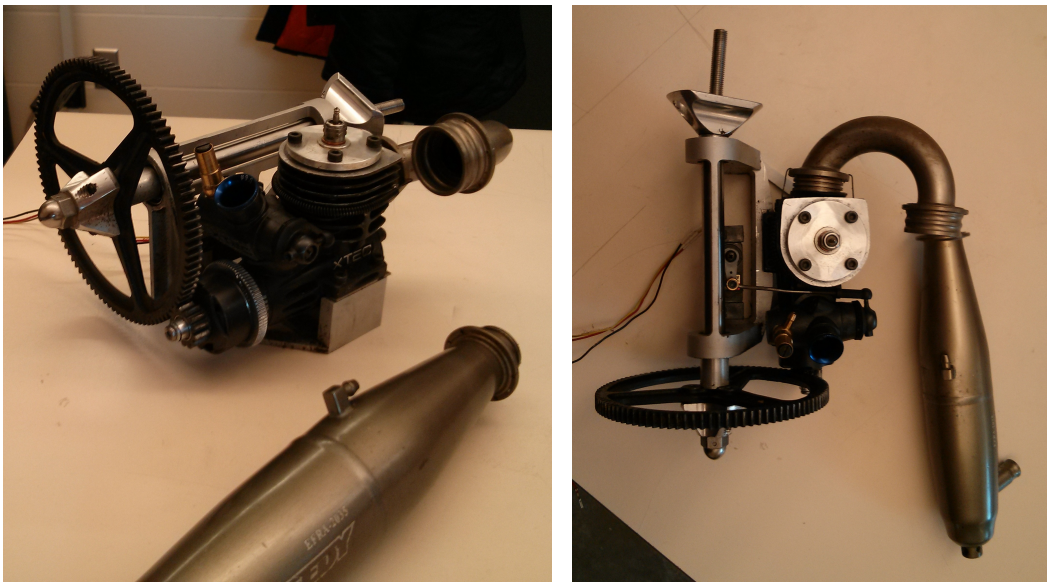

Figure 5.53: Top and rear view of the finalized geared power plant.

slightly after the engine had been run. To remedy this, 0.005 inch feeler gauges were cut in such a way that they fit all around the front and rear bearing. The shaft was then assembled with the feeler gauges between the bearing outer race and the engine mount. After this was done, there was no play between the bearings and engine mount.

The only visible damage from the crash is the bent propeller shaft, shown in Figure 5.53. This shows how strong the power plant design is, and that it is reliable. The bending of the shaft is a rather safe failure mode. Had it fractured and broken off it could show that brittle failure was a possibility.

Overall, the development of the power plant for the UMN SAE Aero Design team using the EPM code proved a success. The power plant impressed many people at the competition, many were taking pictures and asking questions about it. The EPM code and power plant will certainly be of use to the SAE Aero Design teams in the future.

There are several unrealized benefits of the centrifugal clutch as well. RC car engines are often pull started, but there are electric starters that can be mounted to them. Used with a geared power plant, it would be possible to start the engine using the transmitter. It would also be possible to shut the engine off in flight and restart it. If the engine was shut off, it would also be possible to switch to electric power by

gearing an electric motor to the propeller gear. In this way, a power plant could be designed to use solar power or battery power, if possible. The internal combustion engine can be used when high power is needed, if there is no sun or the batteries are depleted. The power plant could also be used in a military UAV where the ICE is used to power the aircraft for most of the flight, but quiet flights over some area could be made with the electric motor.

It would also be possible to use the power plant in a glider with a folding propeller. If the engine was stopped, there could be a brake on the main gear that would stop the propeller from turning. This could be done in such a way that an un-folding propeller stopped level with the wing or in some other way to reduce the drag of the stopped propeller.

Another feature is that many engines could be geared to the same shaft, perhaps a maximum of 4. This would create significant redundancy in the system if one failed. Also, throttled ICEs are more efficient when used with high throttle settings because the pumping losses decrease. This drawback could be used as an advantage by running one engine at full throttle that has been sized to produce the right amount of power for cruise conditions. Then, if more power is needed, such as for takeoff, additional engines can be started to provide the increased power. There would be some loss in efficiency because the freewheeling gears on the clutches that are on the stopped engines would still be engaged to the main gear, and the bearings supporting the clutch gear will have some friction.

Chapter 6

Conclusion

In this chapter we will provide some concluding remarks and suggestions for future work.

6.1 Summary of Findings

It was not clear if methods developed for large scale propeller driven aircraft were applicable to small UAV's. Methods for large scale aircraft were based largely on tables and graphs representing aircraft that had been built. A direct method of comparing different combinations of propellers and engine power curves that takes into account the effect of gear ratio was needed. This thesis describes the creation and testing of such a tool, called engine and propeller matching code.

To verify the results predicted by the engine and propeller matching code, propeller and engine testing apparatus' were constructed. The propeller testing apparatus used a large electric motor to spin 5 different XOAR 26 inch propellers at a range of RPM over a range of velocity. There were some errors introduced due to declining RPM's at high power settings, but these effects were reduced by averaging the data. The engine testing apparatus includes linear sliders and a rotating assembly to measure torque and thrust. Strain gauge instrumented blocks of aluminum from Harbor Freight 70 lb digital scales were used to measure the thrust and torque. Op Amps were built to measure the voltage output from the two Wheatstone bridges. The RPM was measured by taking FFT's of the torque signal. The engine testing apparatus was calibrated by hanging weights in such a way to apply known forces and torques to

the test stand. The calibration showed linear trends in torque or thrust vs. voltage. Severe clipping of the measured thrust and torque voltages was found due to excessive vibration from the LRP ZR.30 X engine. Weights and rubber pads were used to damp out the vibration and remove the clipping. The engine testing apparatus was tested in a closed return wind tunnel to characterize its drag and torque effects with increasing velocity. The torque sensor was found to be extremely sensitive to temperature, but the voltage drift can be subtracted. The LRP ZR.30 X engine vibration also caused a sticking point in the linear slider bearings. There were also unknown resonant peaks in the FFT data.

The LRP ZR.30 X engine was found to produce a maximum of about 2.25 HP at 28-30,000 RPM. Preliminary engine data was used with the EPM code to determine which propeller and gear ratio to use. The preliminary engine data assumed a maximum power of about 2 HP at the same RPM range, but 70% of that curve was used due to uncertainty in the data and unknown losses in gearing. The overall result from the EPM code was that when using the same engine power curve, a propeller with the same diameter, but high pitch, turning at a slower RPM with a higher gear ratio, would produce more thrust at each velocity compared to a propeller with less pitch.

Based on the EPM code results, a XOAR 26 by 16 propeller was used with a (100/13):1 gear reduction with the LRP ZR.30 X engine. The geared power plant was found to produce 17 lbf of static thrust at about 3500 RPM. The geared power plant also produced 3 ft-lbf of torque and 2 HP at static conditions, showing an 11% loss from gearing. The thrust dropped to near zero at about 75 mph. The first geared power plant was optimized further, and the total weight was reduced from 3.3 lbs to 2 lbs by the use of an integrated engine mount, lightened main gear, and lightened propeller and gear hubs. The optimized power plant was used at the SAE Aero Design Competition, and it performed exceptionally well. Compared to a single cylinder gasoline powered 2-stroke engine that weighs about 2.6 lbs and produces 18.7 lbs of static thrust, the optimized geared power plant performs very well [25]. The optimized geared power plant produces 8.5 lbs of thrust per pound of engine, but the other engine only produces 7.13 lbs of thrust per pound of engine. This is an improvement of about 16 percent. Further improvements to the gear and shaft could reduce the weight further.

The measured results are not accurate, however, due to problems with the engine test

stand. The initial predictions were not accurate because the preliminary data did not account for the engine vibration and because the engine power changed with increasing velocity in the wind tunnel. The EPM code was used with a piecewise engine power curve that represented the engines power vs. RPM in the wind tunnel. The measured data was also used to adjust the power absorbed and corresponding thrust curves. When this was done, the EPM code almost exactly predicts the measured data. Even though the measured data is not conclusive, the optimized geared power plant performance and other results show that the EPM code can be used to create much more optimized propeller driven power plants. Lastly, if high RPM engines with high power are used with no restrictions on the gear ratio, it may be possible to get much better thrust vs. velocity performance from fixed pitch propellers.

6.2 Suggested Future Research

As was mentioned, the engine test stand has several known error sources. These could be eliminated so that the results would be more accurate. The drag of the propeller testing apparatus and engine test stand also needs to be fully accounted for so that only the propeller performance is compared. The testing conducted in the wind tunnel also needs to be done more accurately. As the velocity is increased, the engines carburetor needs to be re-adjusted to account for the drop in pressure in the test section in order to maintain the power output. There are several ways that the tools developed in this thesis can be used. It would be possible to use the code developed to make a geared power plant that uses two separate engines. This could be used in the SAE competition again to have even more thrust. Lastly, if a data base was compiled with engine and propeller performance data, it would be possible to test all the available combinations without purchasing a single component. This would help the RC and UAV community and is something that will hopefully begin to happen as the UAV and RC industries grow.

Bibliography

[1] "eCalc," http://www.ecalc.ch/motorcalc_e.htm?castle.

[2] Raymer, D. P., *Aircraft Design: A Conceptual Approach*, American Institute of Aeronautics and Astronautics, Reston, VA, 3rd ed., 1999.

[3] Anderson, J. D., *Introduction to Flight*, McGraw-Hill, New York, 5th ed., 2005.

[4] White, G., "Reno for Gearheads," http://www.supercoolprops.com/articles/gwhitegearheads.php.

[5] "3,500 h.p. RADIAL Pratt & Whitney WASP MAJOR," *Flight*, 1947.

[6] "Liberty 12-Cylinder Engine," http://www.nationalmuseum.af.mil/factsheets/factsheet.asp?id=839.

[7] Hill, P. G. and Peterson, C. R., *Mechanics and Thermodynamics of Propulsion*, Prentice Hall, New York, 2nd ed., 1991.

[8] "O.S. Engines," http://www.osengines.com.

[9] "RCV Engines Limited," http://www.rcvengines.com.

[10] Stone, R., *Introduction to Internal Combustion Engines*, SAE International, Warrendale, PA, 4th ed., 2012.

[11] "Determine a Model's Power Requirements," http://www.horizonhobby.com/pdf/EFLDeterminingPowerRequirement.pdf.

[12] McCormick, B. W., *Aerodynamics, Aeronautics, and Flight Mechanics*, John Wiley & Sons, New York, 2nd ed., 1995.

[13] Tjhai, C., *Developing Stochastic Model of Thrust and Flight Dynamics for Small UAVs*, Master's thesis, University of Minnesota, Twin Cities, 2013.

[14] Kuethe, A. M. and Chow, C.-Y., *Foundations of Aerodynamics, Bases of Aerodynamic Design*, John Wiley & Sons, New York, 5th ed., 1998.

[15] John Stack, Eugene C. Draley, J. B. D. and Feldman, L., "Investigation of the NACA 4-(3)(08)-03 and NACA 4-(3)(08)-045 Two-Blade Propellers at Forward Mach Numbers to 0.725 to Determine the Effects of Compressibility and Solidity on Performance," NACA Report 999, 1944.

[16] Woan, C.-J., "Design of Propellers for Minimum Noise," NASA Contractor Report 155005, 1977.

[17] Vogeley, A. W., "Axial-Momentum Theory for Propellers in Compressible Flow," NACA Technical Note 2164, 1951.

[18] Brandt, J. B. and Selig, M. S., "Propeller Performance Data at Low Reynolds Numbers," *49th AIAA Aerospace Sciences Meeting, Orlando, FL*, 2011.

[19] "RCTECH, Piston and Sleeve Set LRP 0.30X," `http://www.rctech.net/forum/r-c-items-sale-trade/397671-new-piston-sleeve-set-lrp-30x.html`.

[20] "LRP," `http://www.teamassociated.com/lrp/parts/details/LRP32815/`.

[21] "HPI Racing, Aluminum Clutch Shoe Set," `https://www.hpiracing.com/products/en/87196/`.

[22] "HPI Racing 3-Piece Clutch Set Savage," `http://www2.gpmd.com/imagel/h/lhpic8753.jpg`.

[23] "Multipurpose Oil-Hardened O1 Tool Steel," `http://www.mcmaster.com/#drill-rods/=mtptoc`.

[24] "D6800/603C Angular Contact Bearings," `http://www.bocabearings.com/bearing-inventory/Angular-Contact-Bearings/19673/10x19x5-D6800603C`.

[25] "DLE Engines DLE-30cc Gasoline Eng," `http://www3.towerhobbies.com/cgi-bin/wti0001p?&I=LXZZH1&P=0`.

Appendix A

Offset Power and Thrust Curves

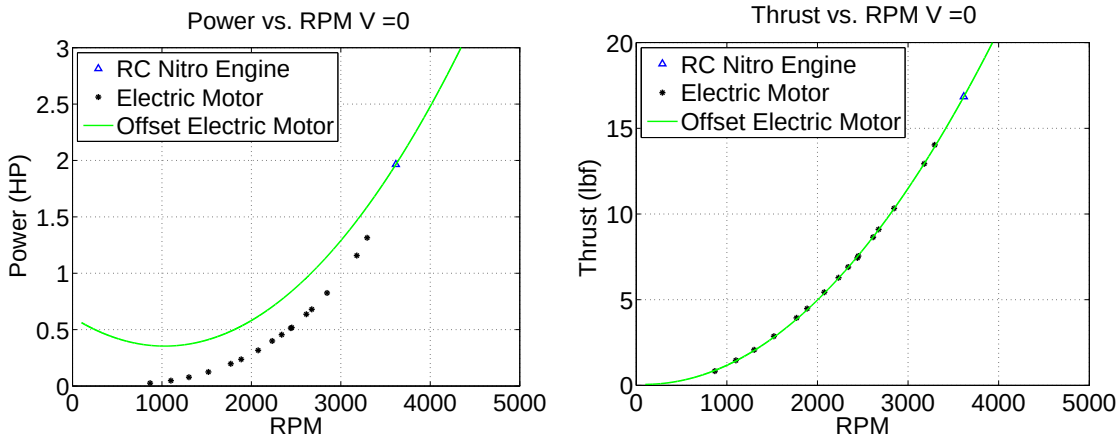

(a) Power (HP) vs. RPM at a velocity of 0 m/sec.

(b) Thrust (lbf) vs. RPM at a velocity of 0 m/sec.

Figure A.1: Figures showing the power and thrust vs. RPM at a velocity of 0 m/sec.

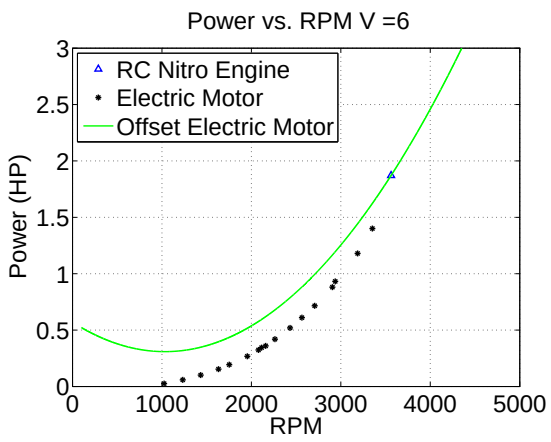

(a) Power (HP) vs. RPM at a velocity of 6 m/sec.

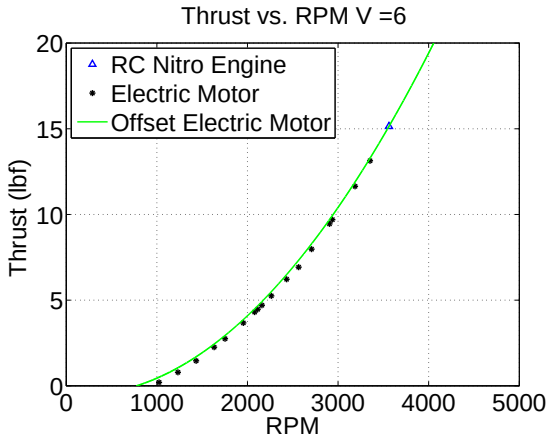

(b) Thrust (lbf) vs. RPM at a velocity of 6 m/sec.

Figure A.2: Figures showing the power and thrust vs. RPM at a velocity of 6 m/sec.

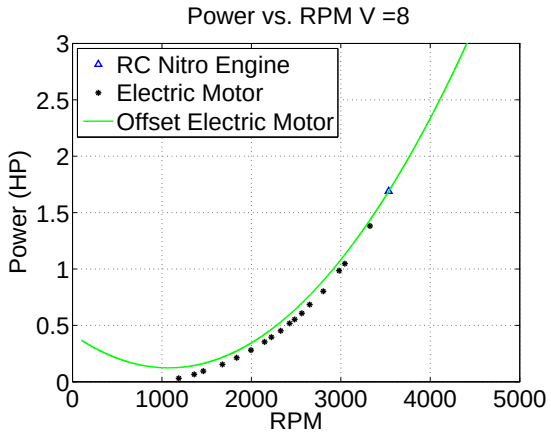

(a) Power (HP) vs. RPM at a velocity of 8 m/sec.

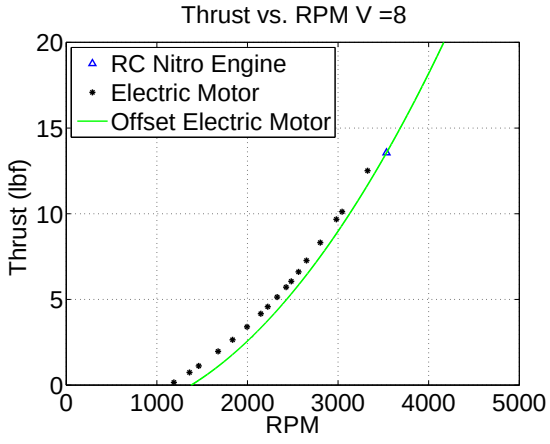

(b) Thrust (lbf) vs. RPM at a velocity of 8 m/sec.

Figure A.3: Figures showing the power and thrust vs. RPM at a velocity of 8 m/sec.

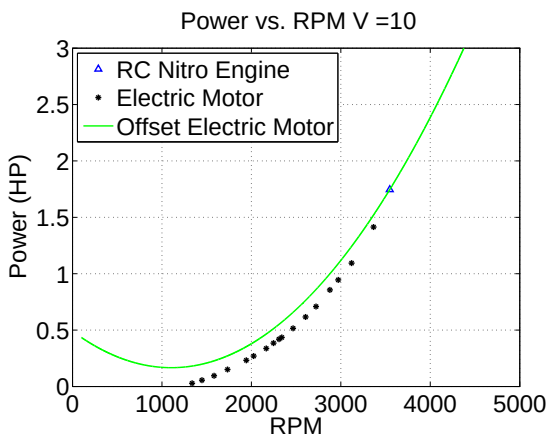

(a) Power (HP) vs. RPM at a velocity of 10 m/sec.

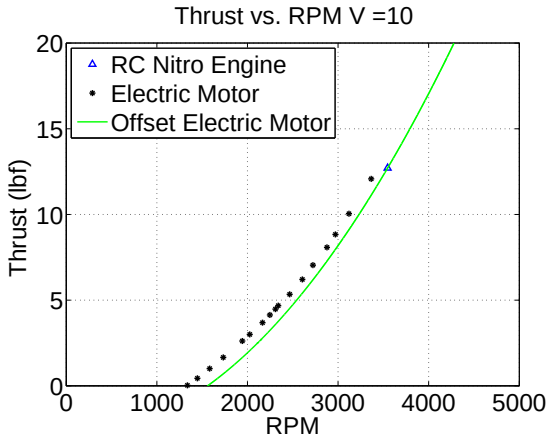

(b) Thrust (lbf) vs. RPM at a velocity of 10 m/sec.

Figure A.4: Figures showing the power and thrust vs. RPM at a velocity of 10 m/sec.

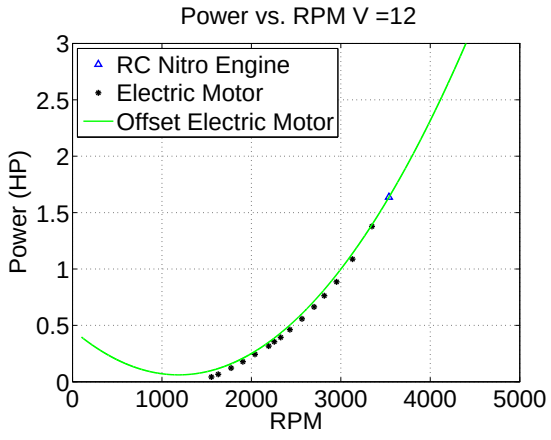

(a) Power (HP) vs. RPM at a velocity of 12 m/sec.

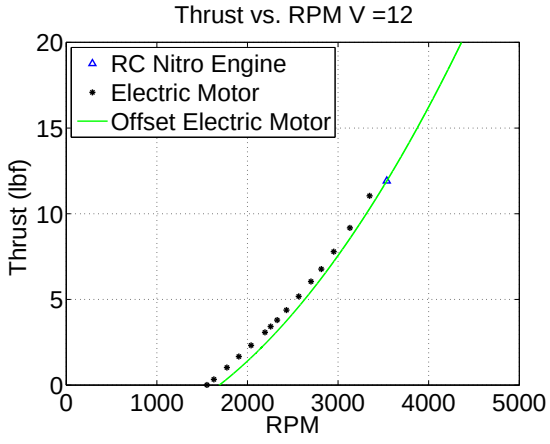

(b) Thrust (lbf) vs. RPM at a velocity of 12 m/sec.

Figure A.5: Figures showing the power and thrust vs. RPM at a velocity of 12 m/sec.

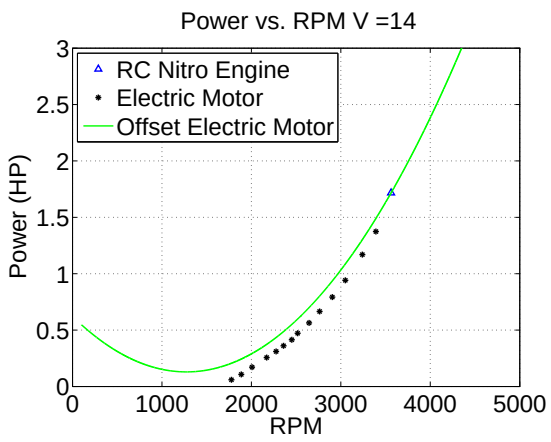

(a) Power (HP) vs. RPM at a velocity of 14 m/sec.

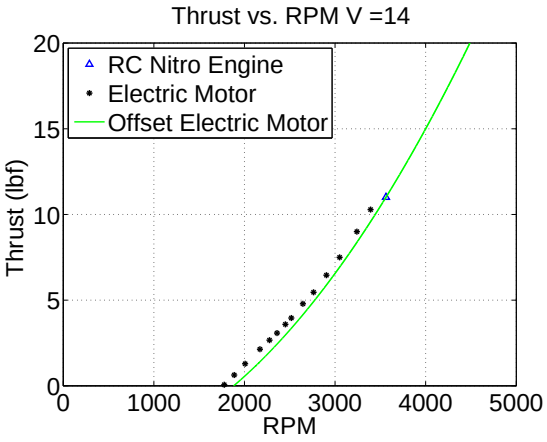

(b) Thrust (lbf) vs. RPM at a velocity of 14 m/sec.

Figure A.6: Figures showing the power and thrust vs. RPM at a velocity of 14 m/sec.

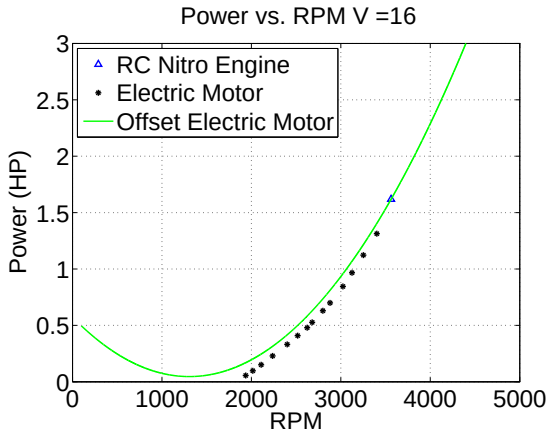

(a) Power (HP) vs. RPM at a velocity of 16 m/sec.

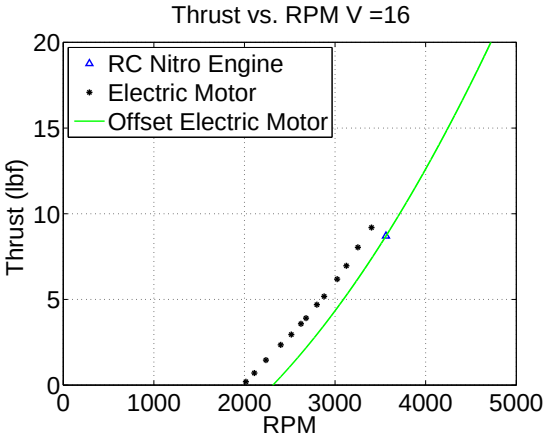

(b) Thrust (lbf) vs. RPM at a velocity of 16 m/sec.

Figure A.7: Figures showing the power and thrust vs. RPM at a velocity of 16 m/sec.

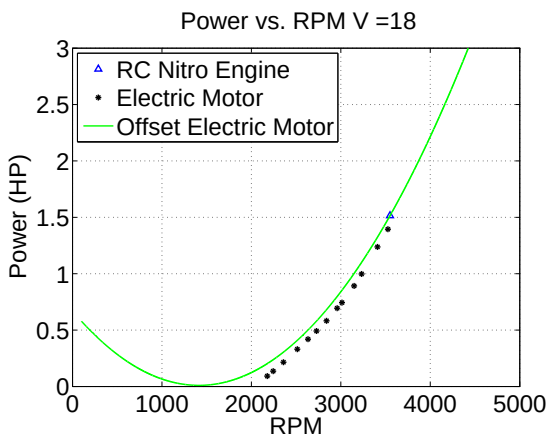

(a) Power (HP) vs. RPM at a velocity of 18 m/sec.

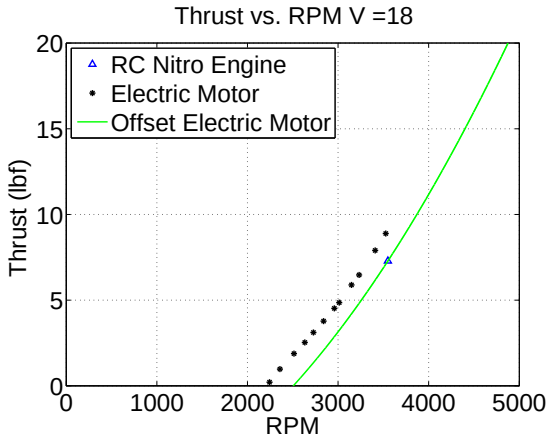

(b) Thrust (lbf) vs. RPM at a velocity of 18 m/sec.

Figure A.8: Figures showing the power and thrust vs. RPM at a velocity of 18 m/sec.

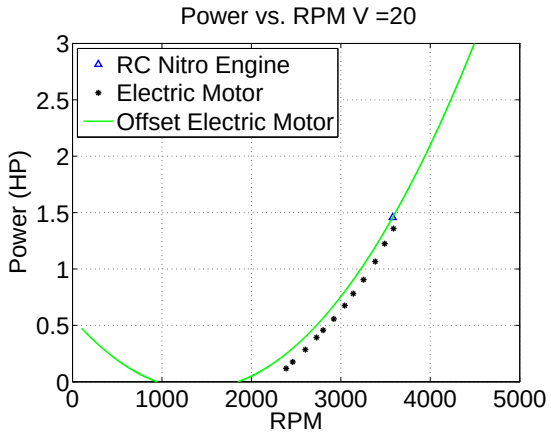

(a) Power (HP) vs. RPM at a velocity of 20 m/sec.

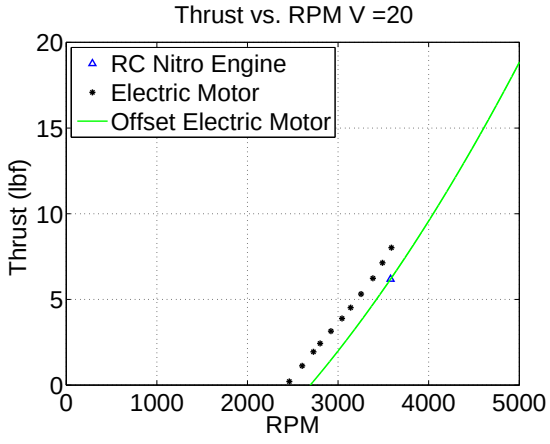

(b) Thrust (lbf) vs. RPM at a velocity of 20 m/sec.

Figure A.9: Figures showing the power and thrust vs. RPM at a velocity of 20 m/sec.

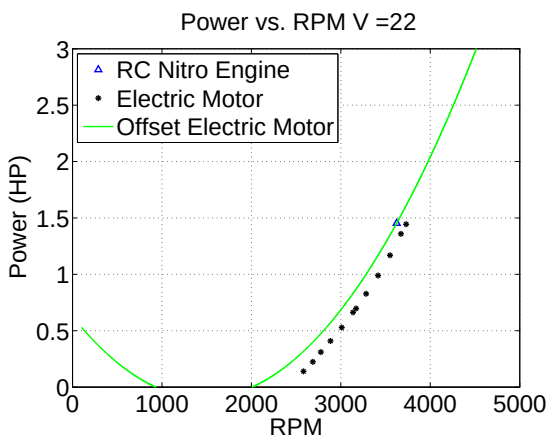

(a) Power (HP) vs. RPM at a velocity of 22 m/sec.

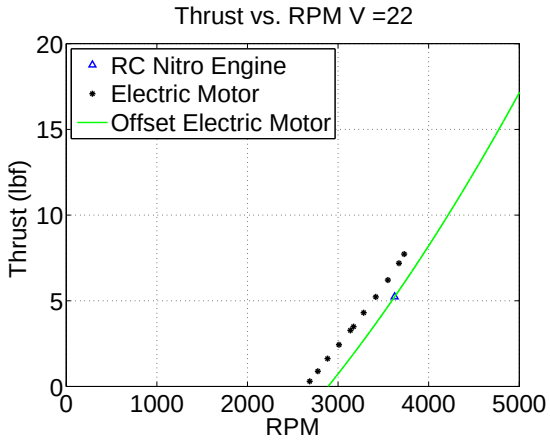

(b) Thrust (lbf) vs. RPM at a velocity of 22 m/sec.

Figure A.10: Figures showing the power and thrust vs. RPM at a velocity of 22 m/sec.

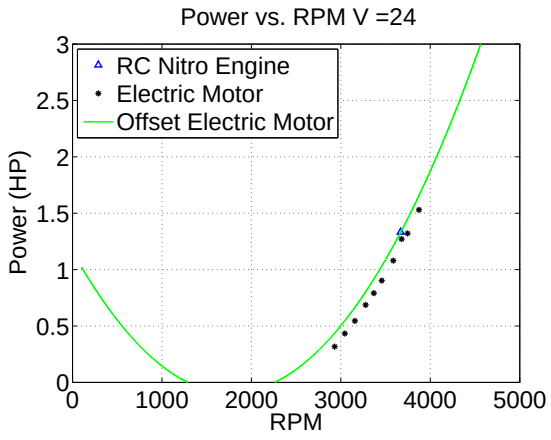

(a) Power (HP) vs. RPM at a velocity of 24 m/sec.

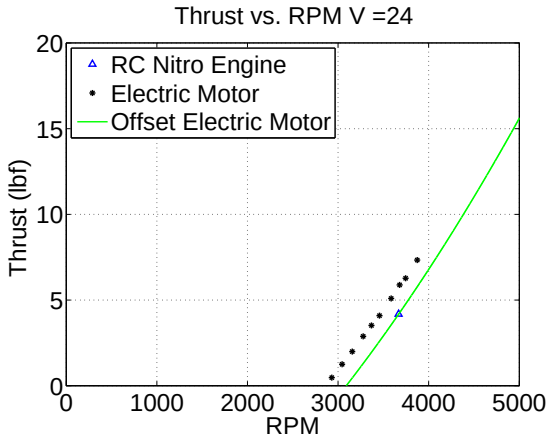

(b) Thrust (lbf) vs. RPM at a velocity of 24 m/sec.

Figure A.11: Figures showing the power and thrust vs. RPM at a velocity of 24 m/sec.

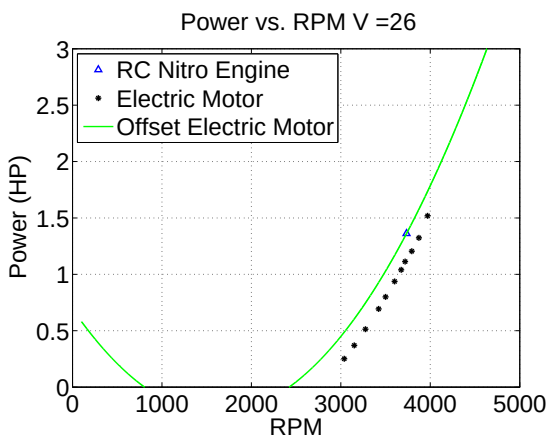

(a) Power (HP) vs. RPM at a velocity of 26 m/sec.

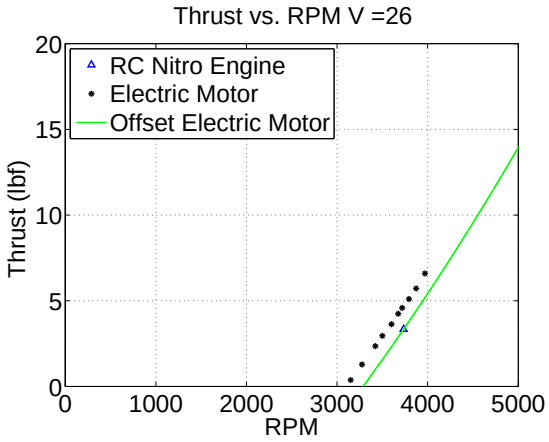

(b) Thrust (lbf) vs. RPM at a velocity of 26 m/sec.

Figure A.12: Figures showing the power and thrust vs. RPM at a velocity of 26 m/sec.

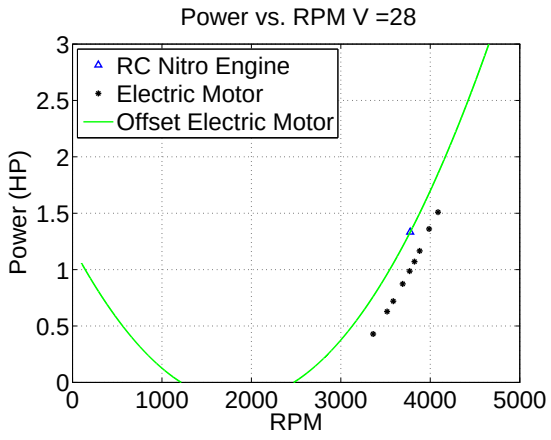

(a) Power (HP) vs. RPM at a velocity of 28 m/sec.

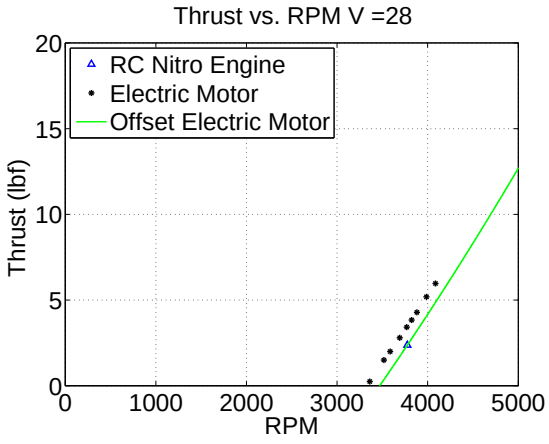

(b) Thrust (lbf) vs. RPM at a velocity of 28 m/sec.

Figure A.13: Figures showing the power and thrust vs. RPM at a velocity of 28 m/sec.

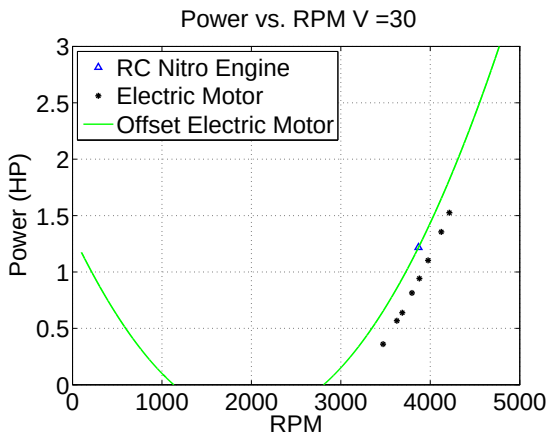

(a) Power (HP) vs. RPM at a velocity of 30 m/sec.

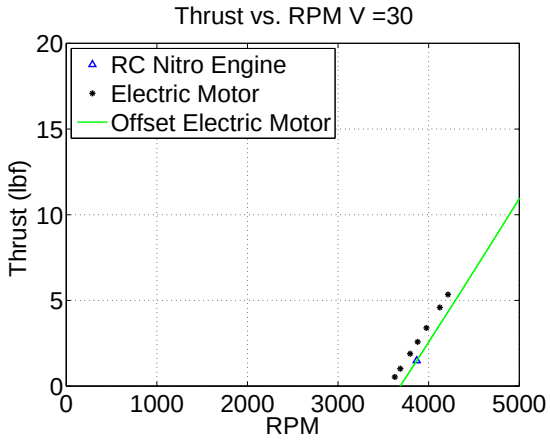

(b) Thrust (lbf) vs. RPM at a velocity of 30 m/sec.

Figure A.14: Figures showing the power and thrust vs. RPM at a velocity of 30 m/sec.